THE PRACTICAL APPLICATION OF A HYDRAULIC POWER RECOVERY TURBINE AT THE VALDEZ MARINE TERMINAL

A

PROJECT

Presented to the Faculty

of the University of Alaska Fairbanks

in Partial Fulfillment of the Requirements

for the Degree of

MASTER OF SCIENCE

PETROLEUM ENGINEERING

By

Brendon John Bruns, B.S., P.Eng.

Fairbanks, Alaska

May 2019

THE PRACTICAL APPLICATION OF A HYDRAULIC POWER RECOVERY TURBINE AT THE VALDEZ MARINE TERMINAL

Approved by:

Dr. Abhijit Dandekar
Chair, Department of Petroleum Engineering
University of Alaska Fairbanks

David Heimke
Director of Engineering
Alyeska Pipeline Service Company

Dr. Richard Wies
Department of Electrical & Computer Engineering
University of Alaska Fairbanks

Date Approved: May 2019

ABSTRACT

A hydraulic power recovery turbine (HPRT) is a machine designed to capture energy from the pressure differential of a fluid. The HPRT recovers energy that would otherwise be lost to entropy in flowing fluid processes. When the shaft of the HPRT is coupled to an electric generator, the electricity produced can be employed for practical purposes. At the terminus of the Trans-Alaska Pipeline System (TAPS) in Valdez, favorable hydraulic conditions and electrical infrastructure exists for the application of an HPRT to generate significant power. This project will study the practical application of an HPRT as a source of clean, reliable electricity to the VMT. Installation of an HPRT has the potential to reduce diesel consumption and emissions of air pollutants at the VMT.

"If I have seen further it is by standing on the shoulders of giants."

Sir Isaac Newton

This work is dedicated to my wife, Ashley Nicole Bruns. This project would not have been possible without her love, patience and support.

ACKNOWLEDGMENTS

I gratefully acknowledge the support of my committee in this multi-disciplinary project: Abhijit Dandekar, David Heimke and Richard Wies. This project would not have been possible without their guidance.

I also wish to thank the following people for their assistance in completing this project: Lyle Sweeney for his practical hydraulic and mechanical expertise; Bryan Tenney who found drawings on the back pressure control system and walked it down in the field; Michael Malvick for sharing his knowledge of the vapor characteristics of crude oil, and my father Randol Bruns for extensive proofreading of the project report.

TABLE OF CONTENTS

LIST OF FIGURES

LIST OF TABLES

SUMMARY

A hydraulic power recovery turbine (HPRT) is a machine designed to capture energy from the pressure differential of a fluid. The HPRT recovers energy that would otherwise be lost to entropy in flowing fluid processes. When the shaft of the HPRT is coupled to an electric generator, the electricity produced can be employed for practical purposes. At the terminus of the Trans-Alaska Pipeline System (TAPS) in Valdez, favorable hydraulic conditions and electrical infrastructure exists for the application of an HPRT to generate significant power.

The elevation of Thompson Pass at pipeline milepost 775 is 2,810 feet above sea level with the terminus at milepost 800 on the Valdez Marine Terminal (VMT) close to sea level. With an incoming differential pressure maintained at 600 pounds per square inch and an average pipeline flow rate of 16,000 gallons per minute, the potential energy available is approximately 3.8 megawatts. Today this energy is lost as heat across a series of backpressure control valves used to maintain hydraulic conditions south of Thompson Pass.

HPRTs are not new or unique; they have been used in industrial processes for decades. The engineers at Fluor who designed TAPS recognized the potential and included tees at Remote Gate Valve (RGV) 125, immediately upstream of the VMT. After startup of the pipeline in 1977 and through the 1980s, Copper Valley Electric Association (CVEA) attempted to utilize this hydraulic resource for local power generation. When the backpressure control system in service today was installed in 1997, 36-inch takeoffs were installed on the piping manifold at East Meters on the VMT specifically for power recovery purposes. Neither effort resulted in an installed HPRT for various technical, economic or legal reasons.

This project will study the practical application of an HPRT as a source of clean, reliable electricity to the VMT. This is a multi-discipline endeavor. Petroleum, me-

chanical, hydraulic and electrical engineering disciplines will be employed to develop a technically viable and economic design. Installation of an HPRT has the potential to reduce diesel consumption and emissions of air pollutants at the VMT.

An overview of the major components of TAPS, the pipeline and the marine terminal is covered in Chapter 1. To understand the origin of the energy resource, static and dynamic hydraulic theory are discussed in Chapter 2 along with the backpressure control system at the VMT. Sizing of the hydraulic turbine is covered in Chapter 3. To choose the appropriate electric generator, the operation of the existing VMT power and vapor system is examined in Chapter 4 as is the electric machine selected in Chapter 5. Projected fuel savings, implementation details and an economics analysis is presented in Chapter 6.

CHAPTER 1
PROJECT BACKGROUND

1.1 Units of Measurement

The United States Customary system (USC) of units remains the dominant unit system in the American oil and gas industry. With a couple minor exceptions, this paper will continue to use USC units with hydrocarbon systems.

Energy: british thermal units (Btu) or million Btu (MMBtu) for fuels, kilowatt-hour (kWh) or megawatt-hour (MWh) for electrical energy.

Energy Density: Btu/SCF for vapor or Btu/gallon for liquids.

Power: horsepower (HP) for hydraulic machines or kilowatts (kW)/megawatts (MW) for electric machines; 1 HP = 746 watts.

Volume: barrels (BBL) or gallons (gal); 1 BBL = 42 gal.

Flow rate (liquid): barrels per day (BBL/day) or gallons per minute (GPM).

Flow rate (gas): thousand standard cubic feet per hour (MSCF/hr) or million standard cubic feet per hour (MMSCF/hr).

Length: foot (ft) or inch (in).

Pressure: pounds per square inch (PSI), absolute (PSIA) or gauge (PSIG) as appropriate.

Temperature: Fahrenheit (°F) for hydrocarbon process, occasionally Celsius (°C) for equipment ratings.

1.2 The Trans-Alaska Pipeline System

The Trans-Alaska Pipeline System was designed and constructed to transport single-phase crude oil from the North Slope of Alaska to tidewater in Valdez. Oil was

discovered at Prudhoe Bay in February of 1968 with the successful flow test of the Prudhoe Bay State #1 well. The field was subsequently delineated with additional wells and confirmed to be a significant accumulation of oil. Shortly thereafter the fjord at Valdez was chosen as the terminus of the pipeline in April of 1968.[1] Valdez is advantageous as it remains ice free during the winter and is due south of Prudhoe Bay. The route chosen maximized year-round utilization of oil tanker transport, the most cost-effective means to transport crude oil.

1.2.1 Pipeline

The original design of TAPS utilized twelve pump stations to supply the hydraulic head differential to move approximately two million barrels of crude oil per day across the Brooks, Alaska and Chugach mountain ranges. With the development and subsequent commercialization of Drag Reducing Agents (DRA) occurring during the construction and startup of TAPS, mainline pumps were omitted from Pump Stations 5 and 11. As throughput steadily declined from its peak in 1988[1], Pump Stations 2, 6, 8, 10 and 12 were gradually removed from service and isolated from the mainline. These pump stations were necessary to handle the frictional head losses induced by flow rates of two million barrels per day. They have since turned into support bases.

Pump Station 7 is configured to circulate oil through a special valve designed to raise its temperature. The pressure drop across the valve induces frictional heating of the oil. The station only operates when necessary to add heat to the crude stream.

Currently four pump stations remain in service: Pump Stations 1, 3, 4, and 9. Each of the active pump stations have been reconfigured in the last decade with centrifugal pumps coupled to 6,500 horsepower induction motors. Pipeline throughput

[1]Throughput today is approximately 500,000 barrels per day. Lower throughput increases system heat losses, resulting in lower crude temperatures. At these reduced temperatures and flow rates, water and wax are increasingly likely to drop out of the crude stream. Consolidated water and wax pose significant risks to system integrity as the mainline crude pumps are vulnerable to damage from ice formation. Wax deposited on the inside of the pipe must be removed to prevent corrosion.[2]

can be precisely controlled as the motors are driven by variable frequency drives. Pump Station 5 remains in service to drain down the southern end of the Brooks Range (south of Atigun Pass) during pipeline upsets or shutdowns.[3]

The pipeline itself consists of 800 miles of 48 inch outside-diameter steel pipe with wall thicknesses of 0.462 or 0.562 inches. The pipeline was designed to traverse highly variable, mountainous terrain in arctic and sub-arctic climates. When soils along the pipeline route were found to be vulnerable to thaw, the pipeline was elevated above ground: 420 miles of the pipeline are installed on 78,000 vertical support members. To prevent the permafrost from thawing, passive two-phase thermosyphons are used to transfer heat away from the ground[2]. When thaw-stable or unfrozen soils were found, the pipeline was buried.[4]

1.2.2 The Valdez Marine Terminal

Facilities at the VMT include infrastructure supporting crude oil storage, metering, vapor recovery, power generation, ballast water treatment, backpressure maintenance and tanker loading. With twelve above-ground storage tanks for crude storage, the terminal's working inventory capacity is 6.12 million barrels with an additional 1.02 million barrels of capacity for relief and drain-down purposes. Given the distance from Valdez to the refineries on the west coast of the continental United States, the designers of the VMT included enough storage capacity to accommodate interruptions to tanker shipping schedules.

The VMT was designed to be self sufficient. Forty years after construction, the terminal remains an islanded system from the city of Valdez. The VMT maintains water purification and wastewater treatment utilities in support of the aforementioned

[2]The thermosyphons are filled with anhydrous ammonia or carbon dioxide as the refrigerant that pools in the sub-grade portion of the tube. During operation, the refrigerant absorbs heat from the permafrost which evaporates and fills the upper portion of the tube inside the radiator. There the refrigerant condenses and falls back to the bottom of the tube, releasing absorbed energy in the process. The cycle continues provided a temperature differential exists between the ground and air. See Figure 1.1

Figure 1.1: An aboveground section of the pipeline at the Kuparuk River crossing during the spring. The iconic vertical support members and thermosyphons are clearly visible.

Figure 1.2: Satellite imagery of the Valdez Marine Terminal. Orientation: North is up. The twelve crude oil storage tanks and two breakout tanks comprising the East Tank Farm are visible in the center of the image. The Power/Vapor facility is west of the East Tank Farm. The four crude tanks west of Power/Vapor are out of service. The Ballast Water Treatment facility is north of the East Tank Farm. In service loading Berths 4 and 5 are in the northwest corner of the image. Image data: Google

crude oil handling operations.

A Rankine steam cycle[3] is utilized to simultaneously generate electricity and manage vapor recovery. A continuously varying mixture of volatile crude oil vapors and diesel are burned in one of three boilers to generate steam. Each boiler can produce super heated steam flows of 175,000 pounds per hour at 620 PSIG and 750 degF. To generate electricity steam is routed via a ring header to one of three 15-stage, 12.5 MW condensing steam turbines. Each turbine is rated for steam flows of 121,500 pounds per hour at 600 PSIG and 750 degF. Steam pressures at the outlet of the turbines is approximately 2 PSIA or 12 PSI below atmospheric pressure to maximize adiabatic[4] energy extraction from the steam. The saturated steam at the output of the turbines is routed to one of three condensers on the roof of the plant where the steam is condensed back to liquid water for reuse in the Rankine cycle. The steam turbines are directly coupled to synchronous generators with nameplate power generation capacities of 15.625 MVA or 12.5 MW each at 13.8 kV.[3]

The inert exhaust or flue gases from the boilers are captured, cooled and used to blanket the crude storage tanks thereby preventing the formation of an explosive atmosphere within the tank. Flue gas is routed to the tank farm when evolved crude oil vapors are insufficient to maintain tank head pressure. Operation of the power and vapor plant is covered in detail in Chapter 4.[3]

As crude oil vapors are a regulated air pollutant, they may not be freely vented into the atmosphere.[6] Though the vapors are valuable in downstream crude oil refining, the difficulty of vapor re-entrainment back into the liquid crude stream lends them for use as a local fuel source at the VMT. Excess crude vapors that cannot be utilized to produce steam in the boilers are destroyed in one of three incinerators. When insufficient crude vapors are available to meet the thermal (steam) load on the

[3]The Rankine cycle is the vapor power cycle frequently used in thermal power plants. The working fluid—typically water—is alternatively vaporized and condensed to convert heat into mechanical work.[5]

[4]A process during which heat does not enter or leave the system. [5]

boilers, diesel is burned as a secondary fuel source. As diesel burned at the VMT is purchased from a local refinery, strategies to maximize utilization of the vapors are employed. The ultimate goal of installing an HPRT at the VMT is to decrease diesel consumption. A reduction in electrical load on the main generators will curtail demand for supplemental diesel.

1.3 Alyeska's History with HPRTs

Previous engineering studies performed on the application of a HPRT at the VMT from the 1960s to the 1980s were typically constrained by the variability of pipeline throughput and the lack of a tie between the VMT power system and CVEA's grid. Suggested configurations were:

1. An HPRT directly coupled to a synchronous generator. This requires steady and predicable flow through the turbine to maintain synchronous speed. This is difficult with crude oil as the production is irregular. Oil is produced with water and gas commingled in the same production line. When the phases segregate in the production tubing or at surface, they form *slug flow*. The variability of pipeline throughput is shown in the Figure 1.3 scatter plot. Use of a synchronous generator is revisited in Chapter 5.

2. An HPRT directly coupled to an induction generator. Unlike synchronous generators, induction generators can tolerate varying shaft speeds as they do not maintain system frequency or voltage. As will be discussed at length in Chapter 5, induction generators must be connected to a power system capable of supplying sufficient reactive power to the machine to maintain excitation. As the early iterations of the VMT power system were smaller than the present configuration, this configuration was deemed technically infeasible.

3. Pumped hydroelectric hybrid. An HPRT in line with the pipeline would be

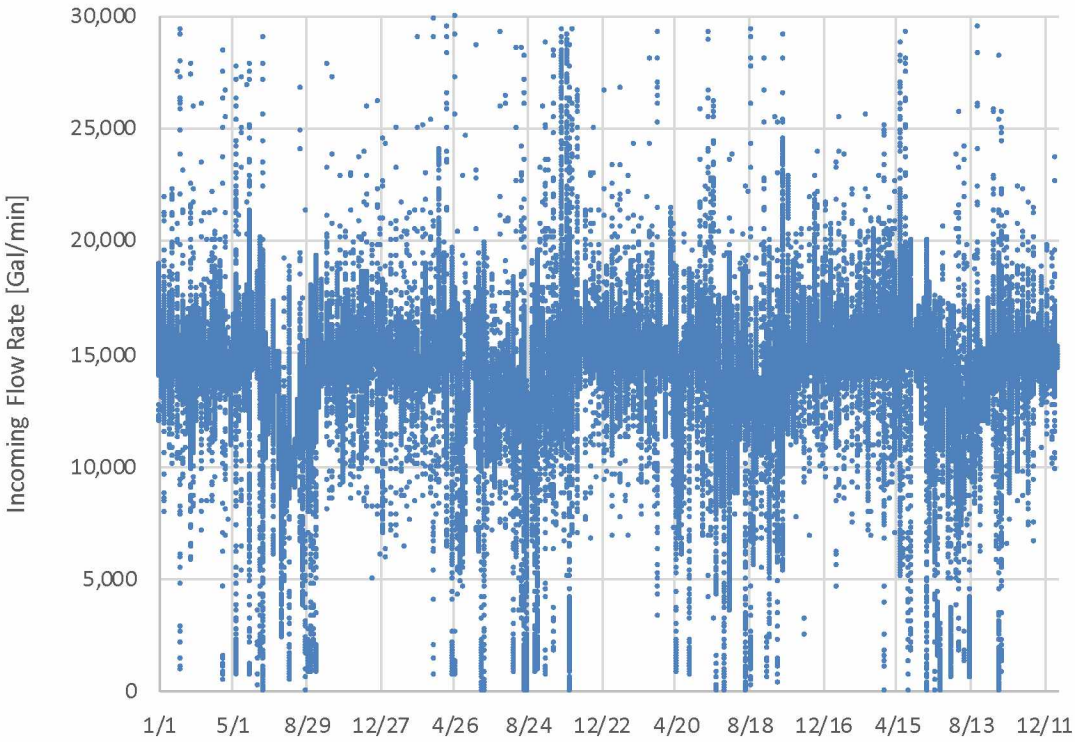

Figure 1.3: Scatter plot of the incoming crude oil flow rate at the VMT versus time.

coupled to a pump that pumps water uphill to a reservoir. The reservoir would be drained through a traditional hydroelectric facility to generate electricity. This configuration was deemed too complicated and inefficient.

In 2018 the Transalpine Oil Pipeline in Europe commissioned a 2.5 MW HPRT to recover energy lost in managing slackline conditions. As shown in Figure 1.4 a Francis turbine is utilized, similar to classic hydroelectric applications.

Figure 1.4: A 2.5 MW hydraulic power recovery turbine installed on the Transalpine Oil Pipeline in Austria. The facility is called the Taimeralm Energy Recovery Station. Source: https://www.ilf.com/company/innovations/

CHAPTER 2
PIPELINE HYDRAULICS

Pipeline hydraulics will dictate the fundamental operation and constraints of an HPRT. Hydrostatics and hydrokinetics will be used to develop the concept of hydraulic head and ultimately a hydraulic gradient. From there the theory behind the 600 pounds per square inch pressure differential developed across the backpressure control system at the incoming of the VMT will be studied. The artificial pressure differential combined with pipeline throughput is the energy resource to be captured.

2.1 Hydrostatics and Hydrokinetics

If a vertical tube that is open at the top is connected to a vessel under pressure, the fluid level in the tube will rise to a height equivalent to the force exerted by the pressure in the vessel. The force due to gravity acting on the fluid in the tube counteracts with the force exerted by the pressure within the vessel. A sight glass mounted to the side of a storage tank used to measure the fluid level operates on the same principle. The vertical tube is a called a *piezometer* and is useful to understand the concept of hydraulic head.

2.1.1 Piezometric Head

Consider a level section of pipeline under constant pressure with no fluid flow. Sight glasses installed along the length of the pipeline would indicate the same fluid level or *piezometric head* at all points within the pipe. This behavior is depicted in Figure 2.1 as the physical manifestation of Blaise Pascal's law of hydraulics. The fluid level will rise to the same level even if the pipeline is traversing uneven ground as shown

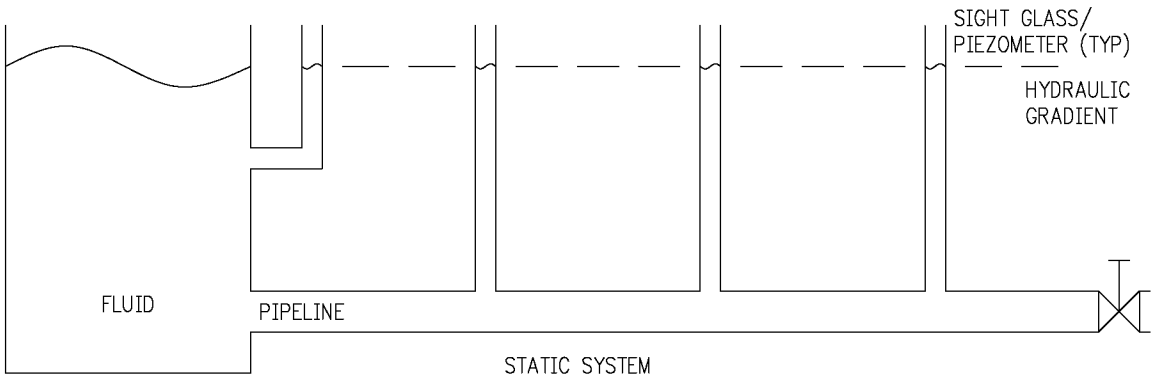

Figure 2.1: Level section of pipeline with sight glasses installed and no fluid flow. The piezometric head is the same at all points along a pipeline with static fluid. Note that the hydraulic gradient is flat under static conditions. *TYP* is short for Typical. Figure adapted from the *Practical Hydraulics Handbook*, reference [7].

in Figure 2.2[1].

If the fluid is set in motion the piezometric head will decrease along the length of the pipeline[2]. The continuous loss of piezometric head is caused by a pressure gradient that develops within the pressure boundary of the pipe as depicted in Figure 2.3. The pressure loss or *head loss* is a result of viscous forces acting within the fluid and frictional forces acting between the fluid and the surface of the pipe wall. If the fluid is then brought to a stop, the frictional forces disappear and the gradient returns to that depicted in Figure 2.1.

Though now at rest, the temperature of the in situ fluid will have increased, a result of the conservation of energy described by the first law of thermodynamics. The net result of a fluid in motion within a pipeline is the formation of a pressure gradient and an increase in the fluid temperature (assuming ideal conditions where no external heat losses occur).

[1] Assuming the fluid density remains constant.
[2] Assuming the fluid density, fluid viscosity and pipe roughness remain constant.

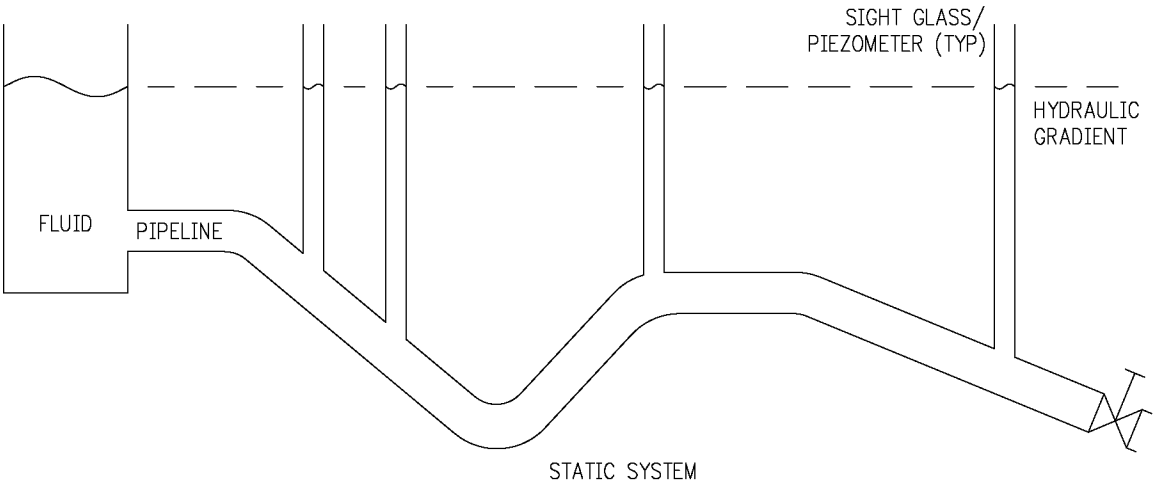

Figure 2.2: A section of pipeline traversing uneven terrain with sight glasses installed and no fluid flow. The piezometric head remains the same under static conditions even if the elevation of the pipeline varies with respect to the datum. Note the hydraulic gradient is again flat and matches Figure 2.1. *TYP* is short for Typical. Figure adapted from the *Practical Hydraulics Handbook*, reference [7].

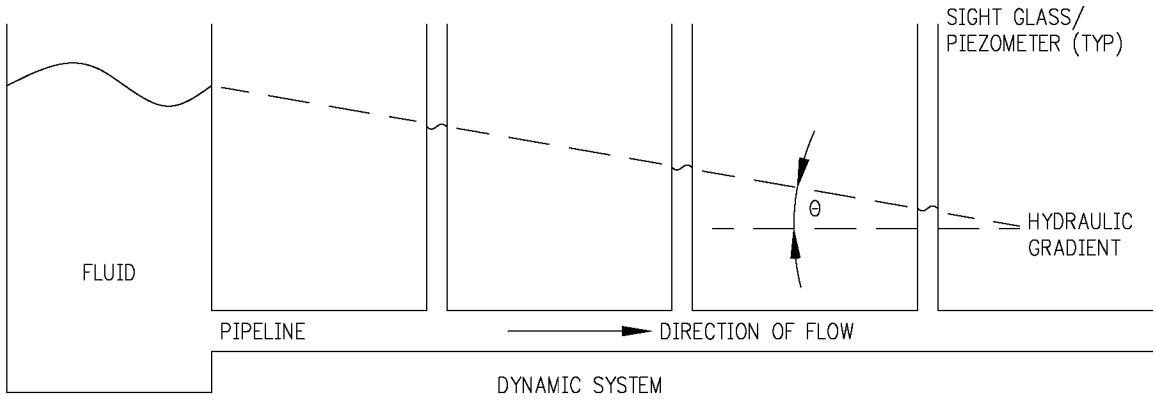

Figure 2.3: When the fluid in the pipeline is set in motion, the piezometric head decreases as distance from the static head increases. This drop is due to the viscous forces and friction between the fluid and the pipe wall. Note the difference in hydraulic gradient between this figure and Figures 2.1 and 2.2. *TYP* is short for Typical. Figure adapted from the *Practical Hydraulics Handbook*, reference [7].

2.1.2 Total Hydraulic Head

The hydraulic pressure in a pipeline can be expressed two ways: feet of head or in pounds per square inch. PSI is useful when considering localized effects such as pressure drops and equipment ratings. Head is useful for pipeline applications as it normalizes the effects of position, gravity, kinetic energy, and friction. The total hydraulic head at any point in a system is the sum of the elevation, pressure, and velocity heads. The Bernoulli equation formulates these effects as follows:

$$h_{total} = z + \frac{p}{\rho g} + \frac{v^2}{2g} \tag{2.1}$$

where h_{total} is the total or energy head, z is the elevation (typically feet) above the datum, p is the in situ pressure, ρ is the fluid density, g is the acceleration due to gravity, and v is the differential velocity of the fluid.[7][8] One of the implications of Bernoulli's equation and the conservation of energy is that the total energy of an ideal hydraulic system remains constant.[9]

The Bernoulli equation can be adapted for pipeline use by including a fourth head term, frictional head losses:

$$h_{total} = (h_e + h_p + h_v) - h_f \tag{2.2}$$

where h_p is the pressure head, h_e is the elevation head, h_v is the velocity head and h_f is the friction head loss.[7] Combining Equations 2.1 and 2.2 yields simple expressions for each component of the total head.

Elevation head:

$$h_e = z \tag{2.3}$$

Pressure head:

$$h_p = \frac{p}{\rho g} \tag{2.4}$$

Velocity head:

$$h_v = \frac{v^2}{2g} \tag{2.5}$$

where h_x is the component of total hydraulic head in feet, p is the pressure, ρ is the fluid density and, g is the acceleration due to gravity. A common simplification of Equation 2.4 is:

$$h = \frac{p}{0.433\lambda} \tag{2.6}$$

where p is the pressure in pounds per square inch and λ is the specific gravity of the fluid[3].[10][8] The frictional head loss h_f will be developed in Section 2.2.

The velocity head is only applicable when the fluid velocity changes within the pipeline. This typically occurs when the pipe size changes. Ignoring short sections of smaller diameter piping at the Pump Stations and assuming incompressible flow with no slackline effects, the velocity head term can be assumed to be zero as the pipe diameter does not appreciably change. Equation 2.2 can be simplified for this project to:

$$h_{total} = (h_e + h_p) - h_f \tag{2.7}$$

If the total hydraulic head of the pipeline and the pipeline elevation are plotted against pipeline length, a *hydraulic gradient* is formed. The hydraulic gradient slopes

[3]Specific gravity is the ratio of the density of the fluid to the density of water at the same conditions: $\lambda = \rho_{sample}/\rho_{water}$. It is standard practice to normalize values to water given its ubiquity in industrial processes.

down in the direction of fluid flow as depicted in Figure 2.3. This is a useful graphical depiction of the hydraulic state of the pipeline:

1. h_e: From the datum to the center line elevation of the pipeline is the potential energy due to fluid position. This is the potential energy with respect to elevation as a consequence of gravity.

2. h_p: Pressure is the force exerted by the in situ fluid. From the pipeline center line elevation to the hydraulic gradient is the pressure energy due to pressure.

3. h_v: Above the hydraulic gradient to the total energy of the system is the *kinetic energy.*

4. The slope of the hydraulic gradient is the head loss due to friction h_f.

2.2 Calculation of the Frictional Pressure Drop

2.2.1 Classification of Fluid Flow

When crude oil is produced from a reservoir it typically undergoes changes in pressure and temperature. Reservoir conditions are almost always at higher pressures and temperatures than those at standard or *stock tank* conditions of 60°F and 14.7 PSIA. Depending on the specific composition of the crude oil, gas is liberated from the oil when the pressure drops below the *bubble point.* This is the pressure at which bubbles of gas begin to form within the liquid oil phase.

2.2.2 Single versus Multi-phase Flow

Single-phase flow occurs when no gas is present in the flow of oil while *multi-phase* flow occurs when gas is present[4]. A single-phase system operating at pressures above

[4]Multi-phase flow can also refer to the presence of water or solids mixed with the oil. Water and crude oil are immiscible. Flow with oil, water and gas present can also be referred to as *three-phase* flow and is typically present during initial production and separation.

the bubble point can become a multi-phase system if the pressure drops below the bubble point. If the pressure of this system then increases above the bubble point, the gas will re-entrain back into the liquid. The system then returns to single-phase. Although TAPS was designed for single-phase flow, multi-phase flow occurs under specific conditions which will be discussed in Section 2.3.

2.2.3 Laminar versus Turbulent Flow

Flow can be characterized as *laminar* or *turbulent*. The laminar regime lacks flow perpendicular to the direction of bulk flow. In a cross section of laminar fluid all laminae are moving in the same direction. Turbulent fluid flow has significant flow perpendicular to the direction of bulk flow. A cross section of turbulent flow has eddy current flowing in every direction.[11] Laminar or turbulent flow regimes have significant impacts on the frictional pressure losses.[8]

Flow is characterized as either laminar or turbulent by the Reynolds number which is calculated by:

$$R_e = \frac{vd\rho}{\mu} \tag{2.8}$$

where R_e is the Reynolds number, v is the bulk fluid velocity, d is the internal pipe diameter, ρ is the fluid density, and μ is the dynamic viscosity in poise[5].

Accounting for the thickness of the pipe wall (0.462 or 0.562 inches with the telescoping design), the internal diameter of the 48 inch mainline pipe is either 47.076 or 46.876 inches, yielding cross-sectional areas of 11.98 or 12.09 feet^2. At a nominal flow rate of 500,000 BBL/day the bulk fluid velocity is 2.70 feet/second. As discussed in Section 1.3 pipeline are highly variable with data from 2018 shown in Table 2.1.

When the Reynolds number is less than 2000, the flow is considered laminar. A

[5]The dynamic viscosity (units of poise) is equal to the kinematic viscosity (units of stokes) multiplied by the fluid density, $\mu_{dyn} = \mu_{kin}\rho$.

Table 2.1: Pipeline throughput at East Meters on the VMT in 2018.

Metric	Unit	Mean	Std. Dev.	Min	Max
East Meters incoming	BBL/day	19,947	3,134	0	43,238

Reynolds number greater than 2500 is considered turbulent. The region between the two Reynolds numbers is the transition region: partially laminar, partially turbulent. The pressure drop due to friction of fluid in a pipeline is directly correlated to the flow regime and is therefore of great importance when calculating the hydraulic gradient.

2.2.4 Crude Oil Density

The density of North Slope crude oil in TAPS is a linear function of crude temperature:

$$\rho = \rho_{oil60}(1 + \beta(60 - t)) \tag{2.9}$$

where ρ is the calculated density, ρ_{oil60} is 0.8615 grams/cm^3, the density at standard conditions, β is the thermal expansion coefficient 0.000461/°F, and t is the in situ temperature of the crude oil in °F.

Crude oil temperatures received at the VMT vary depending on throughput, ambient outdoor temperatures and heat added to the crude oil at strategic points along the pipeline. To ensure that any water entrained with the oil does not freeze, the target crude temperature in the pipeline is 37°F. In 2018 the average temperature of oil received at the VMT was 53°F with a range from 39°F to 65°F. Using Equation 2.9 the average density of 53°F oil received at the VMT is 0.864 grams/cm^3.

Equation 2.8 is plotted against temperature with 2.9 in Figure 2.6.

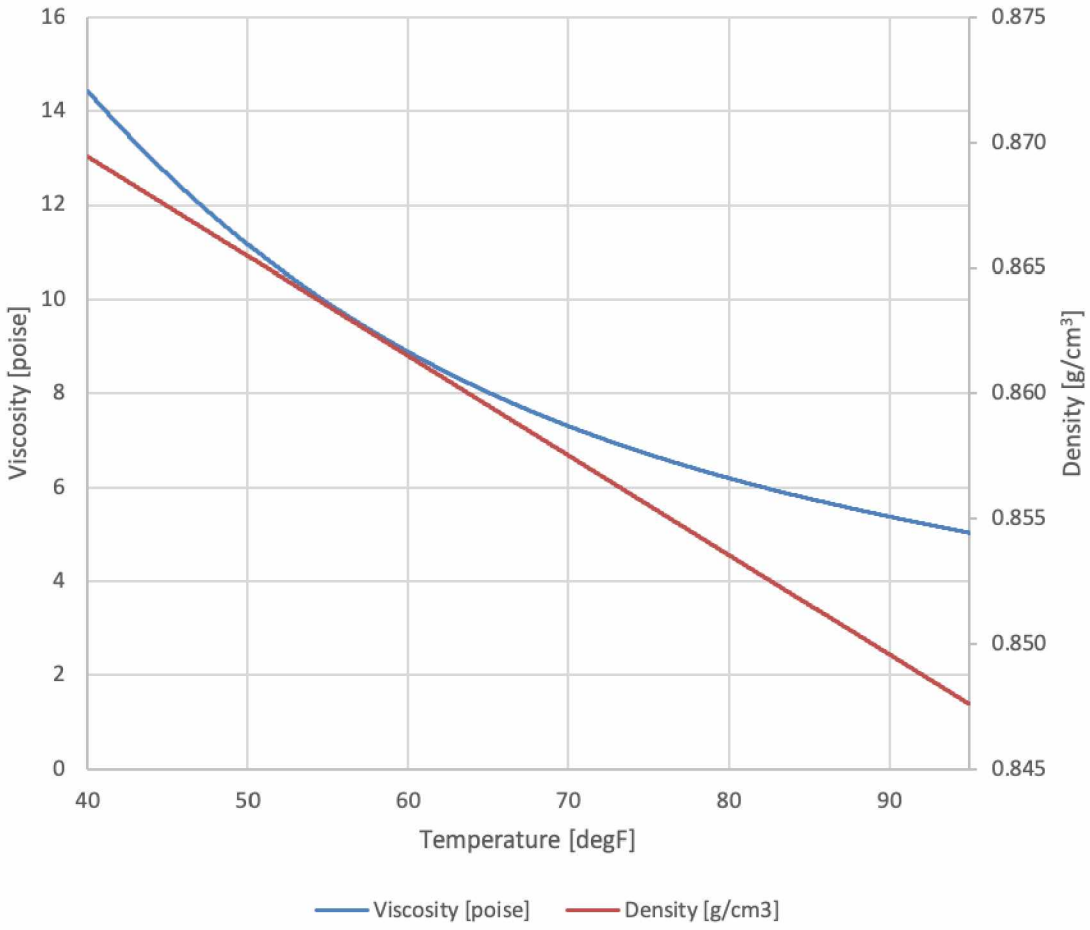

Figure 2.4: Plot of the dynamic viscosity and density versus temperature as calculated by Equations 2.10 and 2.9.

2.2.5 Crude Oil Viscosity

From linear regression of viscosity test data, a fourth-order polynomial provides an excellent correlation ($R^2 > 0.999$) of dynamic viscosity to temperature:

$$\mu = 44.93 - 1.26t + 1.59 \cdot 10^{-2}t^2 - 9.51 \cdot 10^{-5}t^3 + 2.16 \cdot 10^{-7}t^4 \tag{2.10}$$

where μ is the dynamic viscosity in poise, and t is the crude temperature in °F. Using Equation 2.10 the average dynamic viscosity of 53°F oil received at the VMT is 10.4 cP. Equations 2.10 and 2.9 are plotted against temperature in Figure 2.4.

With Equations 2.9, 2.10, and 2.9 the Reynolds number can be calculated using

Equation 2.8. The average Reynolds number is 86,500 at the VMT, well into the turbulent region. In practice the flow regime in TAPS is always turbulent flow. Laminar flow only occurs when pipeline throughput is approximately 100,000 BBL/day or less.

2.2.6 Fanning Pressure Drop

To calculate the frictional pressure drop, the Fanning equation is used:

$$\Delta p_f = \frac{2 f_f \rho v^2 L}{g d} \tag{2.11}$$

where Δp_f is the frictional pressure drop, f_f is the unit-less Fanning friction factor[6], L is the length of the pipeline segment, g is the acceleration due to gravity, and d is the interior dimension of the pipe.[8] Calculating the friction factor is dependent on the flow regime: laminar and turbulent flows use different equations. The laminar Fanning friction factor is calculated by:

$$f_f = \frac{16}{R_e} \tag{2.12}$$

where f_f is the Fanning friction factor and R_e is the Reynolds number. With turbulent flow, the Fanning friction factor is implicitly calculated by the Colebrook-White equation:

$$\frac{1}{\sqrt{f_f}} = -4 \log \left(\frac{\varepsilon}{3.7065} + \frac{1.2613}{R_e \sqrt{f_f}} \right) \tag{2.13}$$

where the roughness of the pipe ε is calculated by:

$$\varepsilon = \frac{k}{d} \tag{2.14}$$

[6]The Fanning friction factor is 1/4 of the Darcy-Weisbach friction factor f_D. Equations 2.12 and 2.13 have the same form but scaled coefficients when f_D is used

Figure 2.5: An exposed (uninsulated) section of 48 inch pipe at Pump Station 8. The surface roughness as calculated by Equation 2.14 is visible.

where k is the size of the surface features protruding from the pipe wall and d is the internal diameter of the pipe in inches.[12] The pipe roughness of 48 inch pipe is approximately $\varepsilon = 0.0018$[7]. This surface texture is readily felt on the inside and outside of the pipe.

As f_f appears on both sides of Equation 2.11, the equation must be solved using numerical methods such as Newton-Raphson[8]. An explicit version of Equation 2.13 to ease computation is the Chen equation:

$$\frac{1}{\sqrt{f_f}} = -4\log\left(\frac{\varepsilon}{3.7065} - \frac{5.0452}{R_e}\log\left(\frac{\varepsilon^{1.1098}}{2.8257} + \left(\frac{7.149}{R_e}\right)^{0.8981}\right)\right) \tag{2.15}$$

[7]Pipe roughness is not measured directly from pipe materials.

[8]Newton-Raphson is a numerical method to find the root of a function. It takes the form

$$x_1 = x_0 - \frac{f(x_0)}{f'(x_0)}$$

where f is the function, x_0 is a guess for the root and f' is the derivative of f. Iteration continues until convergence on a root.

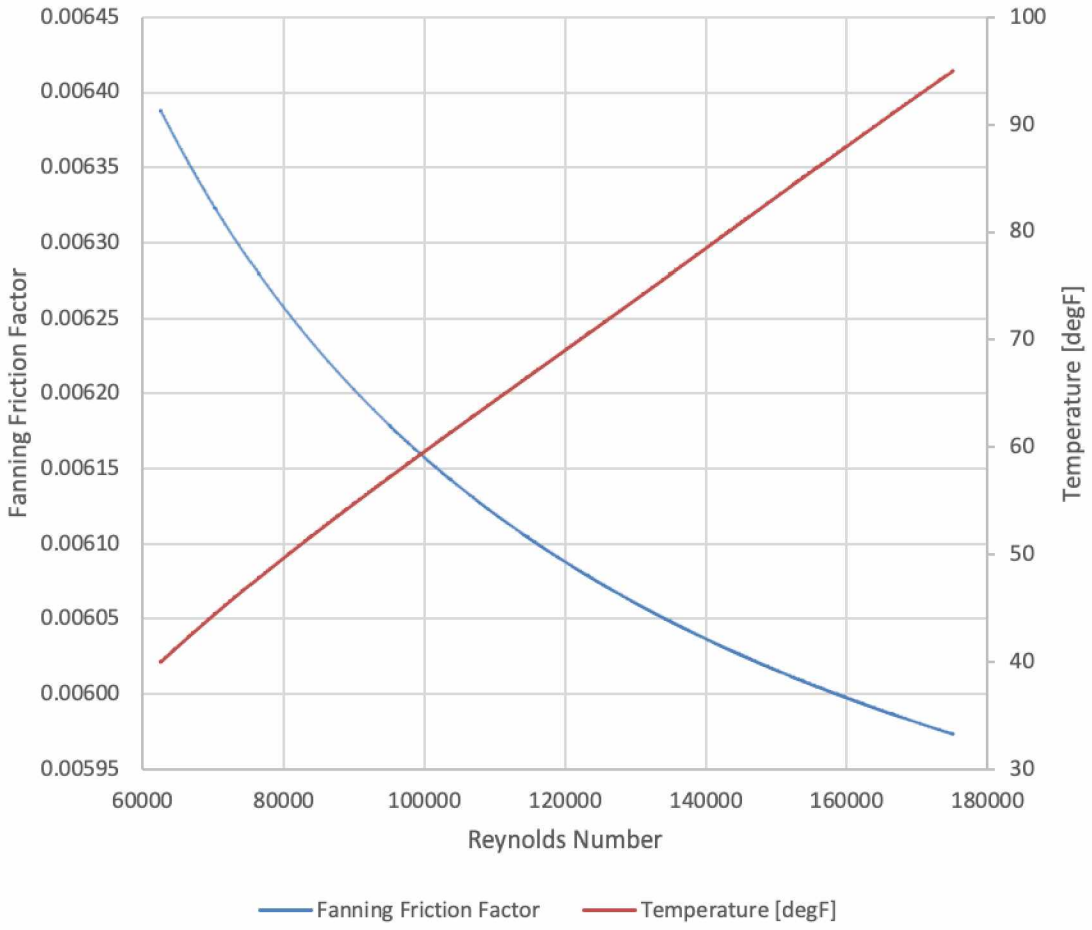

Figure 2.6: Plot of Equation 2.15 versus the expected range of Reynolds numbers (Equation 2.8) at VMT incoming. The Reynolds number is a function of density and viscosity, therefore for a constant crude composition the Fanning friction factor is a function of temperature.

The average Fanning friction factor calculated using Equation 2.15 and an average Reynolds number of 86,500 is 0.00622 (both value are unit-less). Values of the Chen equation are plotted in Figure 2.6 over the expected range of Reynolds numbers at VMT incoming.

Equation 2.11 can now be used to calculate the average frictional pressure drop of the 48 inch pipe at 53°F of 1.596 psi/mile. This pressure drop is converted to feet of head to construct a hydraulic gradient using Equation 2.4, $h_p = \frac{p}{\rho g}$ is 4.265 feet per mile. With this data a hydraulic gradient can be drawn as shown in Figure 2.7.

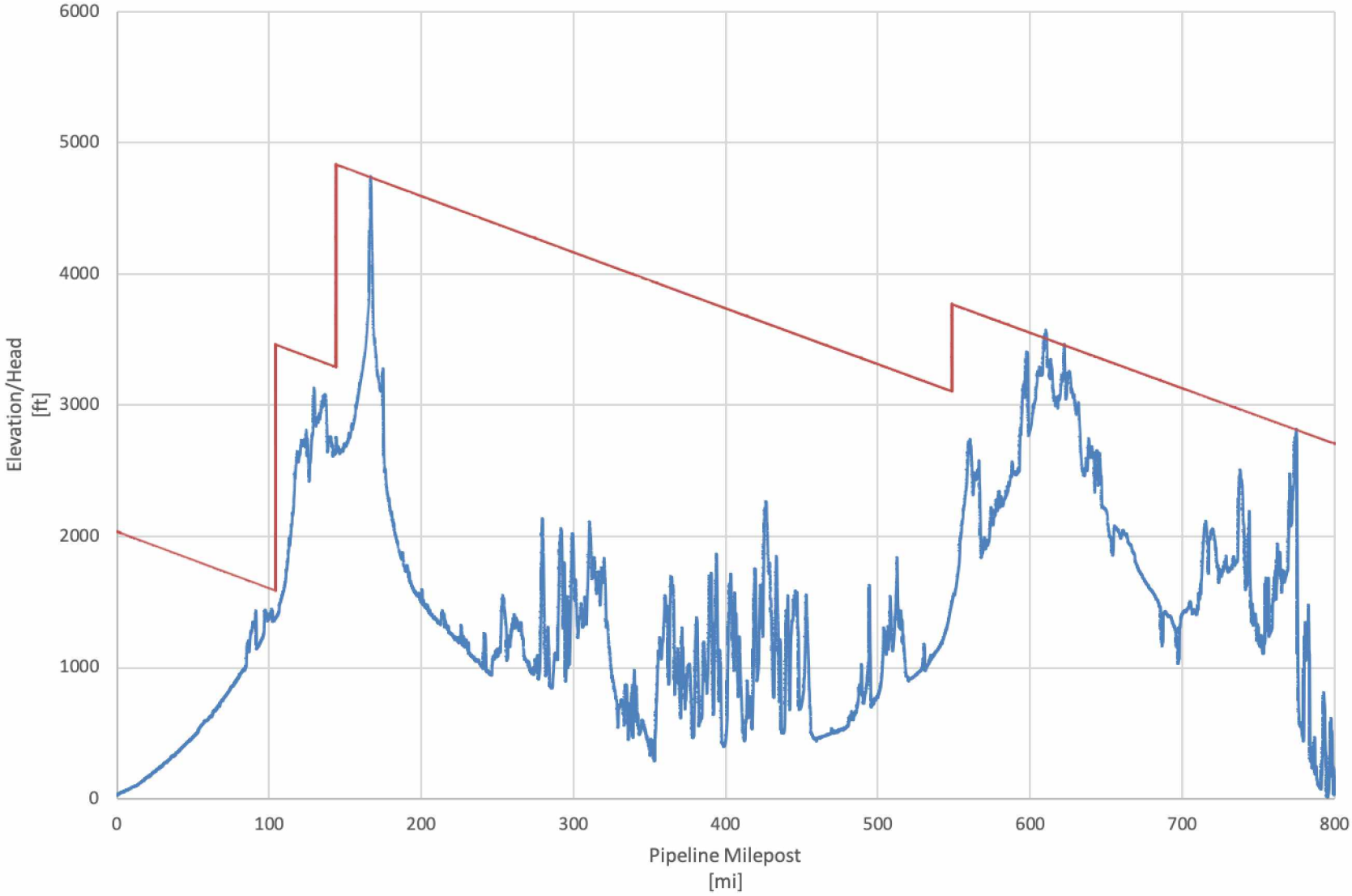

Figure 2.7: Calculated TAPS hydraulic gradient by application of Equations 2.11 and 2.15. Note that the effect of slackline is not included in this plot. This is a demonstration of the frictional effects behind the development of the hydraulic gradient.

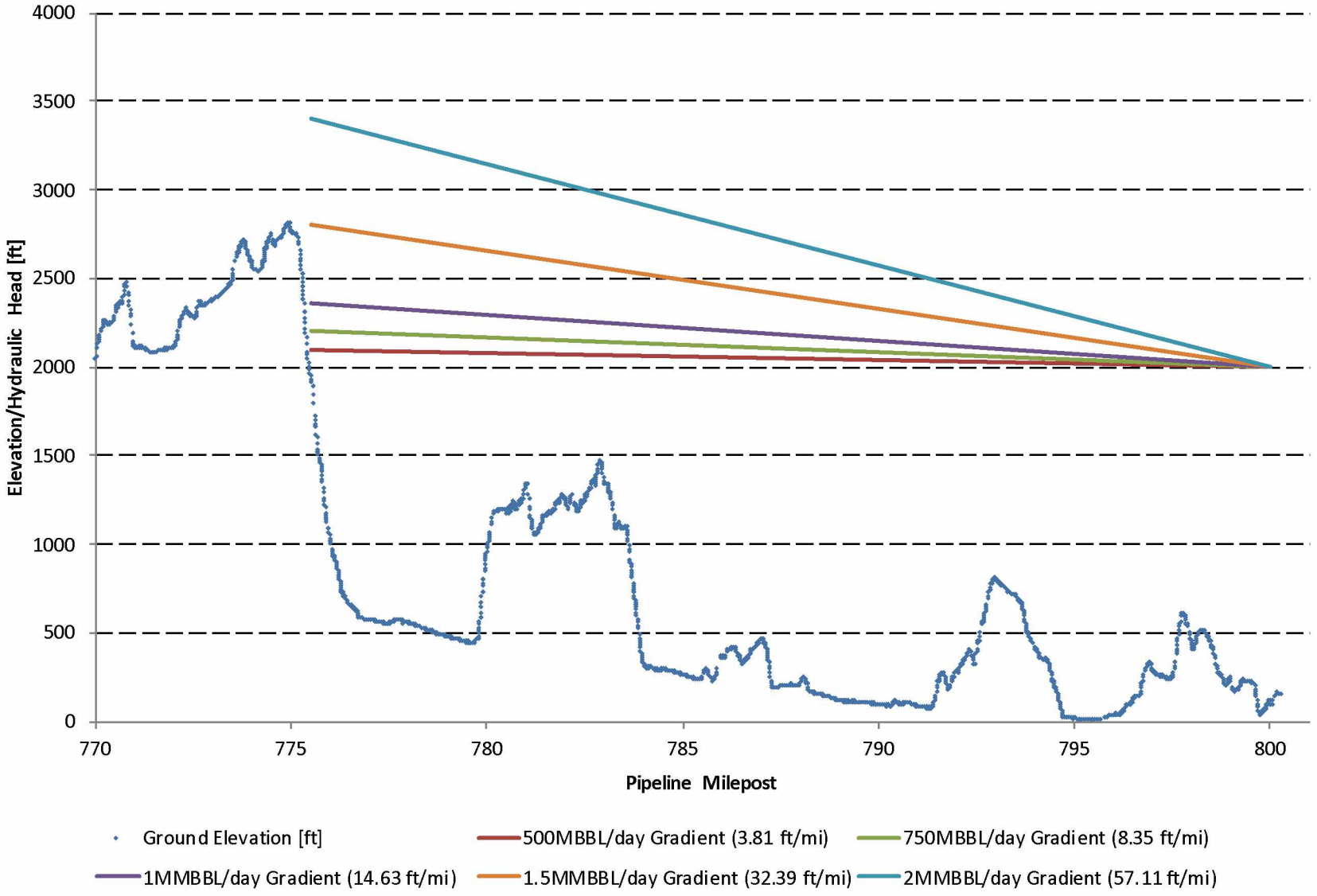

Figure 2.8: Calculated hydraulic gradient in Thompson Pass by application of Equations 2.11 and 2.15 at various flow rates.

It is important to remember that these are average values. Variations in throughput and temperature will change the frictional pressure drop throughout the year. The coefficients in Equations 2.9, 2.9, and 2.10 are based on a sample of crude oil at a specific point in time. The crude oil in TAPS is the summation of all the individual crude streams produced on the North Slope. The commingled composition changes with field production strategies and slug flow. The coefficients in Equations 2.9, 2.9, and 2.10 must be updated with periodic sample draws.

2.3 Slackline and Backpressure Control

With the frictional pressure drop calculated, the conditions at VMT incoming can be reviewed. The pipeline route over Thompson Pass drops for over two thousand feet in Figure 2.12. The elevation profile of the pipeline from the peak of Thompson Pass to the pipeline terminus is shown in Figure 2.8.

Slackline is a phenomena that occurs in closed piping systems where the in situ pressure in the pipe drops below the bubble point of the fluid. On the pipeline hydraulics plot this is where the hydraulic gradient is lower than the elevation of the pipeline. This forms a zone of gas in the pipe yielding two-phase flow. When the pressure increases above the fluid bubble point pressure (the hydraulic gradient is greater than the center line elevation of the pipeline), the process reverses. Gas re-entrainment back into the liquid can be violent and unpredictable, potentially creating pressure pulses that propagate through the pipeline. These pressure pulses can fatigue and ultimately fracture pipe steel or welds. The phenomena is particularly challenging to manage in above-ground sections of the pipeline where lateral restraint is limited and the pipeline was explicitly designed to move[9]. TAPS is particularly susceptible to the propagation of pressure pulses given that 420 miles of the pipeline is installed above ground on vertical support members. It is therefore preferable for

[9]Movement induced by seismic activity, permafrost, thermal expansion etc. See Figure 1.1.

the slackline or vapor-liquid interface to occur in buried sections of the pipeline where lateral restraint is maximized.[7][3]

Slackline typically occurs on the downward slopes of mountain passes. Notable examples on TAPS are at Atigun Pass and Thompson Pass. To maintain slackline conditions in the buried sections of Thompson Pass, a pressure control system was installed to maintain the incoming pressure at the VMT as high as possible. The system is referred to as *backpressure control*. When the backpressure control system is operating, the slackline interface is moved further up Thompson Pass to a stable, buried region.

Shown in Figure 2.2b the backpressure system consists of five control valves connected to common high and low-pressure headers. These valves are located at the VMT within the East Meters facility shown in Figure 2.11. The flow rate through the valves is throttled to maintain a constant incoming pressure of 750 PSI and an outlet pressure of 150 PSI for a total differential of 600 PSI. As the elevation of the VMT tank farm is above the backpressure control valves, 150 PSI is sufficient to overcome the static head pressure of a full tank.

Figure 2.9 demonstrates how the slackline interface can be moved up or down Thompson Pass by adjusting the incoming pressure at East Meters. This plot was calculated by application of Equations 2.11 and 2.15.

2.4 HPRT Integration with Backpressure Control

The necessity to maintain a 600 PSI pressure differential at VMT incoming for control of slackline presents a potential energy source to harness. As will be discussed in Chapter 3 the potential energy recovery is directly proportional to the pressure differential and fluid flow rate.

Today the energy released by dropping pressure across the valves is converted to heat. This is readily observed by monitoring the temperature of the incoming oil at

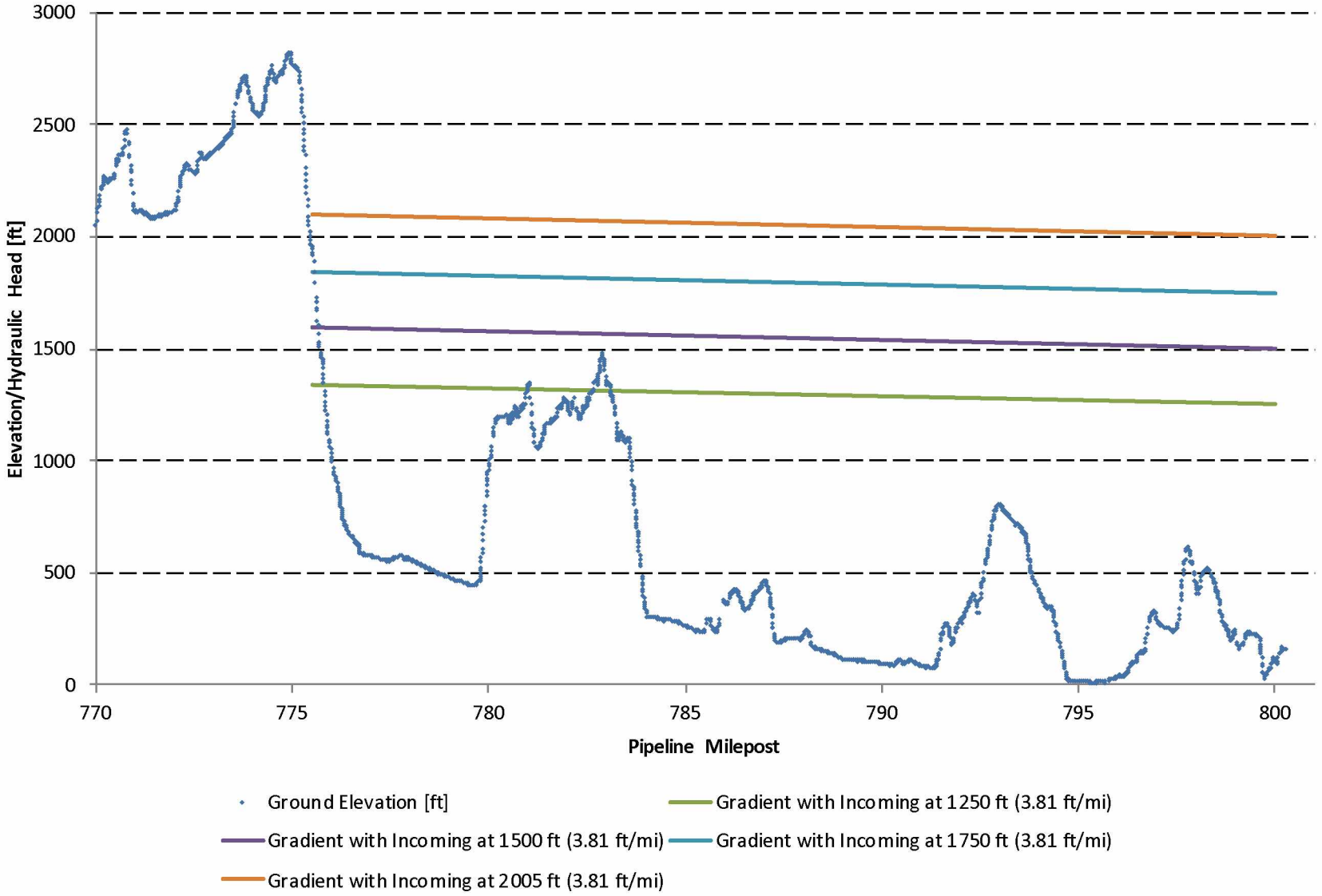

Figure 2.9: Calculated hydraulic gradient in Thompson Pass by application of Equations 2.11 and 2.15 at various incoming pressures at the VMT. Notice how the slackline interface can be moved up or down Thompson Pass by adjusting the incoming pressure at the VMT.

Figure 2.10: Satellite imagery of Atigun Pass, the highest point along TAPS. North is up. The pipeline generally follows the path of the Dalton highway as it crosses Atigun. Three pump stations are necessary to move oil over the pass from the North Slope. Image data: Google

Figure 2.11: Satellite imagery of the East Meters facility, center, at the Valdez Marine Terminal. Orientation: North is up. The proposed location for installation of the HPRT and supporting infrastructure is within East Meters. Image data: Google

Figure 2.12: Photo taken at approximately pipeline milepost 775 (see figure 2.8) near the top of Thompson Pass looking South-West towards the Richardson Highway and the Lowe River. The steep incline of the pass is readily apparent.

East Meters against the temperature of the oil in the storage tank being filled. The tank temperature will be five to seven degrees warmer than the incoming temperature.

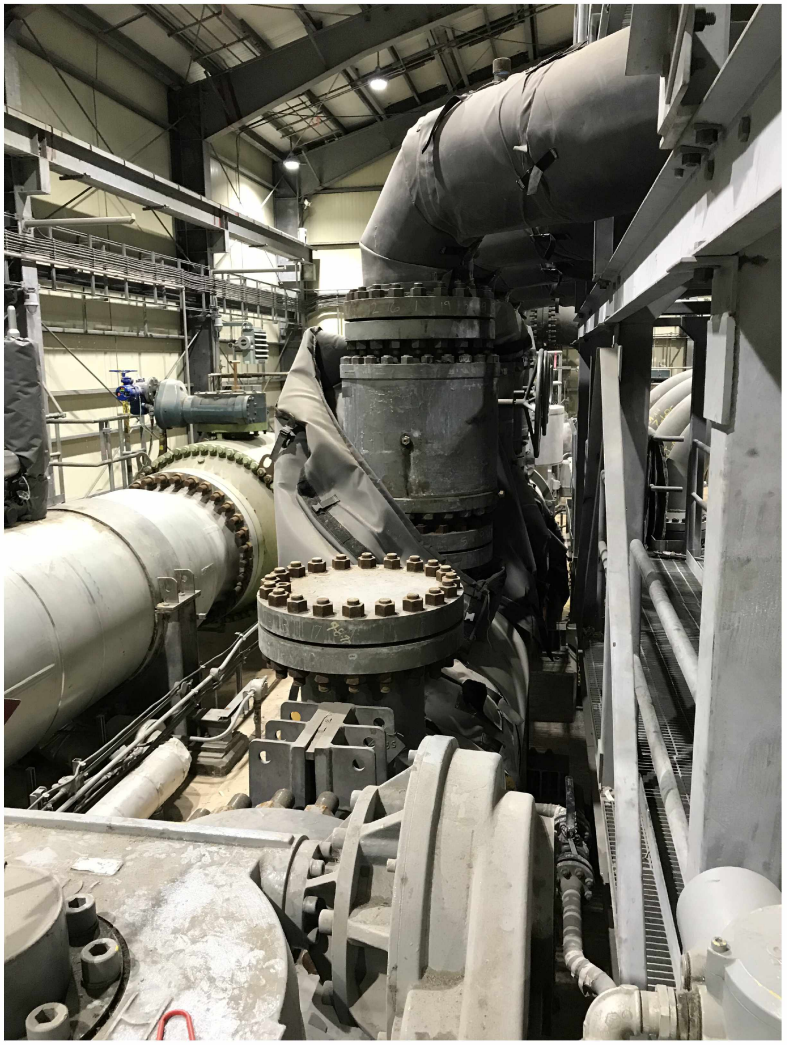

(a) One of the backpressure control valves and a spare flange where an HPRT could be installed.

(b) Lineup of the five backpressure control valves.

Table 2.2: Backpressure control valves used to maintain the 600 PSI pressure differential between VMT incoming and pressure to the tank farm.

CHAPTER 3
HYDRAULIC MACHINES

A hydraulic machine converts mechanical energy to hydraulic energy or vice versa. A machine that converts mechanical energy to hydraulic energy is called a *pump*. A machine that converts hydraulic energy to mechanical energy is called a *hydraulic turbine*.[9] Any process that throttles the flow of liquid from a high pressure to a lower pressure—a common occurrence in transportation and refining of hydrocarbon—is a candidate for an HPRT.

This is accomplished using control valves where flow is modulated to maintain a constant pressure differential across the valve. With the conservation of energy, the temperature of the fluid on the discharge side of the valve increases due to viscous friction.[13] Depending on the specifics of the process, this conversion of hydraulic energy to heat may be advantageous or inefficient. For example, under the current configuration of Pump Station 7, a turbine pump is used to develop a pressure differential across a special drag control valve. As crude oil is forced through the tortuous paths within the valve, the temperature of the crude oil increases as the pressure drop increases. This additional heat can help prevent the formation of ice particles from water entrained with the oil during the winter. An example of the stacks assembled to create the tortuous paths is shown in Figure 3.1a and 3.1b.

At the VMT where crude oil is immediately placed into storage prior to loading on a ship, there is no benefit gained by adding heat to the oil. As discussed in Chapter 2, slackline must be maintained on the downward slope of Thompson Pass. The backpressure control valves (as shown in Figure 2.2b) used to perform this task continuously modulate to maintain a 600 PSI pressure differential across the valves. As expected from this pressure drop, the temperature of the crude oil flowing into the

tank farm increases in temperature by approximately 5°F. To develop a controlled pressure drop and employ the energy for productive purposes, a centrifugal pump operating in reverse can be utilized. From the basic hydraulic theory developed in Chapter 2, characteristics of the turbine will be selected.

3.1 Hydraulic Turbine Properties

To ensure reliable operation, the hydraulic machine must be correctly specified. This is particularly relevant when pumping fluids with bubble points near ambient conditions. Although the oil delivered to Pump Station 1 is degassed[1] by the North Slope producers, two-phase flow can develop within centrifugal pumps. When the impeller cuts through a fluid, a region of low pressure is developed on one side of the blade. If the pressure is below the bubble point, bubbles develop and then migrate through the pump. The expansion and subsequent contraction of these bubbles back into liquid is called *cavitation*[2]. If the situation is not corrected, extensive damage to the impeller, volute and bearings can result.[9]

3.1.1 Hydraulic Machine Selection

Selection of pump or hydraulic turbine requires the same basic data. This application is based on 2018 VMT crude oil data:

1. Type of liquid: single-phase crude oil.
2. Temperature: Average 53°F with a range from 37°F to 70°F.
3. Viscosity: Average of 10.4 cP with a range from 15.7 cP at 37°F to 7.3 cP at 70°F using Equation 2.10.

[1]This process in occurs in pressure vessels called "separators" where fluid is introduced at the the desired pressure. For degassing to atmospheric conditions, the separator operates at approximately 14.7 PSIA.

[2]Cavitation is often described as "pumping gravel". Pump manufacturers provide Net Positive Suction Head (NPSH) curves that specifies the minimum suction pressure a pump can tolerate without cavitation for a specifc fluid. Low suction pressure can be caused by clogged strainers.[14][9]

4. Density: Average of 0.864 g/cm^3 with a range from 0.871 g/cm^3 at 37°F to 0.858 g/cm^3 at 70°F using Equation 2.9.

5. Speed: Specify nominal hydraulic performance for 1800 RPM and bearings for 3600 RPM. In the event of an over-speed condition the bearings are protected from damage. An over-speed condition can occur if the electric generator is suddenly disconnected from the power system or all synchronous machines trip offline.

6. Capacity: Performance of the hydraulic machine will be optimized for this capacity. Flow rates above or below this value will impact machine performance and efficiency. If the single turbine configuration is selected, a nominal flow rate of 16,000 GPM would accommodate expected pipeline flow rates over the next decade[3].

7. Total Dynamic Head: total hydraulic head across the machine, an adaption of Equation 2.4:

$$h_{TDH} = \frac{p_2 - p_1}{\rho g} \tag{3.1}$$

where h_{TDH} is the total dynamic head in feet, p_2 is the pressure in pounds per square inch on the machine inlet, p_1 is the pressure in pounds per square inch on the machine outlet, ρ is the fluid density and, g is the acceleration due to gravity. Maintaining a constant 600 PSI pressure differential as the crude oil density varies, the total dynamic head ranges from 1589 feet to 1613 feet. An average of 1600 feet is therefore a reasonable selection.

8. Efficiency: The machine is selected to optimize hydraulic efficiency based on

[3]The estimates of crude oil production calculated in the *Production History and Forecast by Production Area from Fall 2017 Revenue Sources Book* prepared by the Alaska Department of Revenue is used to estimate future flow rates: http://www.tax.alaska.gov/sourcesbook/AlaskaProduction.pdf

the aforementioned characteristics.

Pump curves from one manufacturer based on the aforementioned operating conditions is shown in Figure 3.1. Selection of a particular machine is ultimately a compromise between the range of acceptable flow rates, efficiency, and power output.

3.2 Hydraulic Power

The classic equation used in hydro power applications is:

$$p = qhg \tag{3.2}$$

where p is the power output, q is the flow rate, h is the available hydraulic head across the machine, and g is acceleration due to gravity. As Equation 3.2 assumes the fluid is water, specific gravity $\lambda = 1.0$ is therefore omitted for clarity.[9] Note that this equation is applicable to pump or turbine configurations as they are the same machine.

In crude oil service where the density is not equal to that of water, ρ is included:

$$p = qhg\rho \tag{3.3}$$

where ρ is the fluid density. A common adaptation of Equations 3.2 and 3.3 is:

$$p = \frac{qh\gamma}{3960} \tag{3.4}$$

where p is the power output in horsepower (convenient for pump prime mover sizing), q is flow rate in gallons per minute and γ is the specific gravity. Expressing p in kW (convenient for turbine electrical power output calculations) yields:

$$p = \frac{qh\gamma}{5310} \tag{3.5}$$

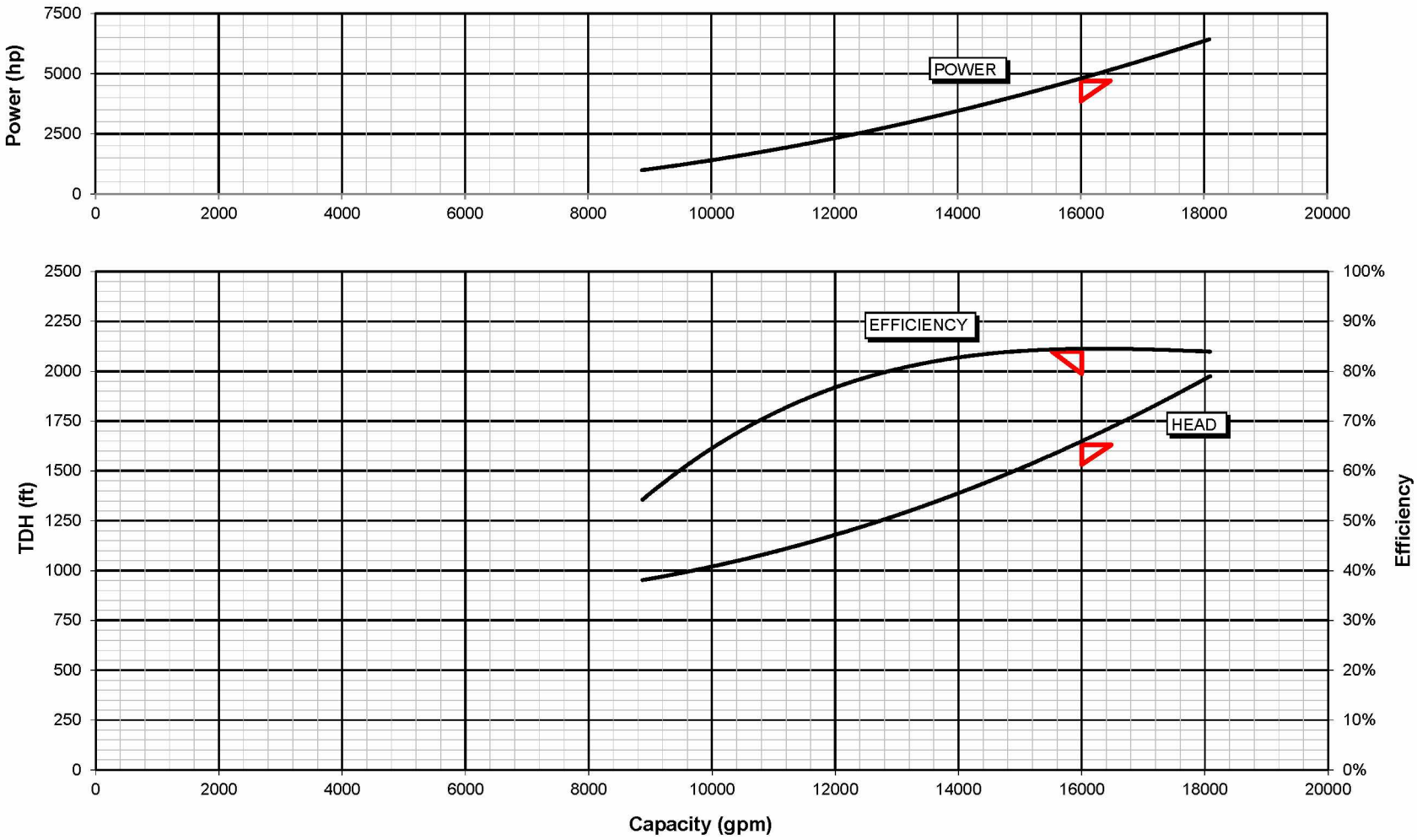

Figure 3.1: Pump curves for an actual hydraulic turbine specified for TAPS crude oil.

These equations do not account for inefficiencies of the energy conversion process. The power available to recover from an HPRT in crude oil service accounting for fluid density, turbine and generator inefficiencies is:

$$p = \frac{qh\gamma\eta_m\eta_e}{5310} \tag{3.6}$$

where p is the power output in kW, q is flow rate in gallons per minute, h is the differential hydraulic head in feet, η_m is turbine efficiency, η_e is the generator efficiency and γ is the specific gravity of the fluid.

From Equation 3.6 the power output is directly proportional to pipeline throughput and fluid density. As previously calculated using Equation 2.9, the specific gravity can vary from 0.871 g/cm^3 at 37°F to 0.858 g/cm^3 at 70°F with an average of 0.864 g/cm^3.

At an average pipeline flow rate of 500,000 BBL/day the energy resource (assuming $\eta_m = 1.0$ and $\eta_e = 1.0$) is 3.81 MW and ranges from 2.29 MW at 300,000 BBL/day to 5.72 MW at 750,000 BBL/day[4]. Accounting for turbine and generator inefficiencies these values will be less. Comprehensive tabulated HPRT power outputs are presented in Section 6.1.

[4]When pipeline throughput peaked at 2.1 million BBL/day the energy resource was in excess of 12 MW.

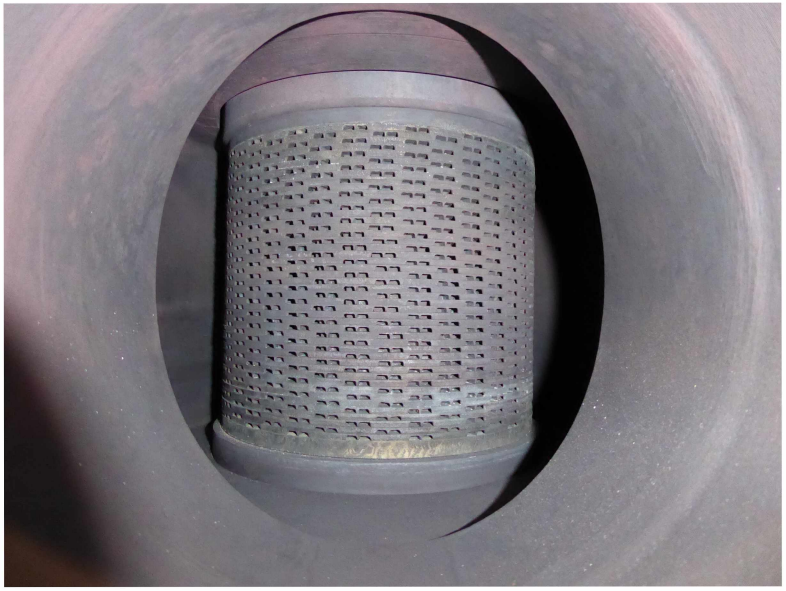

(a) Drag valve with the stack installed.

(b) Drag valve stack removed from the valve. Each hole follows a tortuous path to the other size of the stack.

Table 3.1: A drag valve from Power/Vapor in 600-to-20 PSI steam letdown service that is being rebuilt.

CHAPTER 4

OPERATION OF THE VMT POWER AND VAPOR SYSTEM

This study of pipeline hydraulics and turbine characteristics has identified the characteristics of the HPRT prime mover. To perform useful work, the shaft of the turbine is coupled to another machine, an electric generator in this application. Before the characteristics of the generator can be delineated, the vapor management and power generation systems at the VMT must be understood.

The Power/Vapor facility (P/V) has four core objectives:

1. Safely destroy hydrocarbon crude vapors produced in the tank farm or from a tanker under vapor control during loading operations.

2. Produce inert flue gas to blanket the head space in the tank farm and prevent the ingress of oxygen.

3. Prevent the formation of a pressure differential in each tank with respect to the atmosphere.

4. Generate electricity for use across the VMT.

The facility is visible in Figure 1.2, located directly between the East and West tank farms. A simplified process diagram of the vapor management system is shown in Figure 4.1. A review of the crude oil and vapor recovery infrastructure tied to P/V is necessary.

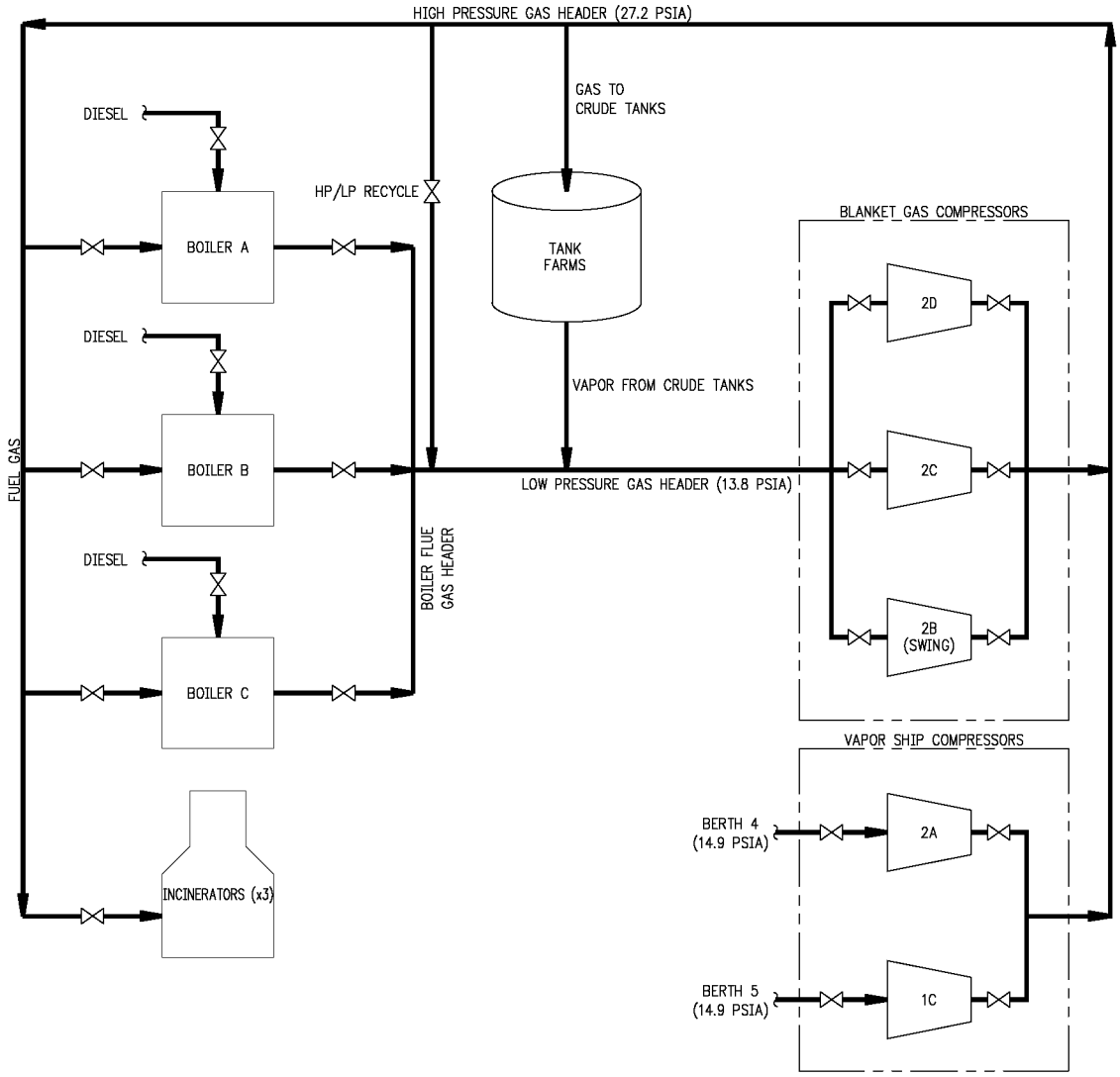

Figure 4.1: Simplified process flow diagram for the Power/Vapor facility. Excluded for simplicity is the steam system, power generation equipment and plant utilities. The entire tank farm is depicted schematically as a single tank as all tanks are tied to the common high- and low-pressure headers.

4.1 Crude Oil Storage

Incoming oil is stored in one of twelve above ground storage tanks[1] at the VMT prior to loading onto ocean-going tankers. At 250 feet in diameter, each tank has a working capacity of 510,000 BBLs. Collectively grouped the tanks form a *tank farm* in industry parlance. The fourteen tanks grouped in Figure 1.2 are known as the *East Tank Farm*. The four tanks to the west are known as *West Tank Farm* and have been taken out of service. The initial design for the VMT called for construction of fourteen tanks in the East Tank Farm and eighteen tanks in the West Tank Farm. A tank farm of that size could have stored one week of production at peak pipeline throughput of two million BBL/day. The fourteen tanks in service today provide approximately twelve days of storage at current throughput.

Storage at the terminus of the pipeline allows TAPS to operate continuously while providing flexibility to tanker shipping schedules. The reliability of TAPS infrastructure from PS1 to the VMT is critically important for the North Slope producers[2]. As most of the oil produced on the North Slope contains some percentage of water prior to separation, it is important to keep production processes online during the winter months to prevent formation of ice plugs. At Pump Station 1 in Prudhoe Bay there is only 420,000 BBL of working storage to buffer North Slope producers against interruptions to pipeline flow, less than 24 hours of production at today's throughput.

4.2 Vapor System

4.2.1 Vapor Pressure

At standard temperature and pressure conditions, crude oil in storage will naturally generate hydrocarbon vapors. This occurs even though the crude delivered to TAPS

[1] Two of the tanks (Tank 1 and Tank 3) are breakout tanks used for pipeline relief and drain-down purposes.

[2] In 2018 the reliability factor for the pipeline was 99.93% per https://www.alyeska-pipe.com.

at Pump Station 1 has been degassed by the North Slope producers to a True Vapor Pressure[3] (TVP) of 14.7 PSIA or below at receipt temperatures. The intent of the TVP specification is to ensure the pipeline operates single-phase at standard conditions and the crude tanks do not become pressure vessels. Typical conditions of receipt at Pump Station 1 are 14.2 PSIA or less.

4.2.2 Pipeline and VMT Vapor Sources

The pipeline and the pump stations are designed and permitted to accommodate crude oil with a TVP of up to 14.7 PSIA. With the exception of Pump Station 1 where a flare is installed in conjunction with the two crude balancing tanks, each active pump station has a *breakout* tank that is used to depressurize the pipeline during relief events and shutdowns. After crude has been diverted to a breakout tank, the tank is pumped down[4] prior to the pipeline resuming operation to ensure sufficient tank space to accommodate another relief event. A small amount of crude oil is maintained in the bottom of the tanks to prevent the ingress of oxygen and the formation of an explosive atmosphere within the tank. The static crude height that remains in an empty tank is selected to prevent formation of vapor pockets in the relief piping connecting the tank to the mainline pipe. Breakout tanks are not classified as storage tanks and do not require a system to manage the hydrocarbon vapors.[15]

The VMT air quality permit issued by the Alaska Department of Environmental Conservation (DEC) prohibits the venting of hydrocarbon vapors to the atmosphere. This includes vapors released during loading of tankers.[6] Unlike the breakout tanks at the pump stations, the fourteen tanks in the East Tank Farm are intended for continuous crude storage. As such the vapor system at the VMT was designed to

[3]The True Vapor Pressure is defined in API Publication 2517 and is the method utilized by regulatory agencies to determine the vapor pressure of the crude stream.

[4]Back into the pipeline.

capture and destroy all vapors generated from the crude tanks. The system can accommodate crude oil with a TVP of up to 13.0 PSIA. The TVP specification at the VMT is lower than Pump Station 1 as the crude oil cools during transportation. Cooler oil has a lower TVP.

During the early 1990s additional vapor recovery infrastructure was installed to capture marine vapors produced during tanker loading from Berths Four and Five. This was done to control emissions of VOCs as mandated by the amended Clean Air Act of 1990.[16]. Figure 4.1 shows the compressors used to capture and compress vapors recovered from a tanker. A tanker must be placed under vapor control prior to beginning oil loading operations.

4.2.3 Vapor Wobbe Index

The composition and energy content of the vapor recovered from the tank farm is not static[5]. Each hydrocarbon constituent releases different amounts of energy during combustion. The energy output of the commingled vapor stream will vary as composition changes. To compare the energy output of vapors with varying compositions the Wobbe Index (WI) is used. The WI determines the degree of interchangeability between different sources of gas. As an example 1 SCF of recovered vapor X may provide 500 BTU while recovered vapor Y provides 700 BTU. Vapor stream Y requires a lower mass flow rate to maintain the same heat rate compared to X. For the control system managing the thermal input to the combustion boilers, accurate calculation of the WI is necessary to maintain predictable steam production. The WI is calculated by:

$$WI = \frac{HV}{\sqrt{\lambda}} \tag{4.1}$$

where WI is the Wobbe Index, HHV is the heating value in BTU/scf and λ is the

[5]The composition of crude oil delivered to TAPS at Pump Station 1 is continuously changing.

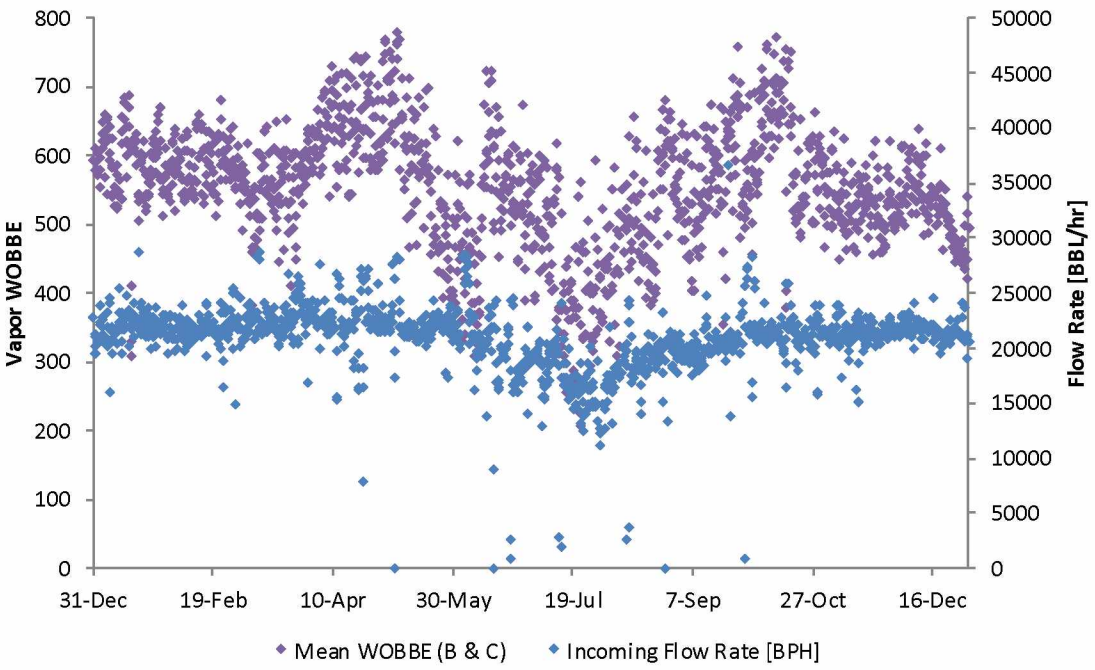

Figure 4.2: Plot of recovered vapor WI and the incoming crude oil flow rate. The WI is the average between boilers B and C.

specific gravity of the gas. This calculation is performed continuously by the control system.

Oil with a higher Gas-to-Oil ratio (GOR) will tend to be more volatile and release more vapor. Blending Natural Gas Liquids (NGLs) with the crude stream will also increase the volatility. Figure 4.3 shows the correlation between the recovered vapor WI and NGLs blended with the crude oil delivered to Pump Station 1. During the summer months when the volume of NGLs drops off on the North Slope, the WI of recovered vapor at the VMT also falls.

The WI is also correlated to pipeline throughput. Figure 4.2 shows the correlation between incoming crude oil flow rate and recovered vapor WI.

4.2.4 Vapor Generation Modeling

Vapor generation from stored crude oil is a function of many interrelated variables. Prediction and modeling is difficult and a rigorous model does not exist for the crude

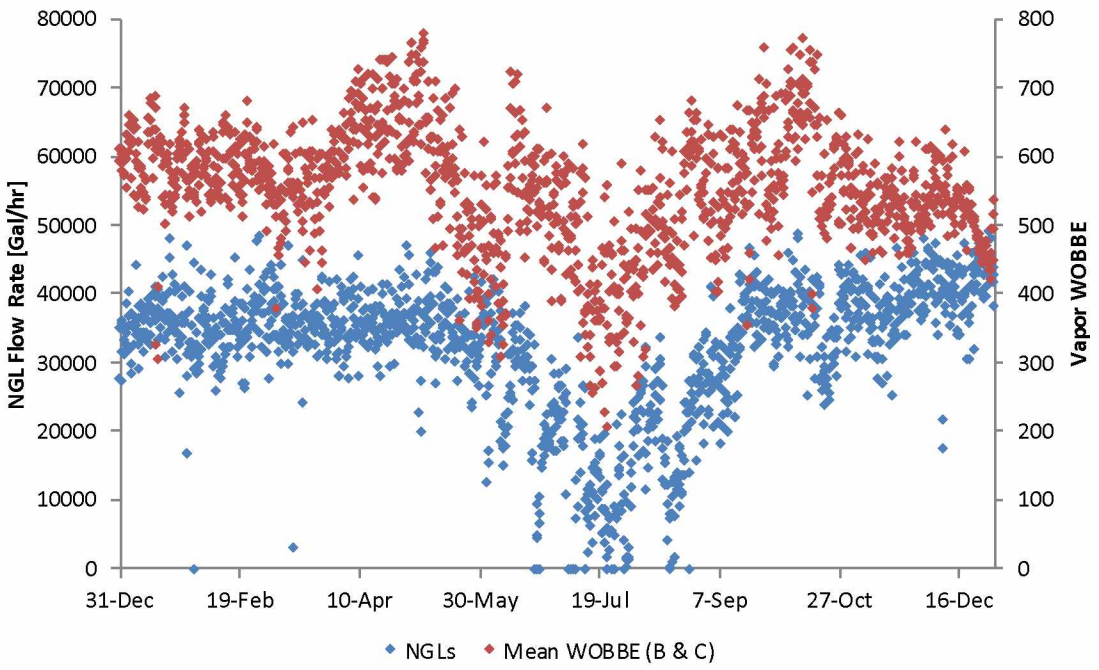

Figure 4.3: Plot of recovered vapor Wobbe Index at the VMT and the volume of blended Natural Gas Liquids delivered to Pump Station 1. The WI is calculated as the average between boilers B and C.

storage tanks at the VMT. To mitigate this uncertainty, vapor management systems are generally oversized by factors of two or more. An oversized vapor systems is not cost effective as the compressors achieve peak efficiency over a narrow operating window. Operating above or below this window increases energy consumption. This effect is visible in the pump curve shown in Figure 3.1 where efficiency drops at volumetric flow rates above or below the specified design (marked by red triangles).

Empirical measurements are useful to understand vapor system behavior. Vapor generation can be modeled as follows:

$$q_{total} = q_{displacement} + q_{flash} + q_{evaporation} - q_{condensation} \tag{4.2}$$

where q_{total} is the total vapor generated, $q_{displacement}$ is the vapor produced by volumetric displacement of crude oil, q_{flash} is the vapor produced by flashing of crude oil or dropping it below its bubble point and $q_{evaporation}$ is the vapor produced from

evaporation at the surface of the crude oil[6]. All units in Equation 4.2 are SCF per unit time (minute, hour etc.).

Total Vapor Generated: q_{total}

On a per-tank or per-tank farm basis q_{total} is the volume of vapor per unit time that must be processed by the vapor management system. This is the value used to size compressors and vapor piping.

Vapor from Displacement: $q_{displacement}$

One barrel of oil occupies 5.615 ft^3. Therefore $q_{displacement} = 5.615 \cdot q_{incoming}$ where $q_{incoming}$ is the crude oil flow rate. Increasing pipeline flow increases the volume of vapor displaced. Unless the tank is being drained during tanker loading operations $q_{total}/q_{displacement}$ will always be at least 1.0 as crude oil is effectively incompressible relative to the vapor. Typical $q_{total}/q_{displacement}$ ratios range from 5 at Pump Station 1 to 1.5–2 at the VMT.

Vapor from Flashing: q_{flash}

This effect is noticeable close to Pump Station 1 where it's possible for crude oil to have true vapor pressures in excess of 14.7 PSIA. The TVP measurements are computed as rolling averages to prevent a producer from being prematurely shut-in[7] for small slugs of off-spec crude. Crude oil with a higher TVP will bubble at standard atmospheric conditions.

[6] Additional terms could also be included for improved accuracy: $v_{absorption}$ is the vapor displaced by being reabsorbed back into the crude oil and $v_{thermal}$ is the vapor displaced by thermal expansion. These terms are omitted for clarity.

[7] Prevented from pumping oil to Pump Station 1 by closing a motor-operated control valve.

Vapor from Evaporation and Condensation: $q_{evaporation}$ *and* $q_{condensation}$

The effects of evaporation and condensation are noticeable when throughput is steady and $q_{total}/q_{displacement} > 1.0$. $q_{evaporation}$ is the vapor added from evaporation at the surface of the oil. Conversely $q_{condensation}$ is the vapor removed by condensation along the cold surfaces of a tank wall.

Each hydrocarbon constituent of the vapor has a different boiling point. Methane and ethane have boiling points below ambient conditions (-258°F and -127°F respectively) and will remain part of the vapor stream regardless of temperature. The boiling points of propane (-44°F), butane (30°F), pentane (96°F) and larger hydrocarbons are in the range of ambient conditions. These components will evaporate and condense when the tanks change temperature. As the storage tanks are exposed to outdoor conditions, sunlight and ambient temperature directly impact vapor generation.

Figure 4.4 shows the relationship between the crude temperature received at East Meters and the vapor WI. During the winter when NGL production is steady (refer to Figure 4.3) the WI is correlated to crude temperature. The correlation is lost during the summer when NGL production drops.

4.2.5 Operational Impact of Vapor Generation

The crude tanks are designed to operate at atmospheric conditions. They cannot tolerate pressure differentials between the atmosphere and the inside of the tank that exceed x inches of water or x PSIA. Two scenarios are possible, over- and under-pressurization.

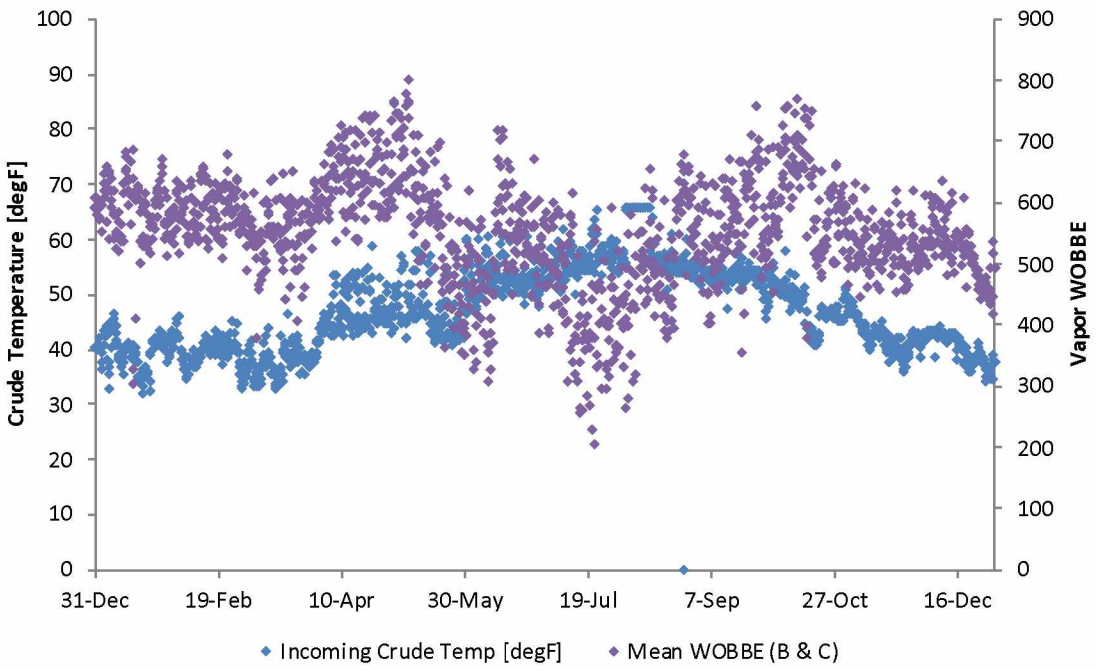

Figure 4.4: Plot of recovered vapor WI and the incoming crude oil temperature over one year. The WI is the mean between boilers B and C.

Tank Over-pressurization

When the crude level[8] in a tank is static or rising, vapor will blanket the head space in the tank. Head space is the region extending from the top of the crude to the tank roof. Crude filling the tank acts as a piston, shrinking the head space and displacing vapor, $q_{total}/q_{displacement} \geq 1.0$. To prevent over-pressurization vapors are removed at the rate at which they are generated, $q_{removal} = q_{total}$, using compressors. This cyclic process is depicted in Figure 4.1.

If the vapor system were not operational, $q_{removal} \ll q_{total}$ and the tanks would vent to atmosphere though pallet relief valves on the top of the tanks. This is a hazardous situation. The gas cloud formed when a tank vents can create a flammable or explosive atmosphere as vapor mixes with oxygen. As the crude vapors contain

[8]Tank levels are measured in feet by suspended or ultrasonic level gauges installed in stilling wells. Footage values are convenient for operators and easily converted to volumes and flow rates when necessary. Stilling wells are used to provide a calm and clean environment within the tank for measurement purposes.

Benzene, they are hazardous to human health. For these reasons the tank farm is immediately evacuated if the vapor system trips offline.

Tank Under-pressurization

When a tanker is loaded and the crude level in a tank drops, the volume of vapors removed is much greater than the rate at which they are generated, $q_{removal} \gg q_{total}$. This can form a vacuum within the tank. As with over-pressurization, even a slight negative pressure differential between the tank and the atmosphere can compromise its structural integrity. In this case, the pallet relief valves are designed to allow air to enter the tank and prevent a vacuum from forming. Again, this is a dangerous condition where a flammable or explosive atmosphere may form within the tank. To prevent the ingress of oxygen, exhaust gases from the boilers are routed back to tanks and fill or *blanket* the newly formed head space. As most of the oxygen has been removed from the exhaust gases as part of the combustion process, the gases are inert[9]. Managing vapor recovery within the tank farm is a dynamic process as the conditions in each tank vary continuously.

Vapor recovery of oil tankers is managed exactly the same as that of the stationary crude storage tanks. Tankers also operate at atmospheric conditions and are vulnerable to over- and under-pressurization.

Flue Gas Management

Flue or exhaust gasses are routed to the tank farm as necessary to maintain pressure in the tanks. The exhaust gas cycle depicted in Figure 4.1 can be represented by:

$$q_{total} + q_{removal} + q_{burned} + q_{flue} = 0 \tag{4.3}$$

[9]The exhaust gases are continuously monitored to ensure the oxygen content remains at or below 4%. The flammable range for hydrocarbon vapor is approximately 13%.

where q_{total} is the total vapor generated from Equation 4.2, $q_{removal}$ is the total vapor removed while draining a tank, q_{burned} is the vapor burned in either an incinerator or a boiler and q_{flue} is the volume of exhaust gasses routed from the boilers to the tank. All units in Equation 4.4 are SCF per unit time (minute, hour etc.). q_{flue} is adjusted by the control system to prevent tank over- and under-pressurization, maintaining equilibrium.

4.2.6 Vapor Combustion

In Equation 4.4 the term q_{burned} is the sum of the vapor destroyed in the incinerators or burned in the boilers. Accounting for vapor destruction Equation 4.4 can be expanded to:

$$q_{total} + q_{removal} + (q_{incinerator} + q_{boiler}) + q_{flue} = 0 \tag{4.4}$$

where $q_{incinerator}$ is vapor routed to the incinerators and q_{boiler} is vapor routed to the boilers. Ideally all of the combusted vapor q_{burned} would be captured and re-entrained back into the crude oil as they have value. Unfortunately vapor re-entrainment is difficult and costly at scale. As the Clean Air Act prohibits their release to the atmosphere, the vapors can be utilized as a fuel source to produce steam and generate electricity.[16]

Vapors captured from the tank farm or a moored tanker under vapor control that are not used to balance tank farm pressure are destroyed in either the power boilers or waste gas incinerators. As depicted in Figure 4.1 three boilers and three incinerators are installed[10].

[10]The thermal inputs of the power boilers are rated at 242 MMBTU/hr each and the three waste gas incinerators are rated for 400 MMBTU/hr each. These are steady-state values.

Vapor Incinerators

The initial design of Power/Vapor used the incinerators to destroy all excess vapors. Unsurprisingly this heat loss was recognized as a valuable energy source to harness. Over the last forty years incremental modifications have been made to the plant to minimize vapors routed to the incinerators. Even with reduced vapor volumes, the incinerators remain an important safety system to destroy vapor surges that occur during pipeline relief events or other process upsets.

The internal temperature of the incinerators is regulated by the Alaska Department of Environmental Conservation to ensure complete destruction of organic components. To ensure temperatures are maintained, the incinerators require a minimum vapor flow rate and Wobbe Index for thermal stability.[6] Two incinerators are normally online for redundancy.

Power Boilers

The boilers shown in Figure 4.1 are configure to burn vapor or diesel. Vapor is the most economical fuel source at the VMT as it requires no refining or transportation. Natural gas is not available in the Valdez area and infrastructure to vaporize Liquified Natural Gas (LNG) does not exist. To minimize diesel consumption combustion of crude vapor in the boilers is maximized where possible. When the energy content of the vapor stream is not sufficient to meet the plant's steam load, vapor is supplemented with atomized diesel in the boilers. Figure 4.5 shows the control system bias towards vapor utilization.

When the energy content of the vapor stream exceeds that required by the boilers to maintain the steam pressure, the excess vapors are destroyed in the incinerators. As expected with such a dynamic system, a continuous source of vapor is not assured. Figure 4.6 shows the relationship between the energy recovered from the tank farm and the volume of diesel consumed in the boilers. The knee of the curve indicates

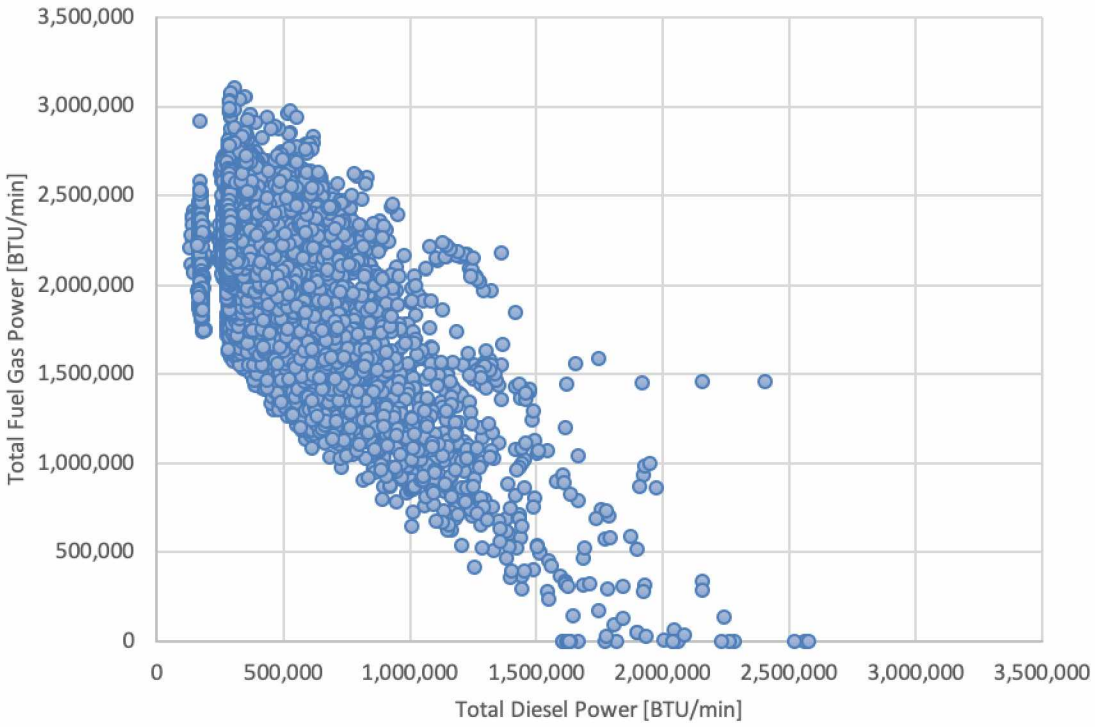

Figure 4.5: Scatter plot of distribution between the thermal inputs to the boilers. The diesel minimums are visible.

maximum vapor utilization in the boilers. Energy extracted from the tank farm and/or tanker under vapor control past the knee is sent the the incinerators.

The plant is typically operates with two of the three boilers online. The boilers supply 730 degF, 600 PSI steam via a common high pressure header to various systems in the plant, the largest of which are the turbine generators. This provides redundancy in the steam system and allows the third boiler to undergo maintenance. When a boiler is online, the minimum diesel flow rate is maintained at 1 GPM, regardless of the incoming vapor energy content or demand for steam. In the event of a rapid collapse of vapor energy content, the diesel flow rate is increased to maintain boiler steam output. The minimums is graphically depicted in Figure 4.5.

The value of an HPRT is that it can supply power when insufficient vapor is available to maintain boiler steam load. This reduces the volume of supplemental diesel.

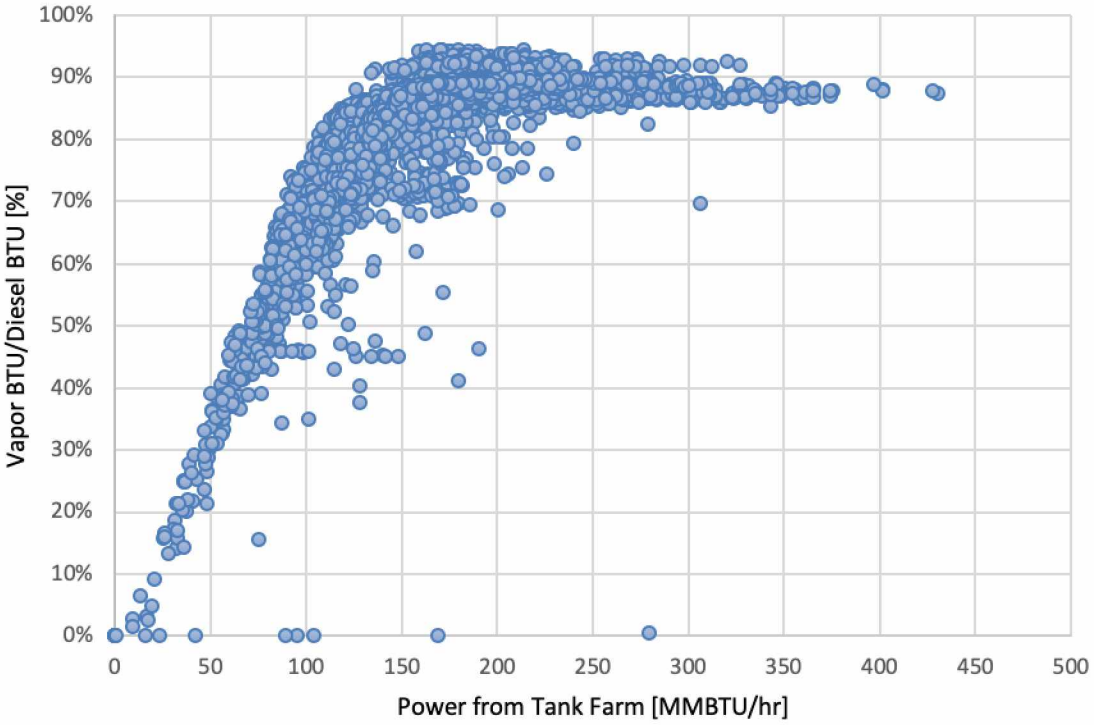

Figure 4.6: Scatter plot of the relationship between the vapor-to-diesel BTU ratio and the power extracted from the tank farm. As power extracted from the tank farm increases, the ratio plateaus. This indicates that there are periods where more power is extracted from the tank farm than necessary for the boilers to operate on minimums.

Table 4.1: Power/Vapor electricity generation statistics.

Metric	Unit	Mean	Std. Dev.	Min	Max
Real power generated	MW	6.7	1.2	4.0	11.3
Plant efficiency (electricity basis only)	%	15.1%	1.3%	10.6%	19.9%

4.3 Power System

The VMT power system is electrically islanded. Although the nearest utility interconnection is only a few miles away, the VMT has never been connected to the Copper Valley Electric Association grid. With the exception of two emergency diesel generators, Power/Vapor is the only source of electricity for the VMT. The plant must be self sufficient and accommodate all load swings and black plant scenarios.

The three main electrical generators in Power/Vapor are 15.625 MVA, 12.5 MW, 13.8 kV synchronous machines. Normal operation is two turbine generators online at any one time for redundancy. Electricity is distributed around the VMT at 13.8 kV. Utilization voltages for large induction motors that drive the vapor compressors is 4.16 kV. General purpose utilization is at 480 VAC or 208/120 VAC.

The yearly VMT electrical load is cyclical and closely correlated to the ambient air temperature. This behavior is visible in Figure 4.7 and 4.8. Summertime loads range from 4-6 MW while wintertime loads peak at 12 MW. A normalized histogram of total electrical load is shown in Figure 4.10. Tabulated data is shown in Table 4.1.

4.3.1 Efficiency

The ultimate justification for an HPRT is one of economics: can the volume of diesel burned in the boilers be reduced? To answer this question the efficiency of the current plant must be calculated.

Three efficiency metrics can be considered for the Power/Vapor facility with re-

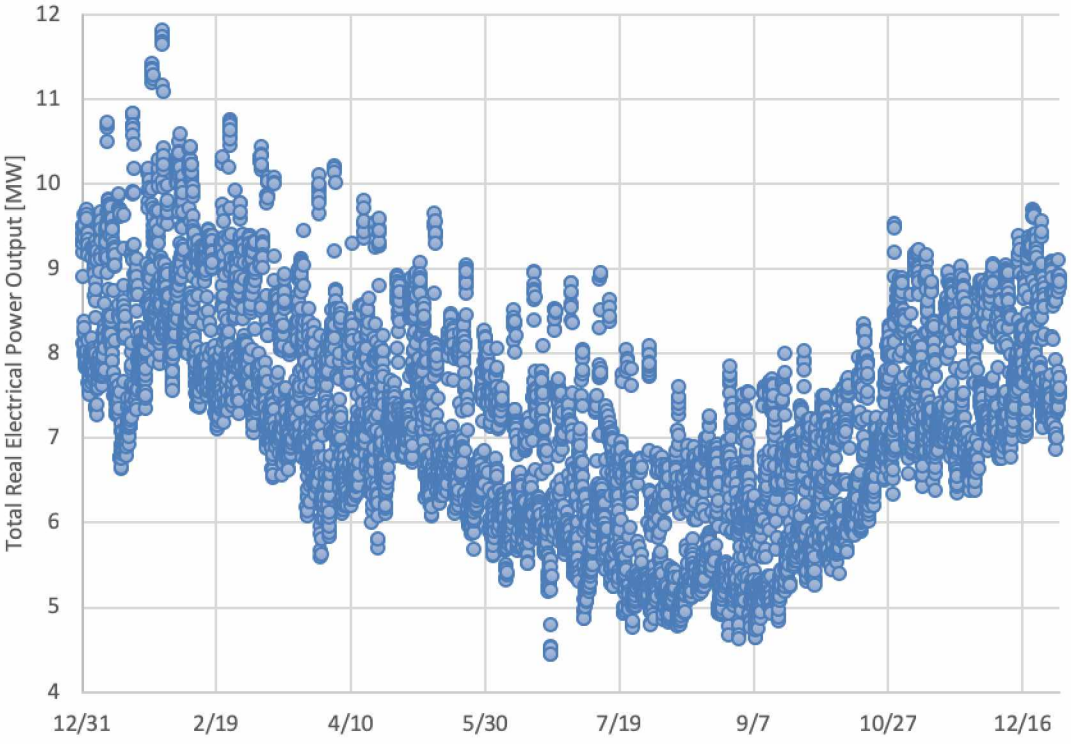

Figure 4.7: Scatter plot of the total VMT electrical load over time.

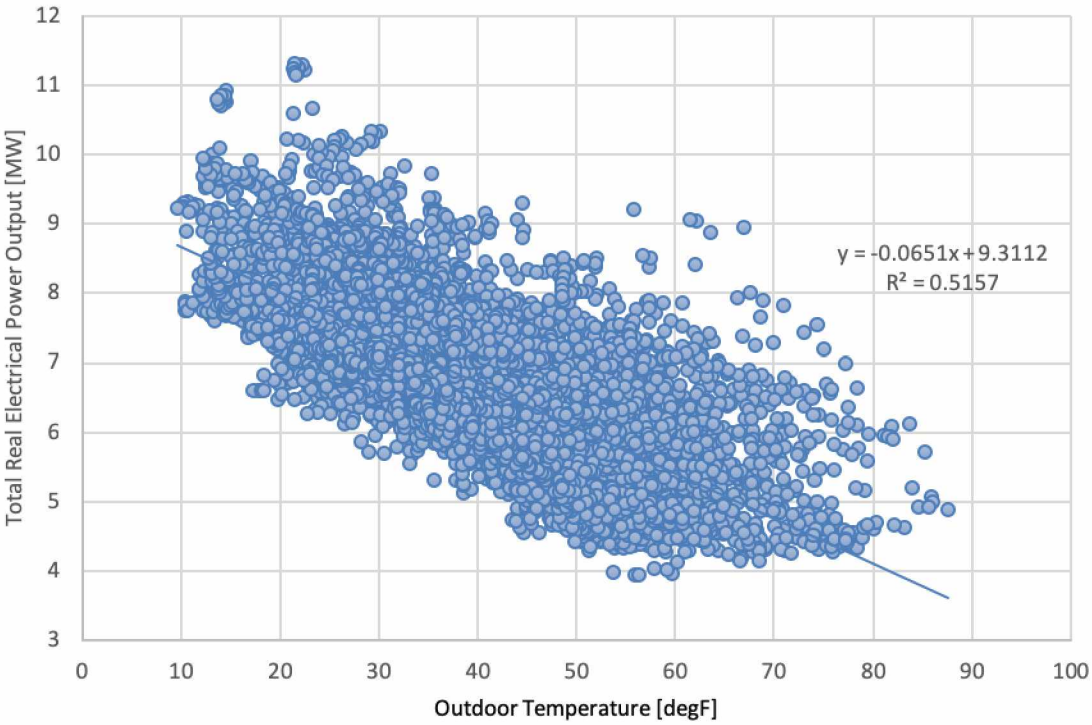

Figure 4.8: Scatter plot of total electrical load versus ambient air temperature.

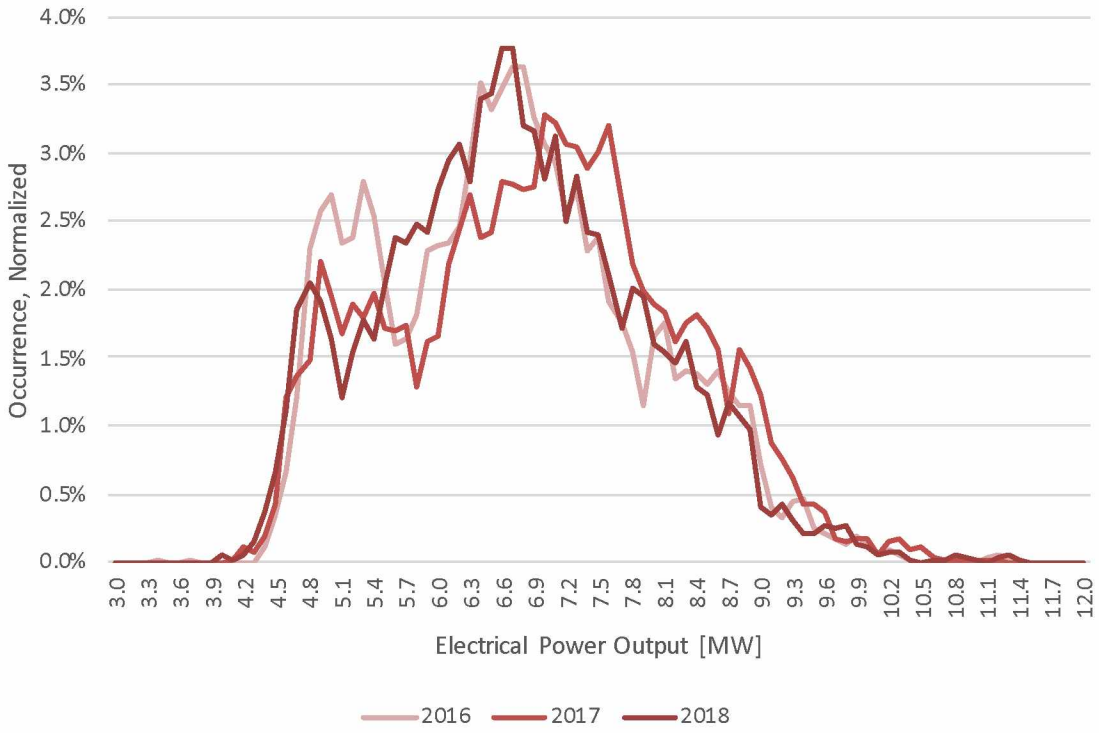

Figure 4.9: Normalized histogram of the total electrical load on the turbine generators. Three years of data is presented, averaged on one-hour intervals. The peaks at 5.3 MW and 6.8 MW are caused by of the number of compressors in operation.

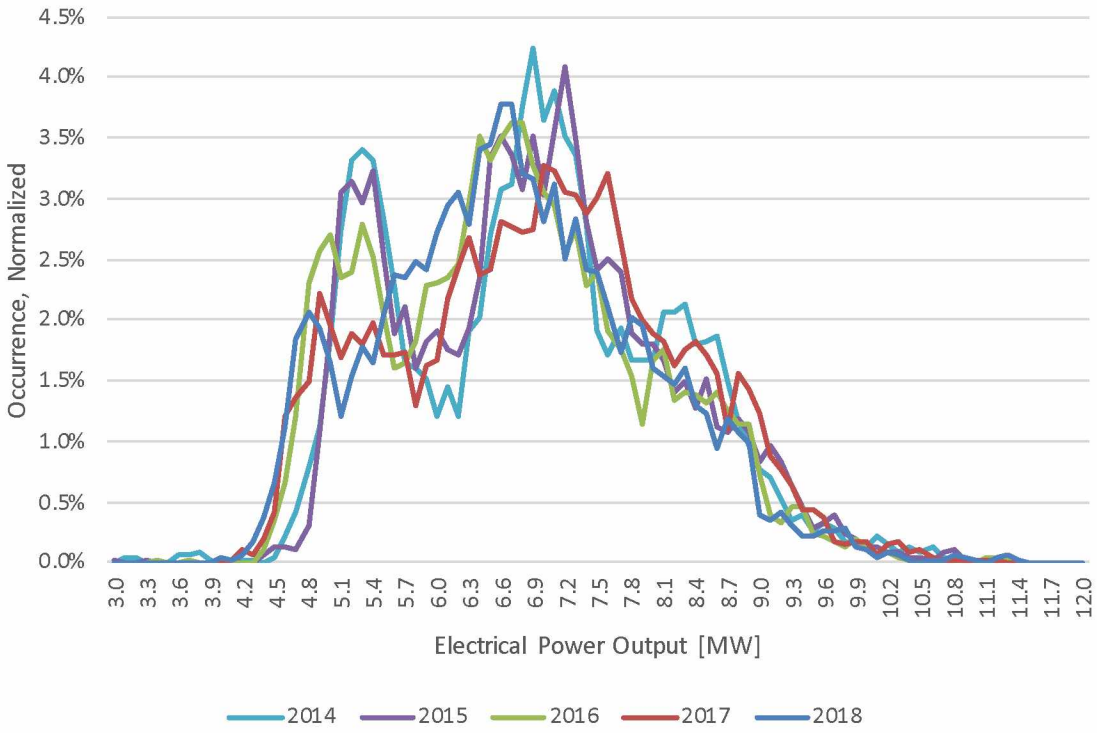

Figure 4.10: Normalized histogram of the total electrical load on the turbine generators. Five years of data is presented, averaged on one-hour intervals. The long-term trend remains consistent.

spect to electricity generation[11]:

1. Efficiency of an ideal (reversible) Rankine cycle.

2. Efficiency of the actual (irreversible) Rankine cycle.

3. Power plant heat rate.

Ideal Rankine Cycle

The ideal Rankine cycle ignores inefficiencies in the plant and calculates the ultimate theoretical efficiency of the cycle. This assumes:

1. Isentropic (constant entropy) compression occurs in the feed water pump.

2. The feed water is heated at constant pressure in the boiler.

3. Isentropic expansion occurs in the turbine.

4. Heat is rejected from steam at a constant pressure in the condenser.

The ideal efficiency of the power vapor Rankine cycle is approximately 28%. This efficiency can be approached by not achieved in a real system.

Actual Rankine Cycle

To determine the efficiency of the actual Rankine cycle a thermal survey of the 600 psi steam system and boiler feed water system was performed. Resistive Temperature Device (RTD) instrumentation is extremely limited on the steam system. Thermographic imagery of the boiler feed water system was used to determine approximate pipe wall temperatures as captured with a FLIR camera. Imagery from that survey is shown in Figures 4.11 and 4.12.

[11]These metrics analyze Power/Vapor as a power plant. Power/Vapor actually operates as a vapor plant where the primary product is flue to blanket and inert the tank farm. If the flue gas is assigned a value, the overall plant efficiency will be higher than as calculated in this paper. An alternative blanketing gas is nitrogen.

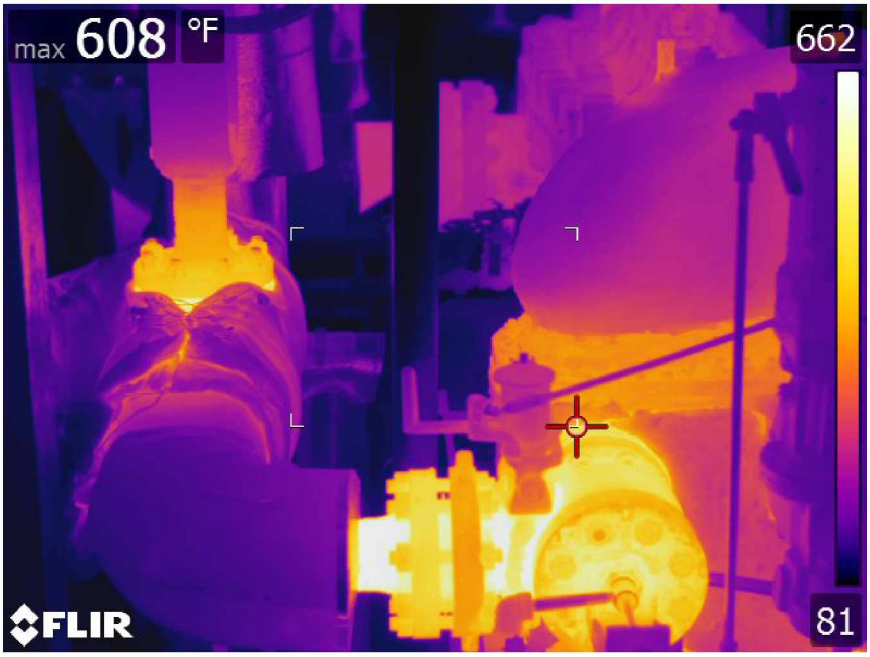

Figure 4.11: Thermal image of the discharge side of the boiler feed water pump.

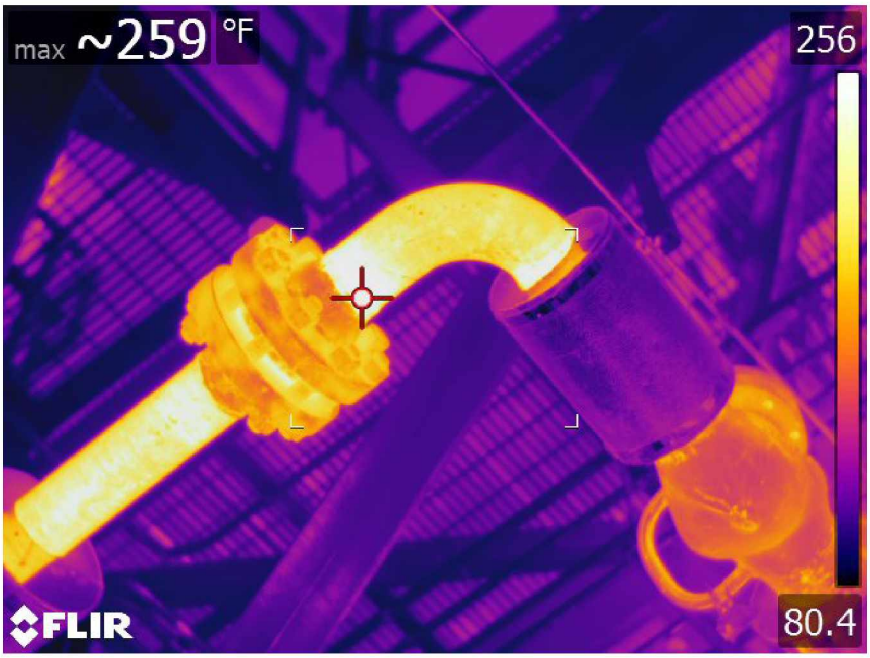

Figure 4.12: Thermal image of the boiler feed water economizer mounted to C Boiler that preheats the water using hot flue gasses.

Table 4.2: Empirical enthalpy values calculated at various points in the Power/Vapor Rankine cycle.

State in Rankine Cycle	Enthalpy Btu/lb
Boiler Output	$h_1 = 1396.8$
Turbine Input	$h_{1'} = 1367.8$
Turbine Output or Condenser Input	$h_2 = 1116.4$
Condenser Output	$h_3 = 86$
Deaerator Output or Boiler Feed Water Input	$h_{3'} = 230$
Boiler Feed Water Output	$h_4 = 232$
Boiler Economizer Output	$h_{4'} = 289$

The enthalpy of steam and water at various points in the cycle is then calculated from steam tables based on temperature and pressure measurements as shown in Table 4.2. Using these enthalpy values, the efficiency of the actual Rankine cycle is calculated using Equations 4.5, 4.6, 4.7 and 4.8:

$$\Delta h_t = h_{1'} - h_2 = 251 \tag{4.5}$$

$$\Delta h_p = h_4 - h_{3'} = 2 \tag{4.6}$$

$$\Delta h_{cycle} = \Delta h_t - \Delta h_p = 249 \tag{4.7}$$

$$\Delta h_b = h_1 - h_4 = 1165 \tag{4.8}$$

where Δh_t is the turbine enthalpy, Δh_p is the boiler feed water pump enthalpy, Δh_{cycle} is the developed Rankine cycle enthalpy and Δh_b is the boiler enthalpy. The units of Equations 4.5, 4.6, 4.7, and 4.8 are Btu/lb. The overall efficiency of the

actual Rankine cycle is calculated by Equation 4.9:

$$\eta_{cycle} = \frac{\Delta h_{cycle}}{\Delta h_b} = 21\% \tag{4.9}$$

It is reasonable for the actual cycle efficiency calculated by Equation 4.9 to be less than the ideal cycle efficiency of 28%. The ideal cycle assumes the plant maximizes enthalpy utilization in the turbines and that the boilers and condensers operate at constant pressures. The actual process deviates from these assumptions.

Plant Heat Rate

The heat rate calculates how efficiently a power plant converts its thermal inputs to electricity. Assuming 100% conversion efficiency, 1 kWh is equivalent to 3412 Btu (1 MWh is equivalent to 3.41 MMBtu). A plant operating at 50% efficiency would have a heat rate of 6824 Btu/kWh (6.82 MMBtu/MWh). Heat rate is used to compare overall efficiency of individual power plants.

As shown in Figure 4.13 and tabulated in Table 4.1, the actual heat rate of Power/Vapor ranges from 10.6% to 19.9% with an average of 15.1%. These values are computed over the range of electrical load fed by the plant. Heat rates below the cycle efficiency calculated by Equation 4.9 are logical. Equation 4.9 does not account for inefficiencies in the 600 PSI steam system or with the electric generators. 600 PSI steam consumed by the turbines driving the boiler feed water pumps and the forced-draft fans on the boilers are not captured by Equation 4.9[12].

"Bottom Line" Plant Efficiency

Of the three calculations, the heat rate is "what you pay" for electricity. Compared to the heat rate of a stationary reciprocating diesel generator, Power/Vapor is ineffi-

[12]Energy is not recovered from the hot flue gasses routed to the tank farm.

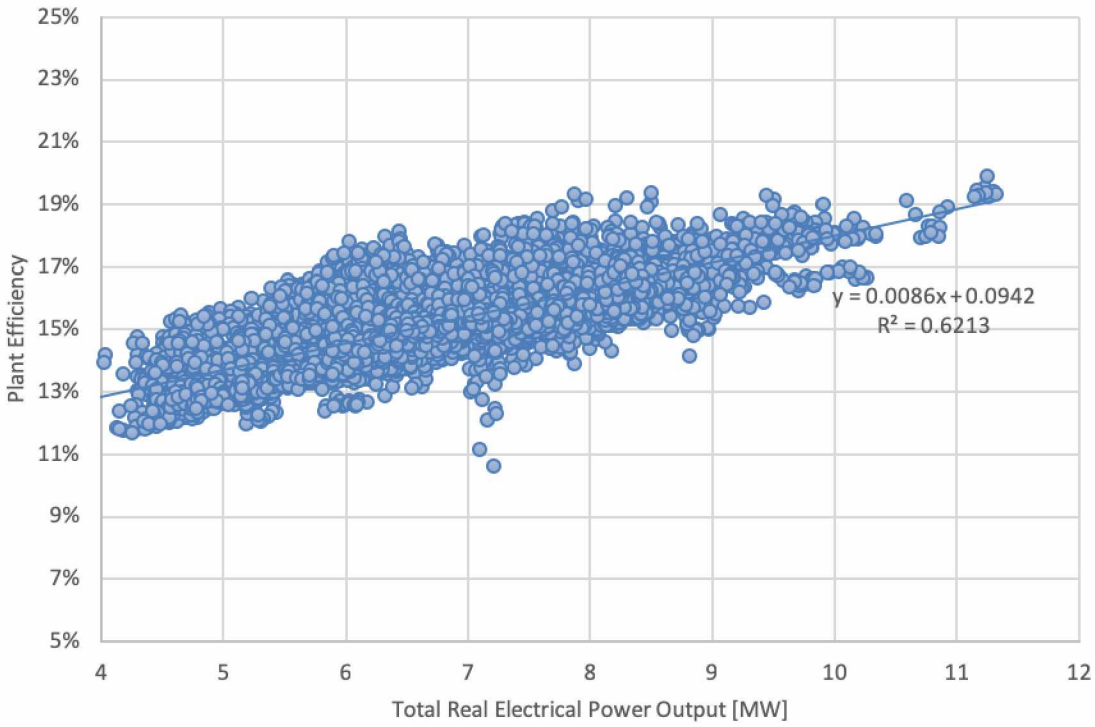

Figure 4.13: Scatter plot of the calculated plant heat rate. Efficiency in this context is calculated by $p_{electrical}/(p_{vapor} + p_{diesel})$. p_{vapor} and p_{diesel} are the same as those depicted in Figure 4.5

.

cient[13]. Reciprocating engines can achieve heat rates of 35% or more. The challenge is designing an engine that can handle the hydrocarbon vapors. Diesel has a predictable energy density, 132–139,000 BTU/gallon, depending on the time of year[14] and the engine design are optimized accordingly. Engine manufacturers queried by Alyeska have expressed concerns about the variability of the Wobbe Index and the ability to meet emission requirements. To date, boilers have proven to be the most versatile tool to extract useful energy from hydrocarbon vapor.

[13]This assumes no value is assigned to the flue gas used to blanket the crude tanks, a product the plant was explicitly designed to produce.

[14]Summer grades of diesel average 139,000 BTU/gallon while winter grades average 132,000 BTU/gallon.

Table 4.3: Tank farm statistics.

Metric	Unit	Mean	Std. Dev.	Min	Max
East Meters incoming	BBL/day	19,947	3,134	0	43,238
East Tank Farm ambient temperature	degF	41	13	10	88
Vapor flow rate from tank farm	Mscf/hr	194	87	-220	1,066
Vapor energy density from tank farm	Btu/scf	349	253	0	867
Vapor power from tank farm	Btu/hr	166	48	0	430

Table 4.4: Boiler statistics.

Metric	Unit	Mean	Std. Dev.	Min	Max
Diesel flowrate to boilers	GPM	3.3	2.0	1.0	19.5
Fuel gas flowrate to boilers	Mscf/hr	222	44	0	292
Fuel gas energy density	Btu/scf	561	96	0	867
Flue gas flowrate to LP header	Mscf/hr	91	56	0	465
Boiler Vapor Btu / diesel Btu ratio	%	82.1%	11.9%	0%	94.5%

4.3.2 Reducing Boiler Deisel Consumption

The largest consumers of 600 PSI steam in the Power/Vapor plant are the turbine generators. Smaller users are the turbines driving the boiler feed water pumps and boiler forced-draft fans. Boiler thermal input is directly proportional to the plant electrical load. An increase in electrical load on the generators will result in greater demand for steam and increase the vapor or diesel burned in the boilers. Figure 6.3 is a histogram of diesel consumption in the boilers. Flow rates above 2 GPM indicate the vapor thermal input to the boilers is insufficient to meet steam load.

Given the relatively poor heat rate of the Power/Vapor plant when considered only as a power plant, an HPRT can improve the efficiency of the entire system. Reducing diesel consumption in a system that is less efficient than a reciprocating diesel generator will cut fuel costs.

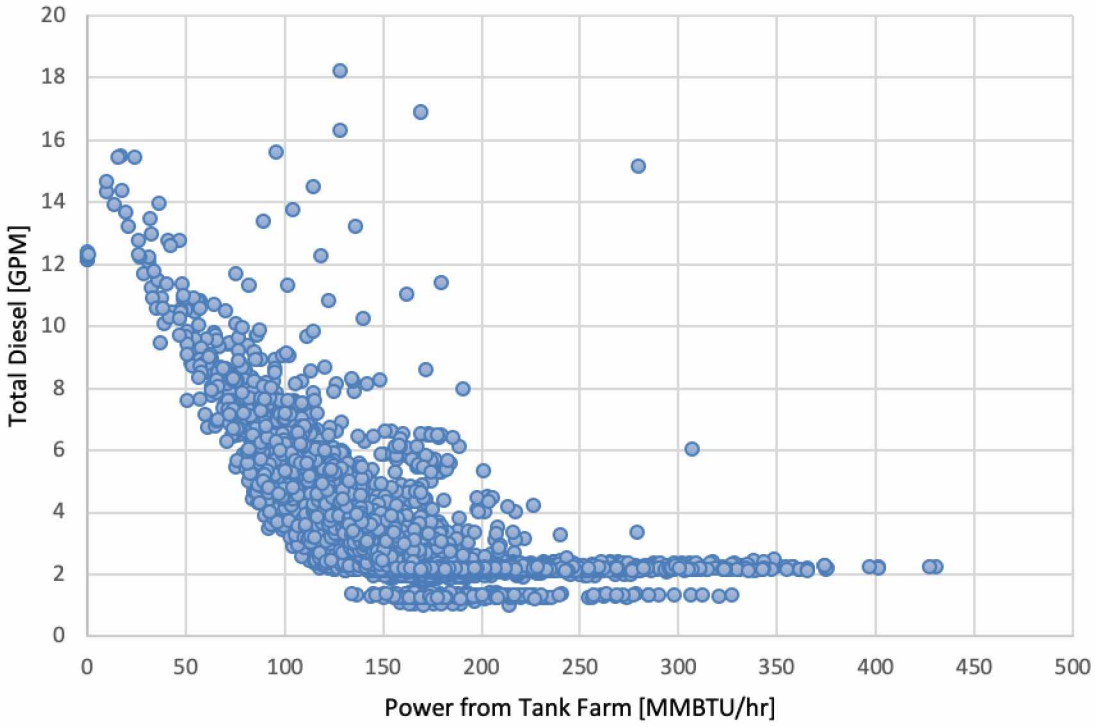

Figure 4.14: Scatter plot of the relationship between the total diesel flow rate to the boilers and the power extracted from the tank farm. As power extracted from the tank farm increases, liquid fuel consumption decreases and plateaus.

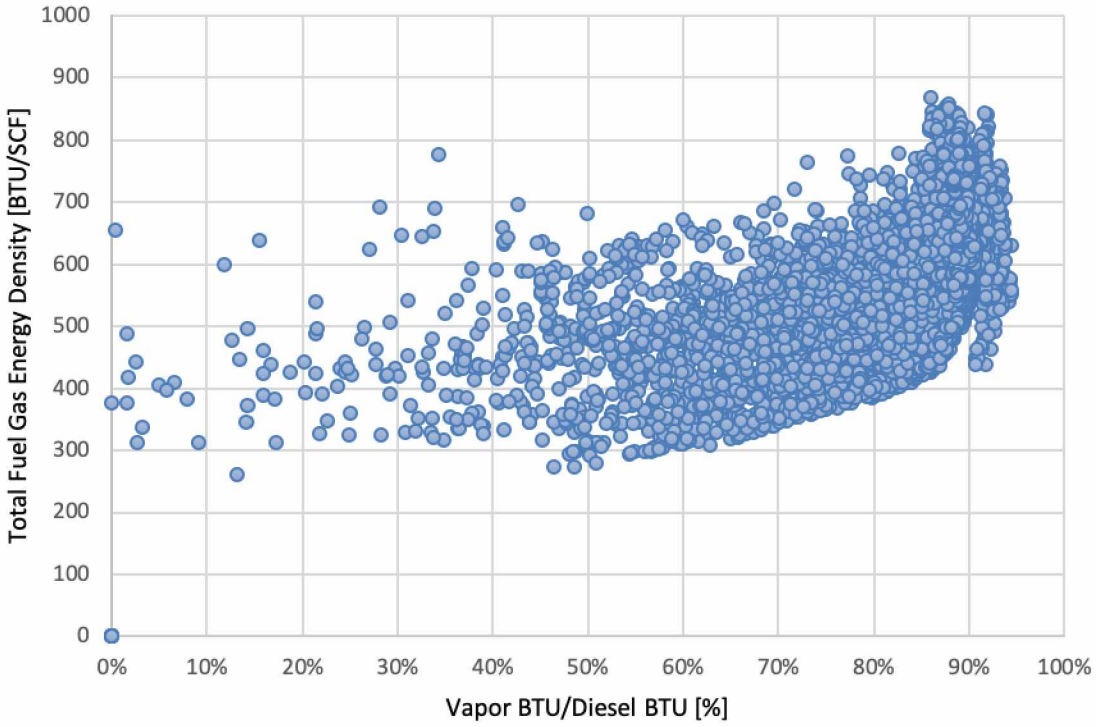

Figure 4.15: Scatter plot of the relationship between the energy density of the vapor used as fuel gas and the vapor-to-diesel BTU ratio. Ratios above 50% have minimum energy densities necessary to meet boiler steam load.

CHAPTER 5
ELECTRIC MACHINES

The choice of the electric machine in power recovery applications has important implications for overall system control and equipment configuration. Machine choice is predicated on two major constraints: the variability of pipeline throughput and the electrical capabilities of the VMT power system.

5.1 Prime Mover Variability

5.1.1 Pipeline Throughput

The first major constraint to consider is that pipeline throughput is not constant. Production on the North Slope varies due to individual well performance, ongoing maintenance in the fields and operator production strategies. The variable distribution of pipeline throughput is depicted in Figures 1.3 and 5.1. Throughput is particularly volatile in the summer when production facilities are taken offline for major maintenance. During the winter maintenance is kept to a minimum to maintain steady throughput. Throughput reductions during the winter are possible due to unplanned equipment outages in the fields or production facilities.

As discussed in Section 1.3 power recovery with an HPRT will always be a secondary function to pipeline reliability and availability. As the brake power output of the turbine, p_{brake}, is directly correlated with flow rate, q:

$$p_{brake} = \frac{qh\gamma\eta_m}{5310}$$

(Equation 3.6 without the η_e term accounting for generator efficiency) the generator must tolerate a prime mover with varying power outputs and angular velocities. This

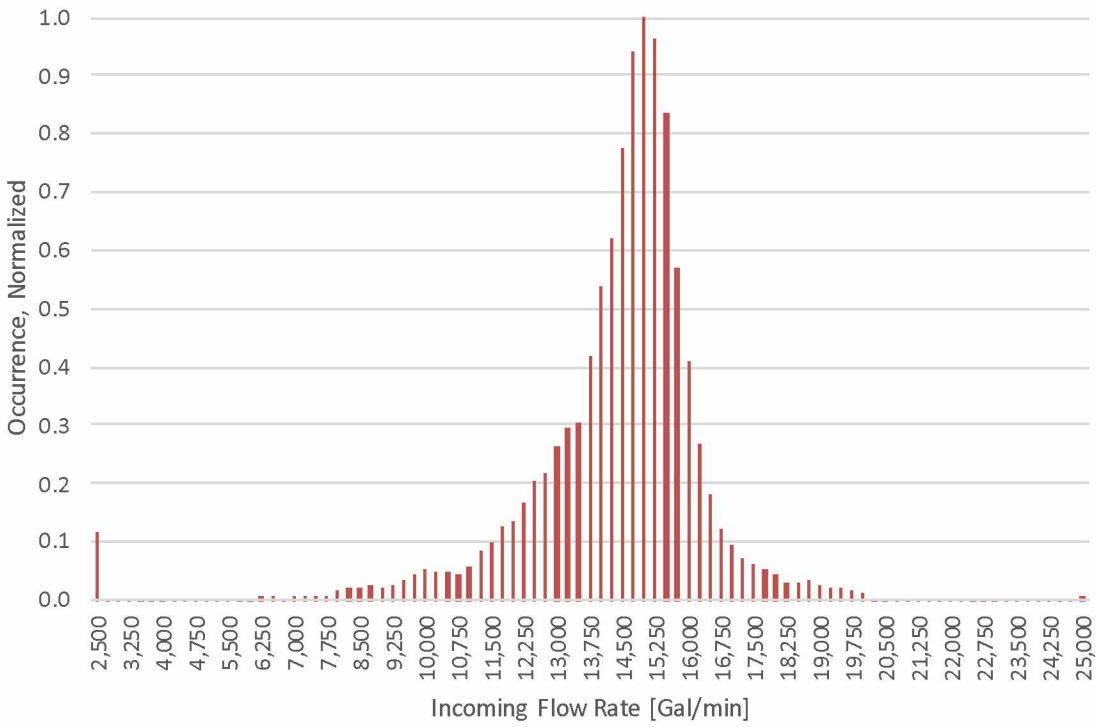

Figure 5.1: Normalized histogram of the incoming crude oil flow rate into the VMT at East Meters.

configuration is not typical of traditional power generation systems where the power output of the prime mover is adjusted to precisely match the power input required by the generator.

5.1.2 System Frequency

Stability of the AC sine wave is essential to electricity generation, distribution and utilization[1]. An uncontrolled change in AC frequency can destroy rotating equipment connected to the power system by inducing excessive torsional stress within the machines[2]. Synchronous machines are particularly vulnerable as the stator and rotor are

[1]In the United States, AC frequency and utilization voltages are standardized by ANSI C84.1. Although the focus of this project is 60 Hz, the theory is applicable to any AC power system.

[2]The anchor bolts designed to support rotating equipment do more than support the static load of the machine. They are designed to resist the sudden changes in angular momentum due to electrical faults. Inadequate anchoring can cause a large machine to "walk", causing extensive damage to the machine.

not designed to slip.

Turbines, generators, motors, pumps and compressors are typically the most expensive equipment connected to a power system. Maintaining steady system frequency for their protection is essential. Industrial power systems will typically initiate under-frequency load shed between approximately 59 and 59.5 Hz in an attempt to maintain system frequency by reducing load. Between approximately 58 and 57 Hz the synchronous generators will trip offline[3]. The under-frequency load shed window is narrow by design to protect the power system. The entire process can occur in milliseconds and leaves little room for error.

5.1.3 Prime Mover Selection

Prime movers with unpredictable power outputs are difficult to integrate into traditional AC power systems. Fossil fuels (coal, natural gas and petroleum liquids such as diesel), hydro and nuclear are the energy sources used to power conventional prime movers. Their energy output is predictable and precisely controlled with Proportional-Integral-Derivative (PID) control systems[4]. These machines tend to be large with low impedance and high available short circuit currents. Large machines are ideal for maintaining system frequency as they have high rotational inertia. An everyday example of inertia is that of a car engine: A flywheel connected to the shaft of the engine adds rotational inertia to the system for smoother operation.

High-inertia machines support the power system during transient loading or unloading events. This is readily understood from Ohm's Law:

$$I_{sc} = \frac{V_{sys}}{Z_{sc}} \tag{5.1}$$

[3]Every power system is unique and these values will vary from plant-to-plant.

[4]Proportional-Integral-Derivative controllers are used to drive and maintain a process value to a specified *set point*. The controller calculates the error between the set point and the actual measured value of the process. Proportional, integral and derivative functions of the error are summed to modulate control of the process. Cruise control in a car is regulated by a PID controller.

where I_{sc} is the available short circuit current, V_{sys} is the operating voltage at the time of the fault and Z_{sc} is the equivalent impedance of the power system feeding the fault. Power systems comprised of high-inertia generation with low Z_{sc} are referred to as *stiff* systems. These power systems can supply high fault current capable of quickly clearing a fault[5] while maintaining system voltage and frequency. Power systems with high Z_{sc} suffer from voltage drop and frequency instability[6] during transient loading. This is why the vast majority of power generation is derived from clusters of large synchronous machines coupled to fossil fuel, hydro or nuclear prime movers.

5.1.4 High Impedance, Low Inertia Power Systems

A brief discussion of renewable resources and the associated challenges is relevant as an HPRT installed at the VMT has many of the same limitations as a solar or wind farm installation. Increasing use of renewable[7] resources such as wind and solar are gradually shifting the profile of domestic and global electricity generation (see Figure 5.2). It is also possible to install renewable resources close to the electrical load, reducing the need for power transmission and distribution infrastructure (e.g. high voltage transmission lines, substations etc.). Compared to traditional synchronous machines used for power generation, these renewable installations are typically three to five orders of magnitude smaller. They have high internal impedance Z_{sc}, low short circuit contributions and cannot maintain steady system frequency. The power grid electrically adjacent to the renewable installation remains heavily dependent on

[5] Circuit breakers and relays are configured to trip faster with higher currents.

[6] An everyday example of this concept: If a 1 kW coffee pot connected to a small 2 kW gasoline generator is turned on, the voltage and frequency of the generator will drop and recover. The frequency change is audible listening to the engine. The generator impedance Z_{sc} and low rotational inertia have difficulty managing the step change in electrical load. Connect the coffee pot to a receptacle-outlet in a home and the power grid has no difficulty managing the step change. The grid has a lower Z_{sc} and significantly higher rotational inertia.

[7] Generally defined as energy sources that can be rapidly replenished. Replenishment of fossil fuels are on the order of tens to hundreds of millions of years whereas wind and solar are replenished continuously. These renewable resources can reduce emissions of carbon dioxide and other pollutants to the biosphere.

Table 5.1: Renewable generation has many of the same characteristics as an HPRT. The lessons learned from modern renewable installations can be incorporated in the design of an HPRT.

	Solar or Wind	HPRT at the VMT
Energy Resource	Highly variable; Dependent on availability of sunlight or wind.	Highly variable; Pipeline throughput changes continuously.
Power Output Ratio	Low relative to grid.	Low relative to synchronous generators at Power/Vapor.
Impedance Ratio	High relative to grid.	High relative to synchronous generators at Power/Vapor.
Inertia Ratio	Low relative to grid.	Low relative to synchronous generators at Power/Vapor.

synchronous machines to maintain stability of system frequency and voltage. When renewable sources are unavailable[8] (e.g. at night for solar or a calm day at a wind farm) traditional synchronous generators must pick up the difference with their spinning reserve as generation must precisely meet instantaneous demand.

Previous attempts (see Section 1.3) to capture the hydraulic head with an HPRT from Thompson Pass failed as the system was designed for prime generation (high-inertia, low-impedance) as opposed to supplemental generation (low-inertia, high-impedance). The difference is significant. Treating an HPRT installation as a low-inertia, high-impedance generator and integrating it into the VMT power system is a practical approach.

[8]When renewable sources abruptly drop offline or come back online, synchronous generators are subjected to sharp loading and unloading. As these machines are designed for steady-state operation, the torsional forces can prematurely wear or cause damage to the machine. Ideally the energy extracted from renewable sources would be stored for later use. Unfortunately electricity is expensive to store in significant quantities. Although grid-connected batteries are increasingly used in specialized applications, improvements to the energy density only average a few percent per year. Batteries also require large quantities of hazardous material such as lead, lithium and cadmium. Flywheels and capacitors are generally limited to run times in tens of seconds. Pumped hydro remains viable though system inefficiencies and space requirements limits application.

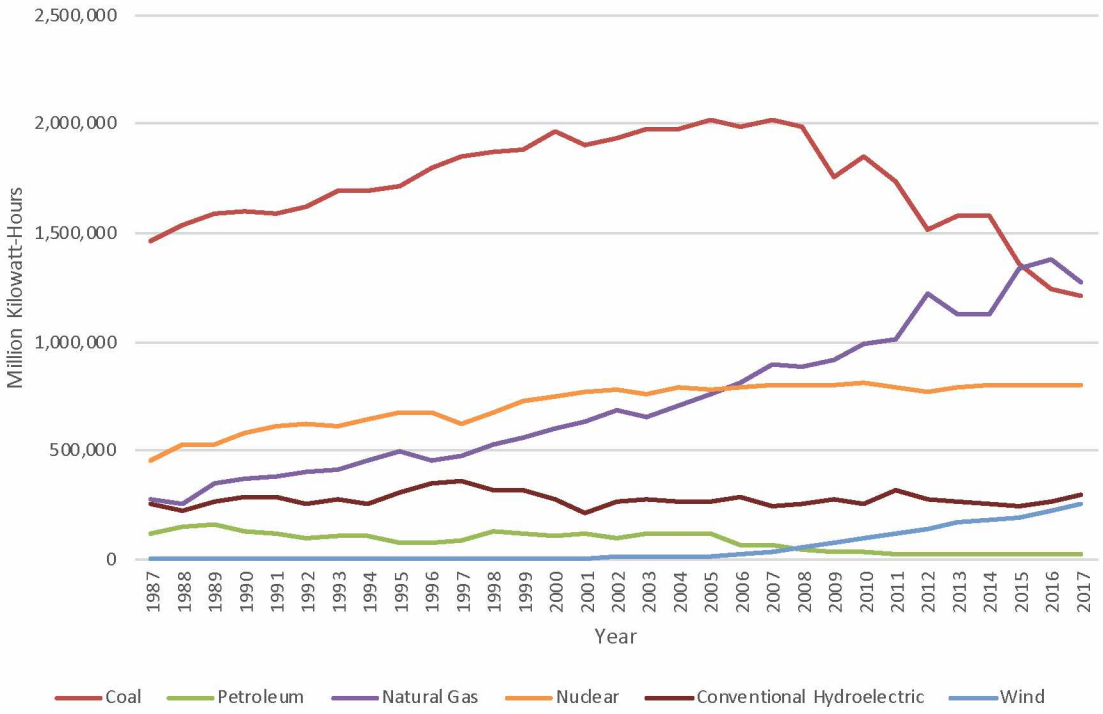

Figure 5.2: Prime mover energy source for electricity generation in the United States. Data from geothermal, pumped storage, biomass and other gases such as propane have been excluded for clarity.[17]

5.2 Electric Machine Choice

The available choices of machine for use as an electric generator in HPRT service will now be studied.

5.2.1 DC Machines

Overview

DC motors and generators are rarely used in modern industrial power systems. It is difficult to step-up the voltage of a DC system high enough to economically transport a large amount of energy. Resistive power losses are proportional to the square of the current as demonstrated by Equation 5.2:

$$P_{loss} = I^2 R \tag{5.2}$$

where P is the power dissipated in watts, R is the resistance in ohms of the distribution system and I is the current in amperes. A power system operating at a higher voltage will have lower resistive power losses than a system with a lower voltage that transports the same power.

DC motors were useful in industrial applications requiring variable speed control before the development and commercialization of power electronics. To change the speed of the rotor in a DC machine, the terminal voltage is adjusted. This was performed using a bank of variable resistors in series with the machine to reduce the machine terminal voltage. A bank of variable resistors is shown in Figure 5.4. Although easy to perform, this process is inefficient, especially with larger machines operating at slow speeds with reduced terminal voltages.[18]

DC generators and motors are effectively the same machine with the shaft of a generator coupled to a prime mover. The terminal voltage of a DC generator is controlled by adjusting the field flux within the machine. The flux is induced by

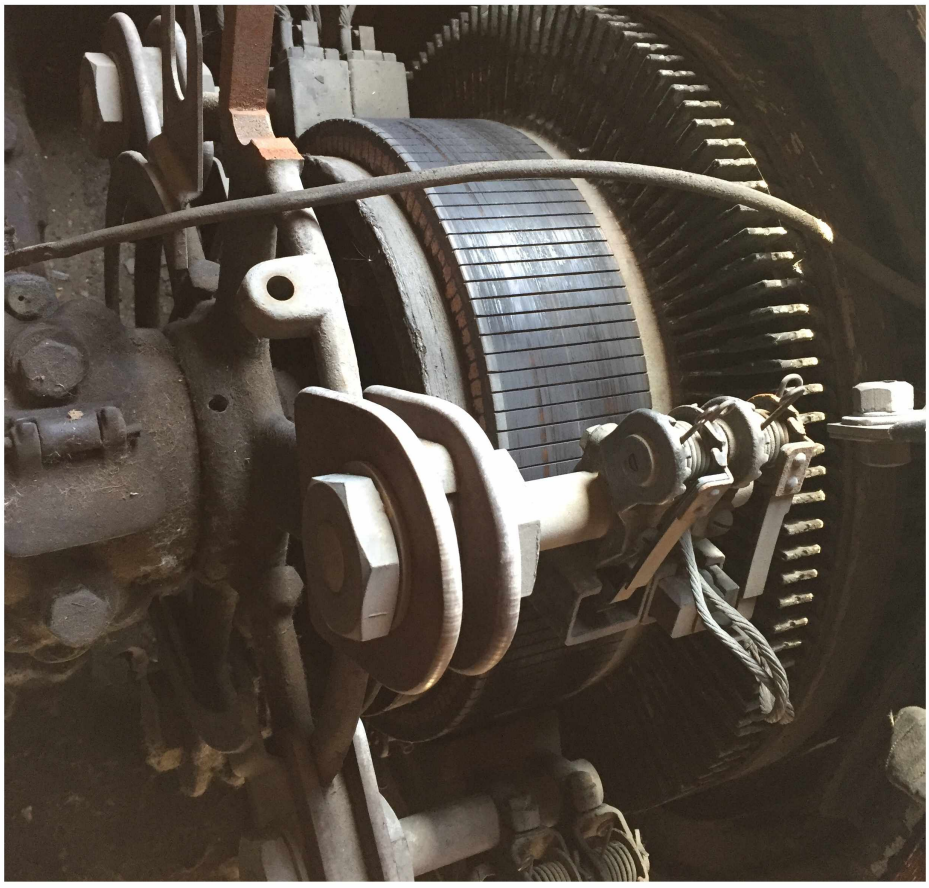

Figure 5.3: Commutator on a DC motor. Picture taken by the author at the abandoned Kennecott Mill in Wrangell-St. Elias National Park.

Figure 5.4: Variable DC resistor. Picture taken by the author at the abandoned Kennecott Mill in Wrangell-St. Elias National Park.

current flowing through the armature. To maintain constant armature current within a rotating machine, all DC machines require commutators. Commutators require regular maintenance and contribute to resistive power losses in the machine. The commutator of a DC machine is shown in Figure 5.3.

VMT Integration

As the VMT power system generates and utilizes AC power, use of a DC machine as the generator of an HPRT would require power electronics to convert DC to AC. This device is called an *inverter*. Large inverters rated for several megawatts are commercially available. They are highly specialized devices and require regular service of the capacitors and other components to maintain operation. The maintenance requirements and specialized equipment required for a DC machine creates a *one-off* installation, increasing upfront engineering and procurement costs. A DC machine is therefore not the best option in this application and will not be studied further.

5.2.2 AC Synchronous Machines

Overview

Modern power systems typically generate power with synchronous generators. Synchronous machines can:

- Generate real power (as a generator).
- Absorb real power (as a motor).
- Generate or absorb reactive power to manage leading loads (as a generator or motor).
- Maintain a fixed generation frequency.
- Maintain a fixed terminal voltage.

The ability of a synchronous generator to supply real power and either supply or absorb reactive power make them highly versatile as generators. The rotor of a synchronous machine spins in synchronism with the frequency of the power system. If the machine is islanded, synchronous speed is established by the electrical frequency of the machine. A change in the speed of the rotor of a synchronous generator will change the frequency of the generated AC sine wave.

When paralleled, the rotors of all other synchronous machines connected to the power system will change in unison. To remain in synchronism, all machines must have the exact same electrical frequency. The scalability of synchronous machines is when many machines are paralleled together on a grid they behave as one large machine. Generation connected to the grid can be added or removed as necessary to accommodate changing loads. With many machines spinning in synchronism, rapid fluctuations must be avoided as severe damage to connected machines can result. A loss of synchronism (the rotor magnetic field is no longer coupled to the stator magnetic field) can lead to the destruction of a machine.

The original capability curve of the 15.625 MVA, 13.8 kV generators at Power/Vapor is shown in Figure 5.5. Depending on the excitation voltage in the generator, the machine can export or import reactive power.

VMT Integration

To maintain constant rotor speeds with synchronous generators, highly predictable prime movers are required. To integrate with existing synchronous machines connected to the power system, the shaft speed must be precisely controlled with a PID controller to keep the machine at or just slightly ahead of the system frequency to generate real power. If the machine slows down relative to the frequency of the power system, the generator will turn into a motor. This is a dangerous operating condition, as prime movers are designed to export power, not absorb power. In the case of an

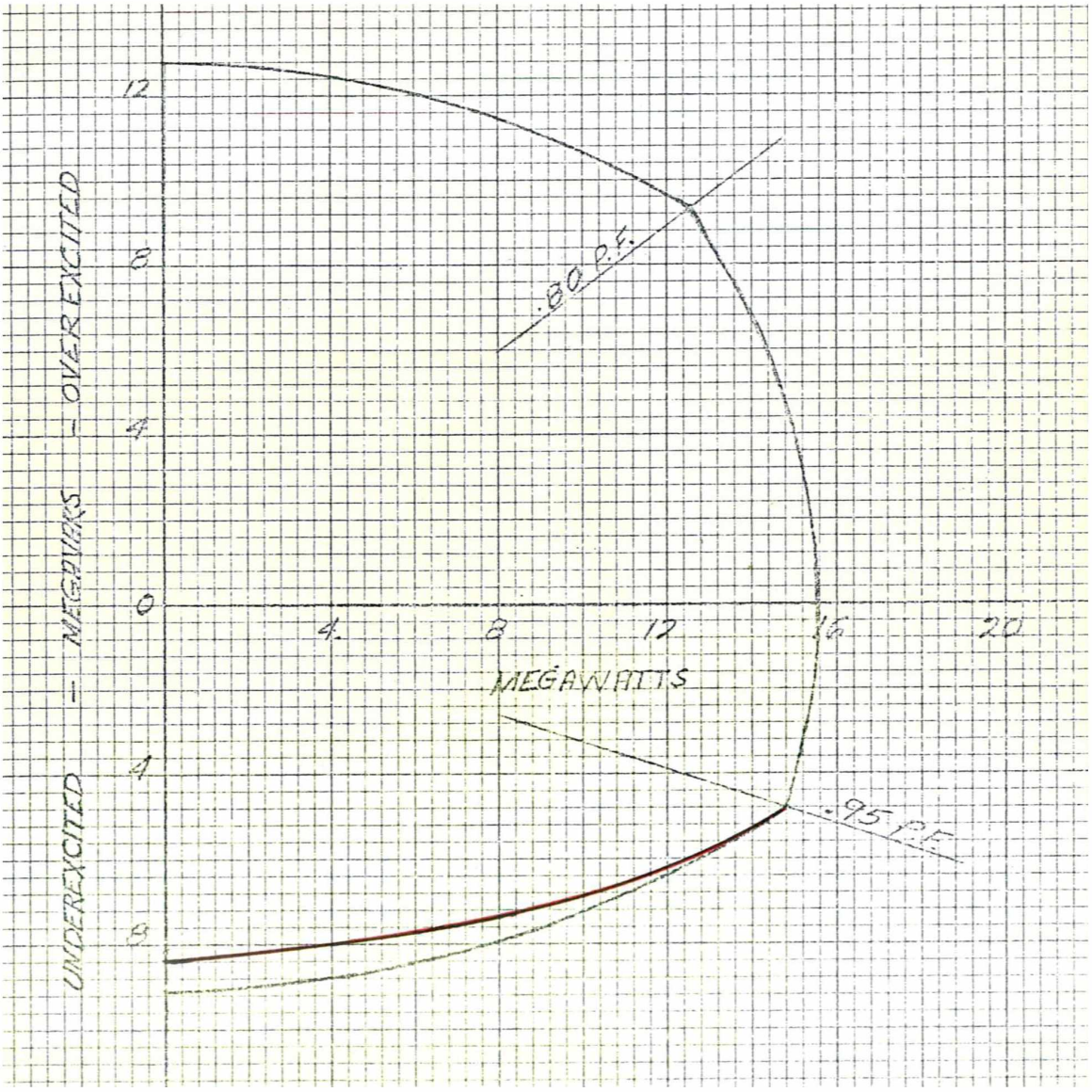

Figure 5.5: Capability curve of the 15.625 MVA Power/Vapor generators coupled to the 12.5 MW Turbodyne condensing steam turbines. Depending on the excitation voltage in the generator, the machine can export or import reactive power. Under-excited is importing reactive power, over-excited is exporting reactive power.

HPRT, the turbine will start to act as a pump, inducing hydraulic transients[9] in the pipeline.

It is possible to place power electronics between the synchronous generator and the grid. The machine would then be free to spin out of synchronism with the power system, relying on the power electronics for AC-to-DC-to-AC conversions. Effectively, this is a Variable Frequency Drive operating in reverse. As with the DC machine, this is a highly specialized application, subject to an undesirable "one-off"installation.

Synchronous machines are electrically the most versatile given their abilities to manage generation or consumption of reactive power and establish system frequency and voltage. The necessity to maintain synchronous speed introduces process control challenges when the prime mover is a hydraulic turbine. The variability of pipeline throughput would likely require extremely fast-acting control valves to maintain predicable flow through the turbine. The control system for an HPRT coupled to a synchronous generator must simultaneously manage variable oil flow rates and variable electrical loads.

5.2.3 AC Induction Machines

Overview

The induction machine is ubiquitous in modern life, by far the most widely used of all electric machines. The success of the induction machine can be attributed to its simple, rugged and efficient design[10]. Modern designs are similar to those developed by Nikola Tesla in the late 19th century.[18] Modern electronics has enabled AC induction machines to replace DC machines in applications requiring speed control[11].

[9]Hydraulic transients propagate at 3,400 feet per second through crude oil. They can be extremely destructive and require detailed engineering to predict and mitigate. Analysis of hydraulic transients is outside the scope of this paper.

[10]The Department of Energy estimates that half of the electricity generated in the United States is consumed by induction machines.[19]

[11]Speed control of a DC motor can be achieved by changing the terminal voltage using variable resistors (see Figure 5.4). Speed control of an AC induction motor is complicated: it requires a

Although the induction design dominates motor applications, induction generators have only recently entered into widespread use. Prior to the 1973 oil embargo in the Middle East, induction machines were almost never used to generate electricity. Unlike synchronous machines, induction machines do not have circuitry to initiate or maintain excitation (magnetic flux) within the machine. This applies to both induction motors and generators. To maintain excitation, reactive power must be supplied by an overexcited synchronous machine or shunt[12] capacitor connected to the power system. Induction generators also cannot maintain AC system frequency or voltage.[18][20] As discussed in Section 5.1, reliable AC power distribution is predicated on maintaining steady system frequency and voltage.

Another significant disadvantage is that an induction machine cannot recover from blackouts[13]. Lacking internal excitation induction generators cannot perform *black start* duties to begin the power recovery process. For these reasons synchronous machines dominate electricity generation while induction machines dominate electricity utilization.[20]

The aforementioned disadvantages of induction machines greatly limit their use as generators. The key advantage of an induction generator is the ability to tolerate a prime mover with varying or inconsistent angular velocities. Provided the power system can support the reactive power requirements of the machine, induction generators can be used in *peak shaving* applications[14]. This configuration is readily applicable to an HPRT at the VMT.

---

change in terminal voltage *and* frequency to avoid saturation and overheating. Use of Variable Frequency Drives has revolutionized speed control applications.[18]

[12]Connected in parallel.

[13]A total power failure where generation is disconnected from the grid.

[14]Peak shaving is the practice of reducing electrical load on the primary generator(s) by temporarily shifting load to supplemental generation.

Induction Machine Operation

The winding of the stator induces a rotating magnetic field within the motor in synchronism with the AC system frequency. When the induction machine is operated as a motor, the stator's rotating magnetic flux induces a voltage and current in the rotor. The rotor is slotted and looks like a cage, hence the name *squirrel cage* rotor. When current is applied to the stator but the rotor is not spinning, the slip is unity $s = 1.0$. The magnetic field induced in the rotor starts to follow the magnetic field of the stator. When operating as a motor, the rotor's magnetic field always lags behind that of the stator. If the rotor was spinning at the same speed as the magnetic field in the stator, i.e. synchronous speed, the induced voltage and current in the rotor would drop to zero and, the magnetic "pull"to drive the rotor would cease to exist. Even unloaded, an induction motor is always *slipping* relative to synchronous speed by several percent. As the load on the induction motor increases, the slip increases and thereby increases the strength of the magnetic field "pulling"on the rotor.[20] The nameplate of an induction motor is shown in Figure 5.6. The synchronous speed of this motor is 900 RPM but the rated speed under load is 880 RPM (actual rotor angular velocity).

When the rotor of the induction machine is rotating at synchronous speed, the slip is zero, $s = 0$. For the machine shown in Figure 5.6, this speed is 900 RPM. Theoretically no power is consumed with zero slip. If the prime mover accelerates the rotor faster than synchronous speed, the slip becomes negative and the polarity of the induced voltage and current in the rotor reverses. With negative slip, the induction machine is begins supplying real power back to the power system. The machine is now acting as a generator.[20]

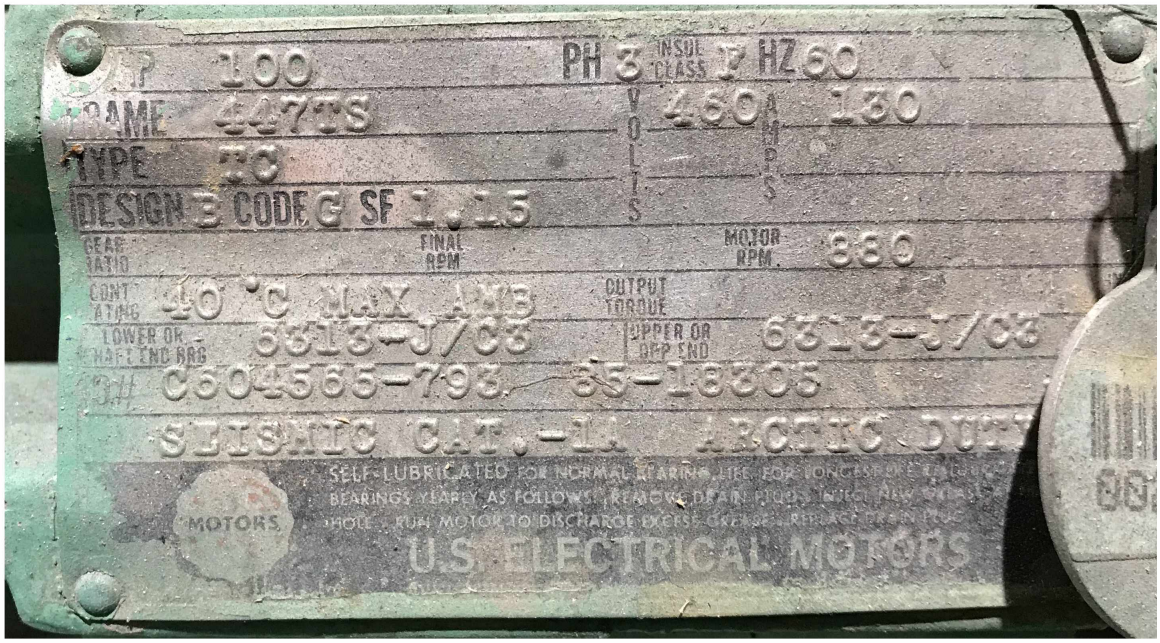

Figure 5.6: Nameplate of a 100 HP, 480 VAC, 8 pole induction motor. The synchronous speed of this machine is 900 RPM but the rated speed under load is 880 RPM. The rotor slips with respect to the stator.

Induction Generator Calculations

Use of an induction machine in HPRT service at the VMT is promising. To verify the existing power system has has sufficient reactive power capabilities, a model of an actual machine will be developed and analyzed.

Two manufacturers provided resistance and reactance values for the equivalent circuit of a squirrel cage induction machines suitable for HPRT service. The values are tabulated in Table 5.2.

The equivalent circuit of an induction machine is shown in Figure 5.7 where r_1 is the stator resistance, x_1 is the stator reactance, r_2 is the rotor resistance, expressed in terms of the stator voltage and frequency, x_2 is the rotor reactance, expressed in terms of the stator voltage and frequency, x_m is the magnetizing branch reactance and s is the slip between the rotor and the stator calculated with Equation 5.4.

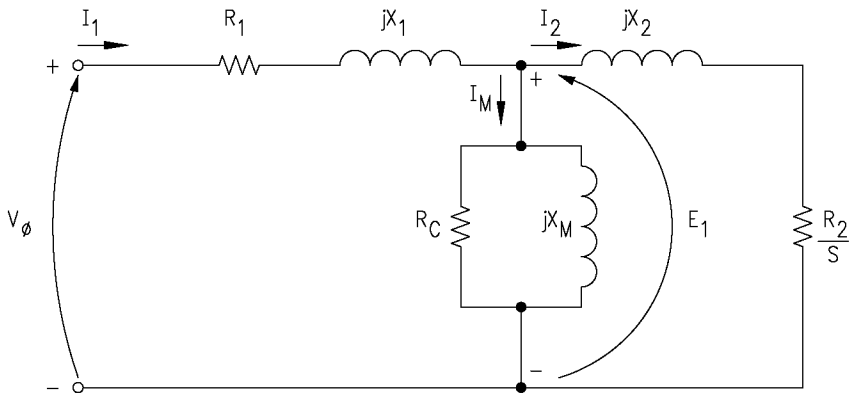

Figure 5.7: The equivalent circuit of an induction machine. This circuit is useful to calculate the performance of the machine under various operating conditions. r_1 is the stator resistance, x_1 is the stator reactance, r_2 is the rotor resistance, x_2 is the rotor reactance, x_m is the magnetizing branch reactance and s is the slip.

Table 5.2: Manufacturer-provided resistance and reactance values for the equivalent circuit of a 7 MW (9387 HP), 13.8 kV, 4-pole, 3 phase, 60 Hz squirrel cage induction machine suitable for HPRT service. Values are for a machine running at 110°C. Operating as a motor the machine draws 310 A with an efficiency of 96.6% and a power factor of 0.94. Note that r_c was not provided.

Coefficient	Value
r_1:	0.11144 Ω
x_1:	j3.0933 Ω
r_2:	0.13214 Ω
x_2:	j1.7263 Ω
x_m:	j189.01 Ω

Synchronous speed of the machine is calculated by Equation 5.3:

$$n_s = \frac{2f}{p} \tag{5.3}$$

where n_s is synchronous speed or the stator electrical speed in RPM, f is the power system frequency, p is the number of magnetic poles in the machine. For the machine in Table 5.2, $n_s = 1800$ RPM and the machine shown in Figure 5.6, $n_s = 900$.

Slip in the machine is calculated by Equation 5.4:

$$s = \frac{n_s - n_r}{n_s} \tag{5.4}$$

where s is the slip, n_s is synchronous speed or the stator electrical speed in RPM, n_r is the rotor mechanical speed in RPM. Values of slip are tabulated and used for subsequent computations.

The impedance of the machine determined by solving the equivalent circuit in Figure 5.7 for the Thévenin equivalent circuit. At the terminals of the machine the impedance is calculated using Equation 5.5[20][18]:

$$Z = r_1 + jx_1 + \left(\frac{\left(\frac{r_2}{s} + jx_2 \right) jx_m}{\frac{r_2}{s} + j(x_2 + x_m)} \right) \tag{5.5}$$

An important consequence of Equation 5.5 is the impedance of the machine is a function of the rotor slip (Equation 5.4). With the values listed in Table 5.2 and Equations 5.5 and 5.4 the current in the stator can be solved using Equation 5.6:

$$I_s = \frac{V_\phi}{Z} \tag{5.6}$$

where I_s is the stator current, V_ϕ is the terminal voltage:

$$V_\phi = \frac{13800}{\sqrt{3}} = 7977$$

and Z is the machine impedance calculated with Equation 5.5.

In an induction machine operating below synchronous speed (as a motor) the real component of the stator current I_s and the imaginary component are supplied by the power system. If the induction machine is operating above synchronous speed (as a generator) the real component of the stator current I_s is exported back to the power system while the imaginary component is still supplied by the power system. The two scenarios are expressed by Equations 5.7 and 5.8 where the sign of I_{real} flips[20][18]:

$$I_s = I_{real} + jI_{imaginary} \tag{5.7}$$

$$I_s = -I_{real} + jI_{imaginary} \tag{5.8}$$

After solving Equation 5.5 for the impedance of the machine over the range of rotor slips and then calculating the stator current at each slip, the real and reactive power consumed or exported by the machine is found. Equations 5.9 and 5.10 are used to calculate the real and reactive power:

$$P = \sqrt{3}V_L I_s cos(pf) \tag{5.9}$$

$$Q = \sqrt{3}V_L I_s sin(pf) \tag{5.10}$$

where P is real power consumed or generated by the machine, Q is reactive power consumed or generated by the machine, V_L is the line-to-line voltage, 13.8 kV, I_s is the stator current as calculated by Equation 5.5 and pf is the power factor or the

phase angle of I_s.[20][18]

Values computed using Equations 5.9 and 5.10 are plotted in Figures 5.8, 5.9 and 5.10. Figure 5.9 and 5.10 focus on the rotor angular velocity where the machine transitions from motor to generator.

At synchronous speed, $n_s = 1800$ RPM, the stator current, real and reactive power all approach to zero. At this speed the slip is zero and the machine is idling, neither consuming or exporting energy. In HPRT service this is the speed at which the machine is to be electrically connected to the system. Above synchronous speed, $n_s > 1800$ RPM, the real power reverses polarity while the reactive power retains the same polarity. The machine is now acting as a generator, exporting real power and importing reactive power. In all three figures positive power values are consumed by the machine while negative power values are exported from the machine.

5.3 Electric Generator Comparison

The operation of DC, AC synchronous and AC induction machines has been discussed. A summary of the advantages and disadvantages of each machine is tabulated in Table 5.3.[20][18]

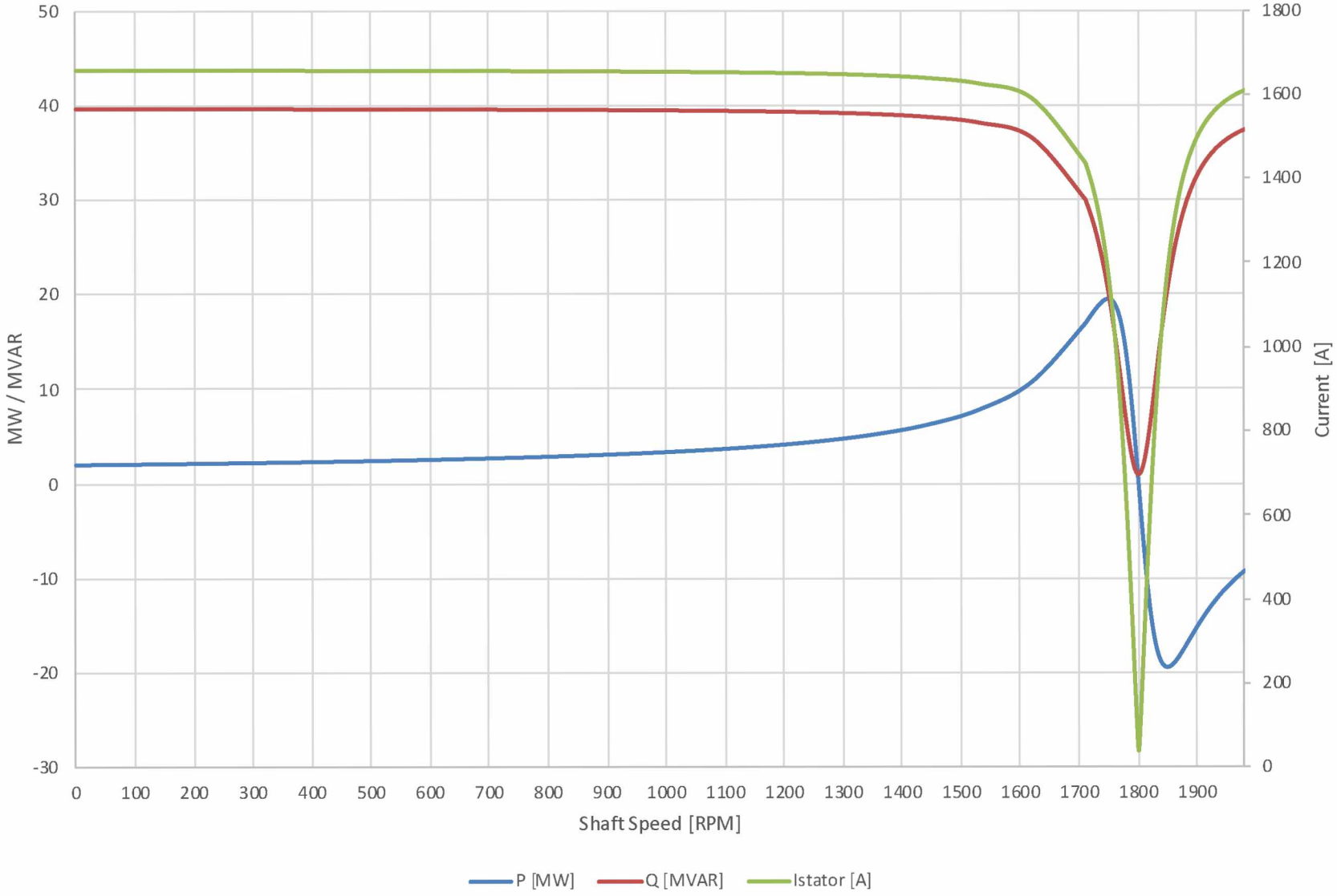

Figure 5.8: Plot of the real power, reactive power and stator current consumed or exported by the machine as calculated by Equations 5.9 and 5.10. Positive power values are consumed by the machine while negative power values are exported from the machine. At 1800 RPM the transition from motor to generator is apparent.

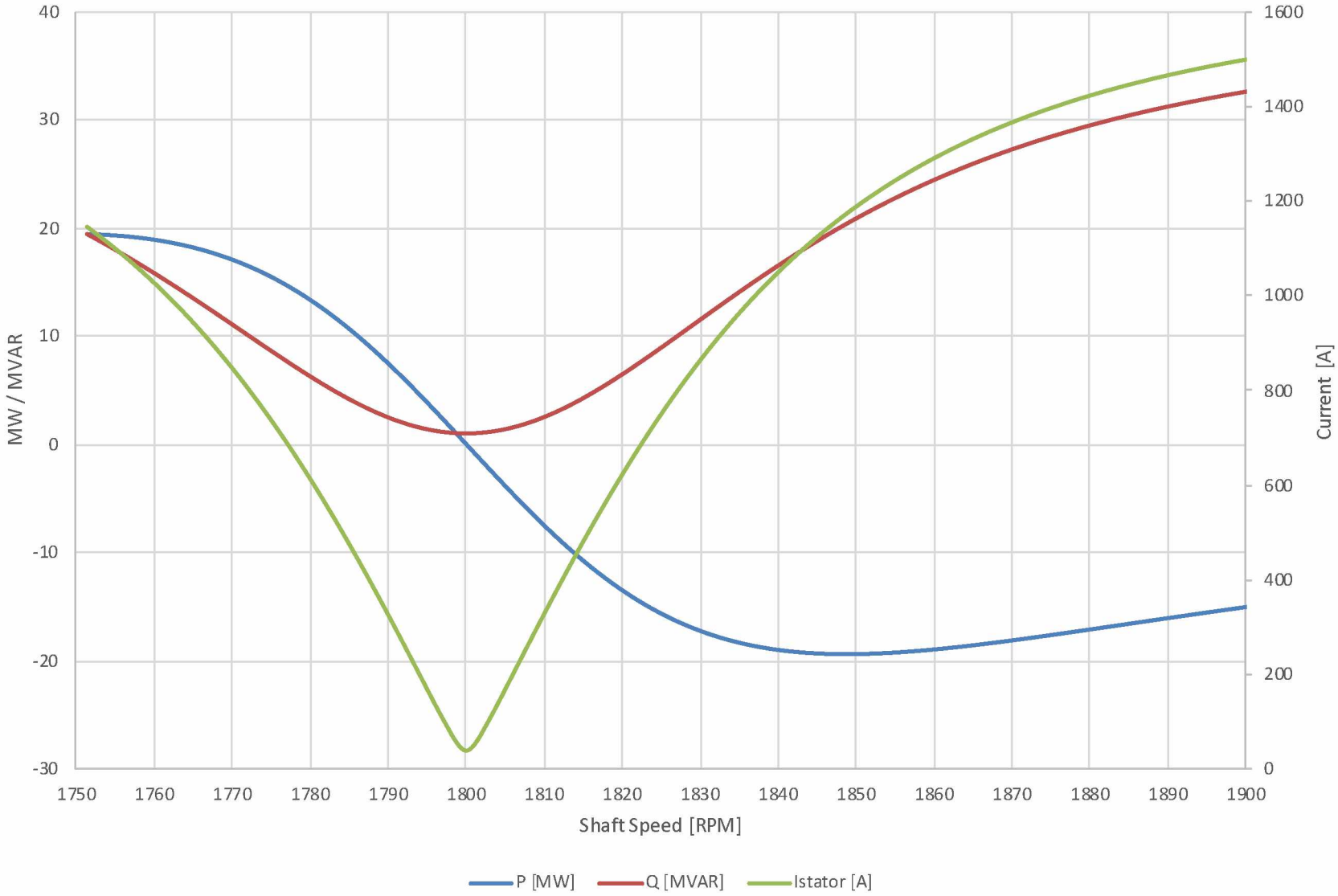

Figure 5.9: Enlarged plot of when the machine is operating as a generator. At synchronous speed, $n_s = 1800$ RPM, the stator current approaches to zero. Above synchronous speed, $n_s > 1800$ RPM, the real power reverses polarity while the reactive power retains the same polarity. Positive power values are consumed by the machine while negative power values are exported from the machine.

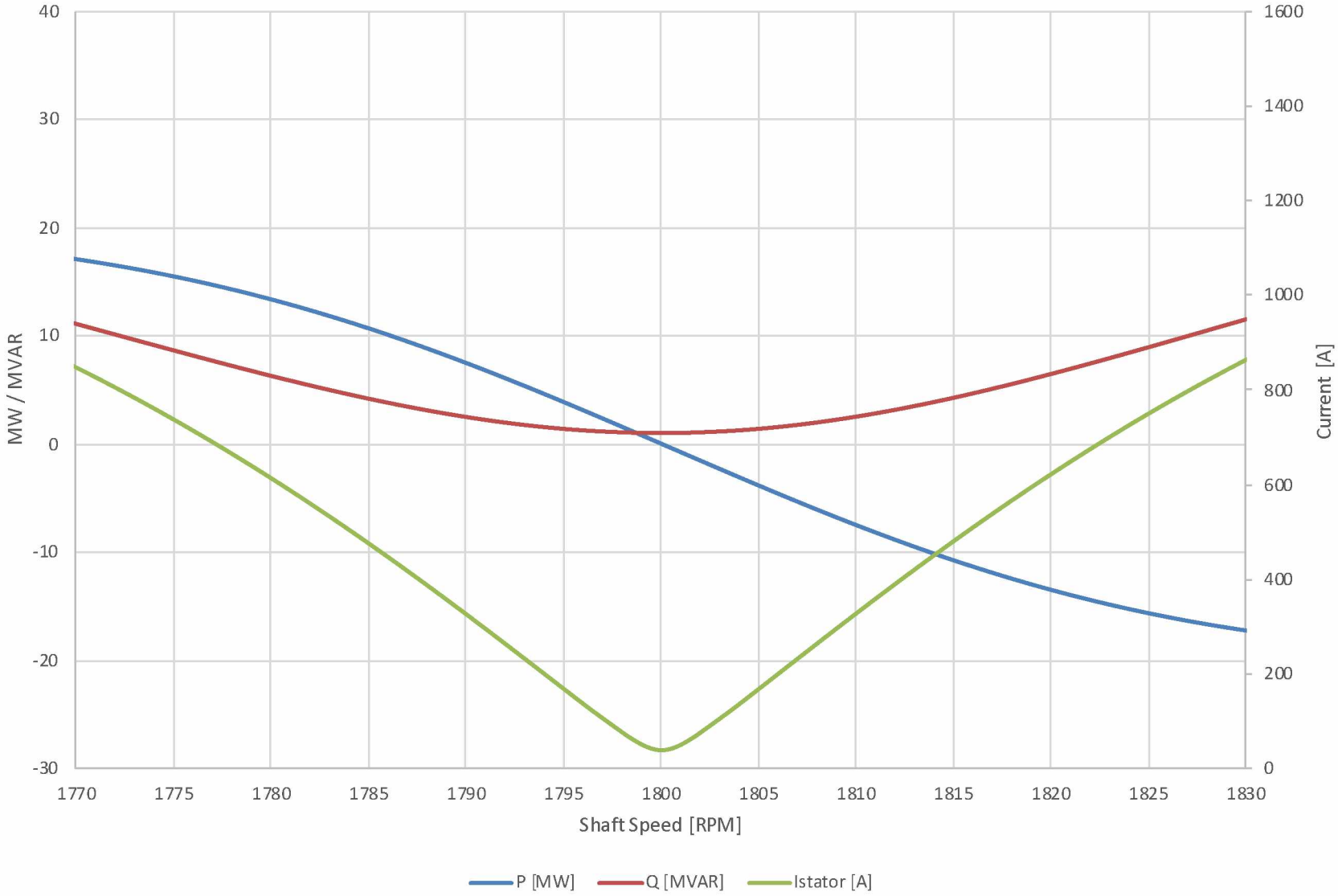

Figure 5.10: Enlarged plot of the transition region between motor and generator operation. Positive power values are consumed by the machine while negative power values are exported from the machine.

Table 5.3: Summary of the strengths and weaknesses of the major electric machines in HPRT service at the VMT.

Characteristic	DC Machine	Synchronous Machine	Induction Machine
Voltage	Fair: Requires power electronics to generate AC output	Best: Establishes power system voltage. Easily adjusted.	Poor: Cannot establish power system voltage.
Frequency	Fair: Requires power electronics to generate AC sine wave.	Best: Establishes power system frequency.	Poor: Depends on a synchonous machine to establish power system frequency.
Maintenance	Poor: Commutator brushes require regular servicing. DC machines are not common in power generation.	Good: Low maintenance requirements. Electrically more complicated than an induction machine.	Best: Lowest maintenance requirements. Simple, rugged design with few components.
Protection[a]	Fair: Power electronics will limit the available fault current to the AC system. Circuit breakers and protective relays must accommodate limited fault current.	Best: Typical decrement curve and protection requirements for a synchronous machine.	Fair: Short circuits will cause the machine terminal voltage to collapse and greatly limit contribution to the fault. Circuit breakers and protective relays must accommodate limited fault current.
Control	Good: Prime mover shaft may rotate at any speed compatible with commutators. Power output varies with prime mover shaft speed.	Fair: Prime mover shaft must closely match synchronous speed (typically 1800 or 3600 RPM). Cannot tolerate variations in prime mover shaft speed. Use of control valves to precisely regulate throughput will be complicated.	Best: Prime mover shaft may rotate at any speed. Below synchronous speed, the machine will act as a motor and will be disconnected from the power system
Islanding[b]	Fair: Power electronics will limit the ability to start loads with high inrush currents.	Best: Capable of independently carrying loads on the VMT power system.	Poor: Cannot operate without a synchronous machine tied onto the power system.
Black Start	Fair: Possible to independently startup typical plant heating, lighting, and process control loads.	Best Capable of independently starting loads on the VMT power system.	Poor: Cannot operate without a synchronous machine tied onto the power system.

[a] Considerations when designing protective relaying schemes.

[b] Ability to operate without being paralleled with other generators.

CHAPTER 6

IMPLEMENTATION

6.1 Power Output

The power output of an HPRT at the VMT is tabulated in Table 6.1 and plotted in Figure 6.6. Table 6.1 was calculated using Equation 3.6

$$p = \frac{qh\gamma\eta_m\eta_e}{5310}$$

with the following assumptions:

1. Average temperature of crude oil received at the VMT is 53°F.
2. Average density of crude oil received at the VMT is 0.864 g/cm^3.
3. Head differential across the turbine is 1604 feet.
4. Efficiency of the turbine is $\eta_{turbine} = 0.85$.
5. Efficiency of the electrical generator is $\eta_{generator} = 0.95$.

In Table 6.1 q_{HPRT} is the crude oil flow rate routed through the HPRT, $p_{theoretical}$ is the theoretical hydraulic power prior to accounting for turbine and generator inefficiencies, p_{brake} is the shaft power available at the generator accounting for pump inefficiencies and $p_{electrical}$ is the real electrical power exported to the power system accounting for generator inefficiencies. As indicated by q in the numerator of Equation 3.6, the power recovered is directly proportional to the flow rate through the HPRT.

Diverting 100% of pipeline throughput through the HPRT is not practical (although theoretically possible). In the event of a process upset and the HPRT electrical

Table 6.1: Tabulated power outputs of an HPRT at the VMT. q_{HPRT} is the crude oil flow rate through the turbine, $p_{theoretical}$ is the theoretical hydraulic power, p_{brake} is the shaft power at the generator and $p_{electrical}$ is the real power exported from the machine.

q_{HPRT} [BBL/day]	$p_{theoretical}$ [MW]	p_{brake} [MW]	$p_{electrical}$ [MW]
300,000	2.29	1.94	1.85
350,000	2.67	2.27	2.15
400,000	3.05	2.59	2.46
450,000	3.43	2.92	2.77
500,000	3.81	3.24	3.08
550,000	4.19	3.56	3.39
600,000	4.57	3.89	3.69
650,000	4.96	4.21	4.00
700,000	5.34	4.54	4.31
750,000	5.72	4.86	4.62

load drops offline, flow must quickly transition back through the backpressure control valves to maintain control of slackline in Thompson Pass. Hydraulic transients will be attenuated if there already is crude flowing though the valves.

6.2 Fuel Savings

Given the complexities of the vapor management system and the unpredictability of utilizing hydrocarbon vapor as a fuel source, diesel fuel savings calculations based on empirical data are challenging. The following calculations are based on the most recent operational data from calendar year 2018.

6.2.1 Calculation of Fuel Volumes

The control system calculates the instantaneous diesel flow to each boiler (refer to Figure 4.1) by monitoring one of three flow indicating transducers. The raw diesel flow rate is scaled by the transducer calibration and reported in units of gallons per minute via 4-20mA instrumentation circuits. Total volumes can be calculated by integrating the instantaneous flow rate to each boiler from the starting time and

date, m to the end time and date, n:

$$Q_{total} = \int_m^n q_A dt + \int_m^n q_B dt + \int_m^n q_C dt \tag{6.1}$$

where q_x is instantaneous flow rate to each online boiler and Q_{total} is the total fuel burned. To verify accuracy of the instrumentation, the integrated volumes are periodically compared by field technicians to the physical fluid levels in the diesel tanks.

The control system and data historian[1] have finite memory and computational capacity to record and process this data (along with thousands of other control inputs and outputs). The instantaneous flow rates are recorded by the data historian every two seconds. To calculate fuel savings retroactively with a finite data set, diesel volumes are calculated as follows:

$$Q_{total} = \sum_{i=m}^{n} \overline{q_A} \cdot \Delta t + \sum_{i=m}^{n} \overline{q_B} \cdot \Delta t + \sum_{i=m}^{n} \overline{q_C} \cdot \Delta t \tag{6.2}$$

where m is the starting date (December 31, 2017 for this analysis), n is +365 days, q_x is instantaneous flow rate to each boiler and Q_{total} is the total fuel burned in the online boilers. The data historian retrieves the average of the reported flow transducer values q_x over the interval Δt directly on the server and only reports the average[2]. Using Equation 6.2 the calculated boiler fuel total in 2018 is 1,728,392 gallons.

Reviewing Figure 4.1, the minimum diesel flow rate to each boiler is 1 GPM. With two boilers online—the typical operating scenario—diesel minimums total 2 GPM. A

[1]A data historian is a computer database that stores process and control variables over time. Data can be retrieved from the database on-demand for analysis. Data historians are important tools used to monitor and analyze commercial or industrial processes and the systems that control them.

[2]By offloading computation to the data historian, the volume of data queried is significantly reduced. One I/O point sampled every hour over a year is 8760 points, sampled every 60 seconds is 525,600 points and every 30 seconds is 1,051,200 points. Five-minute intervals were chosen for yearly analysis of data as a compromise between accuracy and file size.

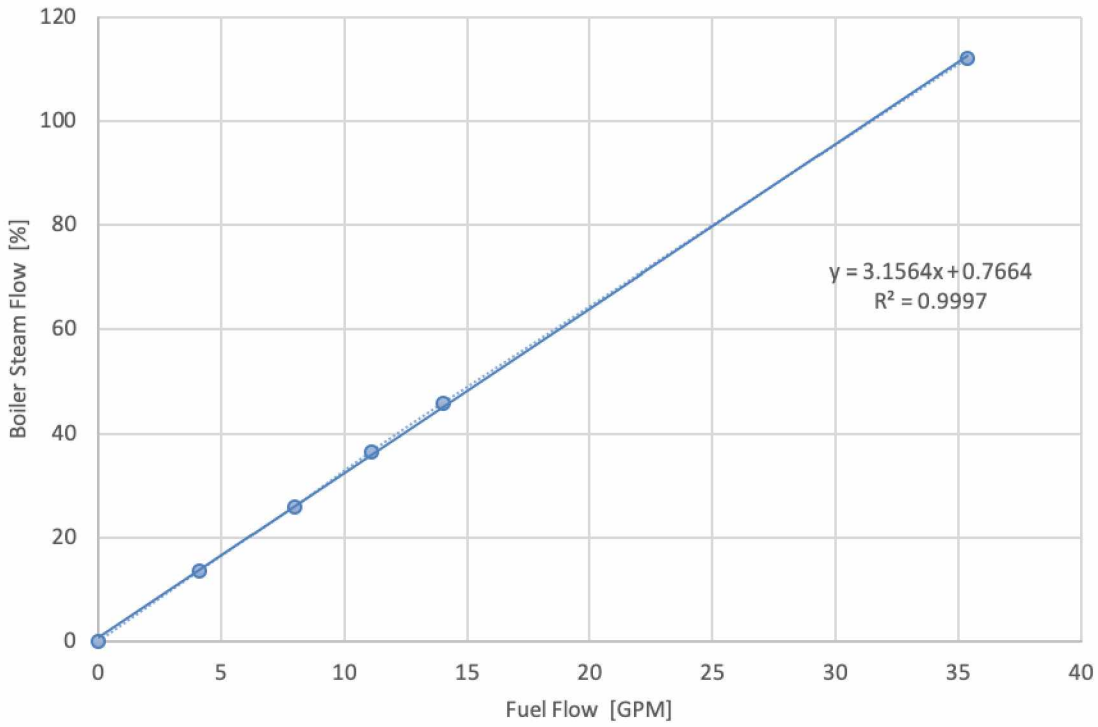

Figure 6.1: Boiler curve relating normalized steam output to diesel input. This data is extracted from the control system and used in HPRT fuel consumption calculations.

boiler operates on minimum diesel flow when the vapor energy content and volume are maximized. If the vapor Wobbe Index or volume declines, diesel combustion can be increased to maintain steam output.

Diesel flow rates above 1 GPM per boiler are the result of the control system detecting insufficient vapor thermal input. Figure 6.1 shows the linear relationship between steam output and diesel fuel flow. Any diesel flow rates above 1 GPM per boiler are an opportunity to utilize more cost effective power generation. This range is graphically depicted in Figure 6.2.

6.2.2 600 PSI Steam Flow

As shown in Figure 6.1 the ratio of steam output to diesel flow input is a linear function. This is expected behavior: doubling the fuel rate doubles the thermal input and steam production. These boiler curves are recomputed during every boiler

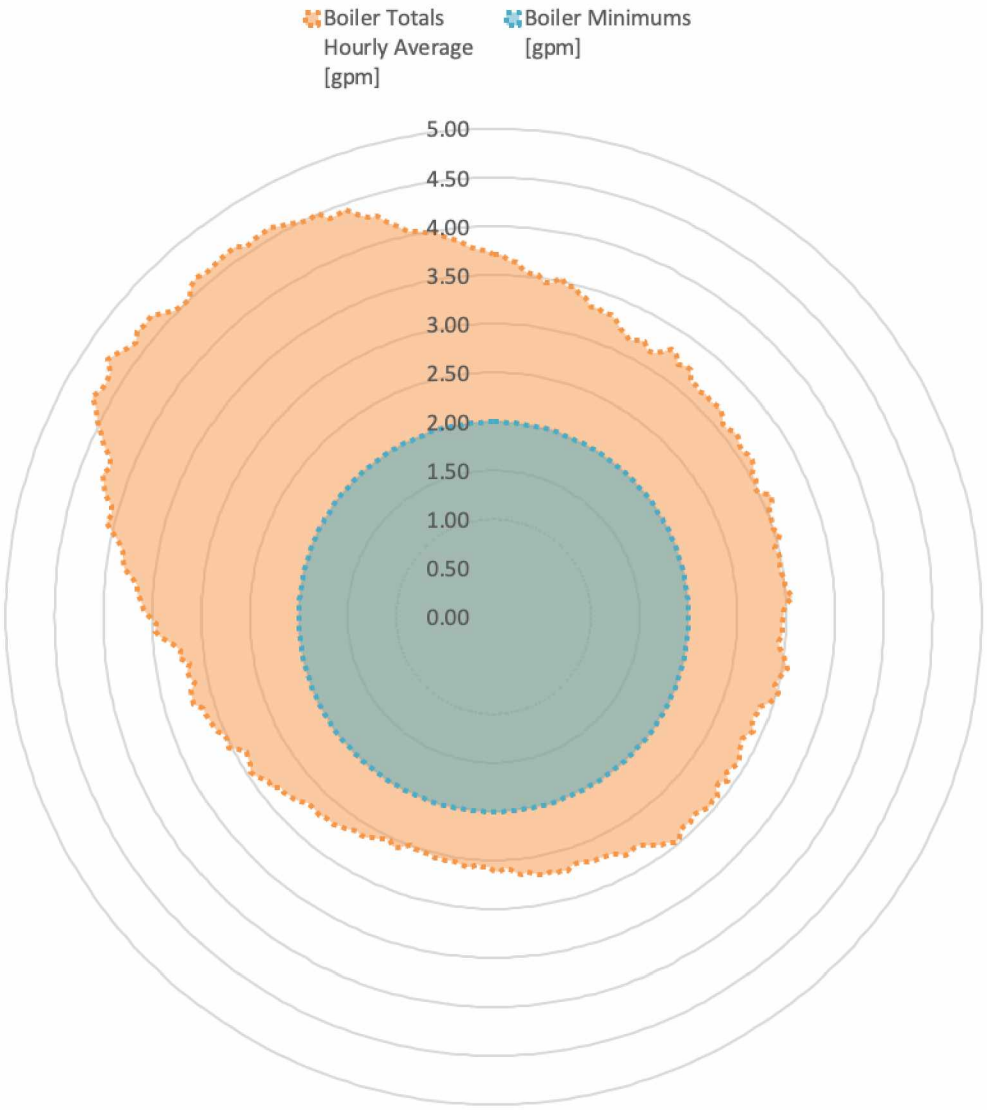

Figure 6.2: Hourly average diesel consumption. Top of figure is 00:00 hours, bottom of figure is 12:00 hours with the right and left edges at 06:00 and 18:00 hours respectively. Boiler fuel minimums are depicted. Diesel flow rates ranging from the boiler minimums to the average hourly consumption is the economic sweet spot of an HPRT. An HPRT can "shave" the edge of the curve yielding fuel savings.

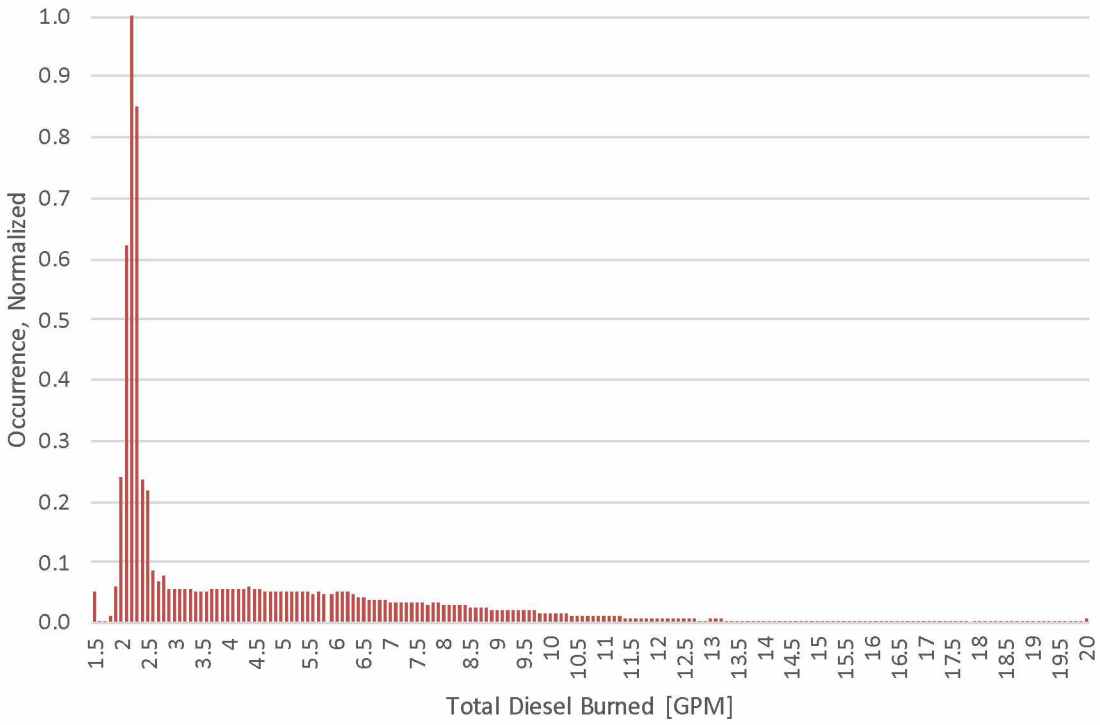

Figure 6.3: Normalized histogram of diesel consumption in the boilers. As the minimum flow rate into each boiler is 1 GPM and two boilers are typically online at any one time, flow rates of 2 GPM occur most frequently. Flow rates above 2 GPM indicate the vapor thermal input is insufficient to meet steam load.

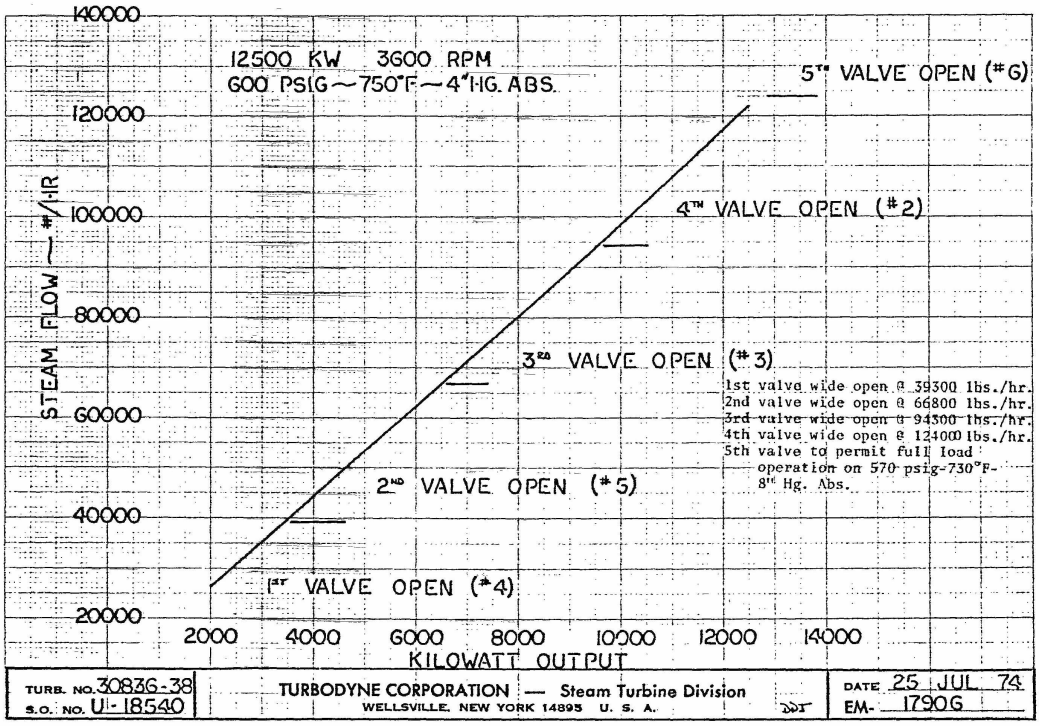

Figure 6.4: Performance curve for the three main Turbodyne 12.5 MW condensing steam turbines.

startup to ensure the control system correctly supplies the boiler with the appropriate volume of fuel to maintain pressure and temperature in the 600 PSI steam header.

The conversion between steam flow in percent to the mass flow rate is as follows:

$$Q_{steam} = 0.03206 \cdot \int_{m}^{n} q_{steam} dt \tag{6.3}$$

Where the units of the coefficient 0.03206 are $\frac{\%steam}{second}$, q_{steam} is the instantaneous steam flow percentage as reported by the control system, and Q_{steam} is thousands of pounds of steam produced.

The 12.5 MW Turbodyne condensing steam turbines exhibit a linear relationship as shown in Figure 6.4 between the mass flow rate of steam into the turbine and shaft power out. Figure 6.5 demonstrates the linear correlation between the thermal input to the boilers and the real electrical power output of the generators. Finally a linear

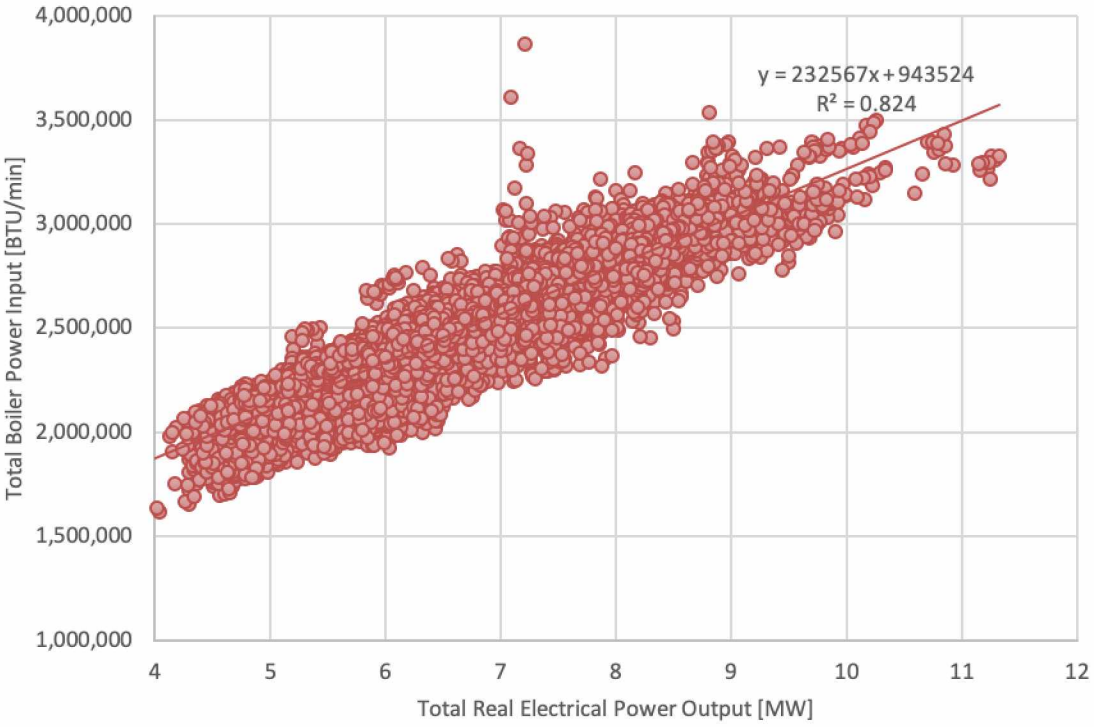

Figure 6.5: Scatter plot comparing the thermal inputs to the boiler against electrical power output.

function relating the thermal input to the boilers in MMBtu/hr to MW derived from data in Figure 6.5 is:

$$p_{boiler} = 13.954 \cdot p_{electrical} + 56.611 \tag{6.4}$$

where p_{boiler} has units of MMBtu/hr and $p_{electrical}$ has units of MW.

The efficiency of the plant is then be calculated on a per-Btu basis. This is a calculation of the power plant heat rate described in Section 4.3.1. Figure 4.13 shows the efficiency distribution relative to real power output.

The diesel burned in the boilers has an energy density ranging from 132,000 Btu/gal to 138,000 Btu/gal. Due to the boiler minimums, a fuel rate greater than 2 GPM could be accommodated by loading the HPRT. To calculate the diesel replaced by the HPRT, the electrical power output of the generator tabulated in Table 6.1 is converted to equivalent gallons of diesel burned using Equation 6.4 and performing the unit conversion from MW to Btu. Assuming an energy density of 132,000 Btu/gal for diesel is assumed as peak electrical loads occur during the winter.

Using the tabulated fuel consumption data collected using Formula 6.2, logic functions are used to determine periods where the fuel flow to the boilers is above minimums and less than or equal the HPRT equivalent gallons of diesel. During these periods all excess diesel flow could be displaced by the HPRT. These values are summed using Equation 6.5:

$$Q_{diesel,saved} = \sum_{i=m}^{n} q_{diesel,eq} \cdot \Delta t \tag{6.5}$$

where m is the starting date (December 31, 2017 for this analysis), n is +365 days. The volumes of diesel are then summed to determine total savings and tabulated in Table 6.2. When diesel flow is in excess of the volume displaced by the HPRT *and* boiler minimums, the balance will still be burned in the boilers.

Table 6.2: Calculated fuel savings in the boilers based on the flow rate through the HPRT. $q_{diesel,eq}$ is the equivalent diesel flow rate in the boilers to generate the power output of the HPRT. $q_{diesel,saved}$ is a summation of the total fuel saved based on data from 2018 using Equation 6.2.

q_{HPRT} [BBL/day]	$q_{diesel,eq}$ [gpm]	$Q_{diesel,saved}$ [gallons]
300,000	3.25	502,012
350,000	3.80	536,458
400,000	4.34	563,694
450,000	4.88	585,372
500,000	5.42	603,036
550,000	5.97	617,693
600,000	6.51	629,469
650,000	7.05	639,110
700,000	7.59	646,806
750,000	8.13	652,825

A quadratic fit of the fuel saved based on HPRT flow rate is Equation 6.6.

$$Q_{diesel,saved,fit} = -6.59 \cdot 10^{-7} q_{HPRT}^2 + 1.01 q_{HPRT} + 2.61 \cdot 10^5 \tag{6.6}$$

6.3 Hydraulic Turbine and Generator Integration

6.3.1 Loading Profile

To maintain stable operation and avoid generating pressure transients in the pipeline, the HPRT generator must operate under constant load. The power input to the synchronous turbines in Power/Vapor would swing to accommodate changes in the VMT electrical load. The turbines would continue to establish system frequency and voltage as the induction machine is not capable of performing this function. When large loads are started, flow rate through the HPRT would not increase.

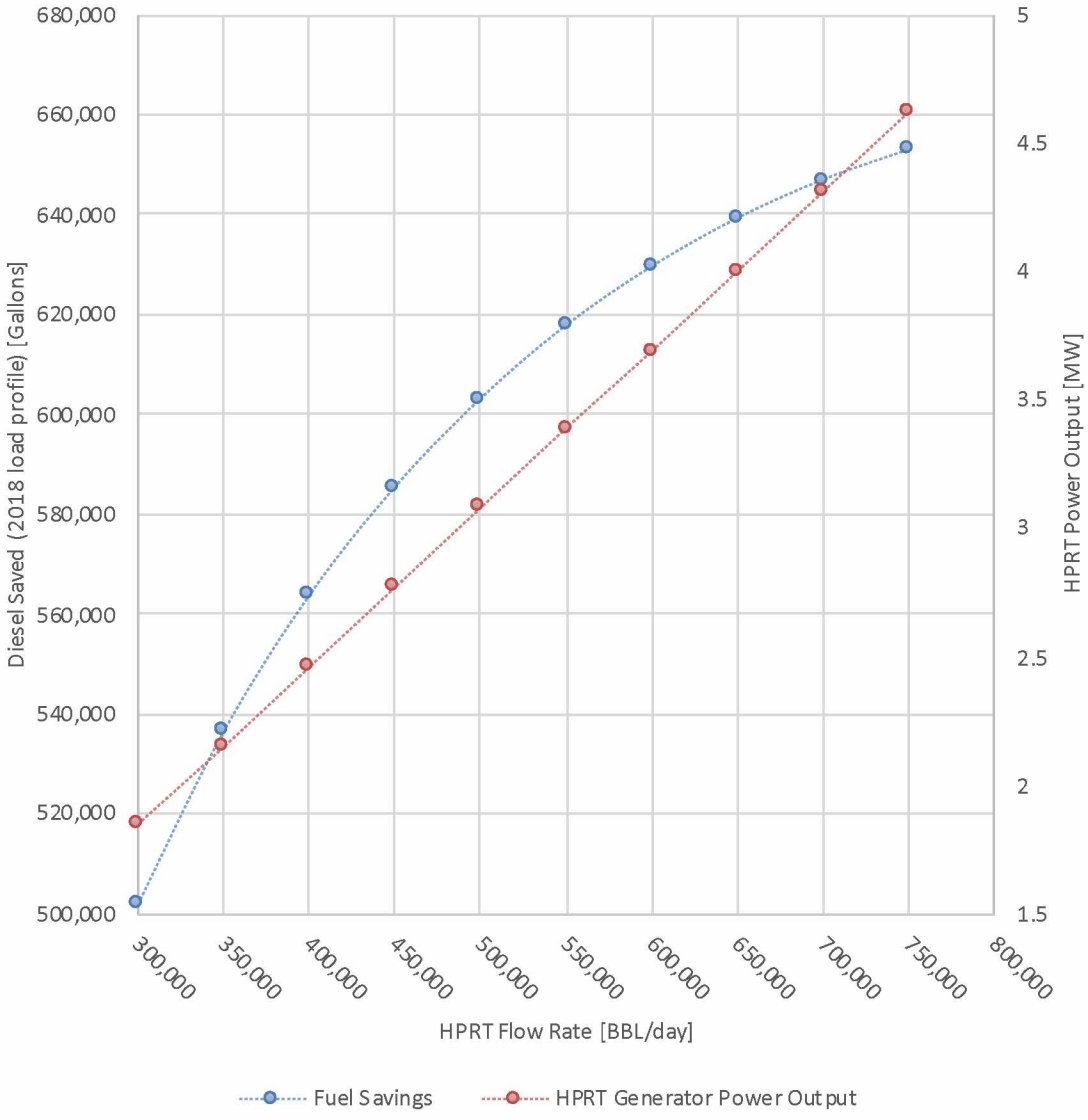

Figure 6.6: Calculated fuel savings based on the flow rate through the HPRT.

6.3.2 Piping Interconnection

The turbine would be installed in parallel with the existing backpressure control valves. Although it would be theoretically possible to route all flow through the HPRT, some flow must always be moving through the backpressure control valves to maintain pressure stability in the event of an upset.

Two pressure and flow control schemes are recommended. Figure 6.7 is designed strictly to maintain the pressure differential across the turbine without adjustments for speed. This is compatible with an induction machine. Figure 6.8 is designed to regulate the speed of the turbine while simultaneously maintaining the pressure differential. Required for use with a synchronous machine, the control system for this scheme is more complicated.

6.3.3 Reactive Power Supply

The normal power generation configuration in Power/Vapor is two turbine-generators operating in parallel. The VMT load distribution as shown in Figure 4.10 indicates that one generator would be sufficient to meet demand year-round. At any one time the generators are operating at approximately 50% load. From the capability curve of the generators shown in Figure 5.5 the machines have sufficient capability to meet the reactive power consumed by the induction generator as calculated in Figures 5.9 and 5.10.

6.4 Economics

As with any practical endeavor, an economic analysis is necessary. To install an HPRT at the VMT and justify the endeavor with an economic rationale, the volume of diesel saved is only part of the equation. All *annualized* costs (and savings) associated with design, procurement, installation, commissioning and operation must be considered.

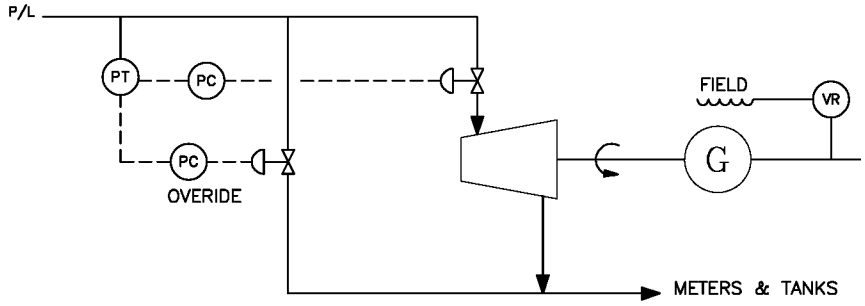

Figure 6.7: HPRT Scheme 1. Flow through the HPRT is uncontrolled. This is applicable to use with an induction machine.

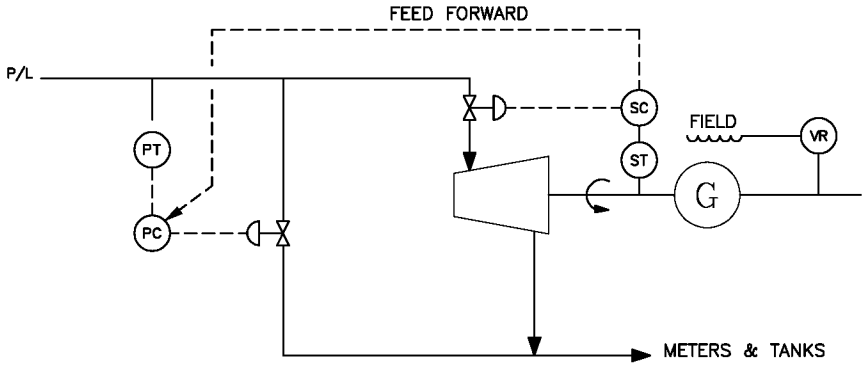

Figure 6.8: HPRT Scheme 2. Flow through the HPRT is directly controlled. This is applicable to use with a synchronous machine.

By allocating costs and savings over time as they are realized, the cash flow of the project is constructed.

Corporations have a fiduciary duty to their shareholders to maximize shareholder value. As capital is a finite resource, an economic analysis will compare projected cash flows against alternative uses for that capital. The alternative that optimizes returns on invested capital and perceived risk will be the chosen alternative[3]. Across a portfolio of possible projects, a corporation can build a suite of work that maximizes value.

Unfortunately, comparisons only on cash flow are difficult. One project may have very high upfront capital requirements but yield steady, predicable returns over the long run. An alternative project that requires less capital upfront could have lower, unpredictable returns. Which alternative maximizes long term shareholder value? To ease comparison, the Internal Rate of Return (IRR) method is used. The IRR calculates the overall return on a given cash flow on an annualized basis. It is calculated as follows:

$$\sum_{t=0}^{n} \frac{v_n}{(1+irr)^t} = 0 \tag{6.7}$$

where n is the number of periods in the cash flow, v_n is the specific value of the period and irr is the Internal Rate of Return. With Equation 6.7 outgoing cash (spent to build or maintain the system) in a given period is negative while incoming cash (returns or avoided costs) is positive.

The IRR excludes taxes, inflation, cost of capital and other financial risks. Accounting for these risks is generally outside the scope of engineering and the responsibility of corporate financial analysis. Acknowledging these complexities, the IRR remains a powerful tool engineers can use to compare alternatives and maximize time

[3]One common alternative that must always be considered is to do nothing. Could a dollar invested in another project or the capital markets yield better returns?

spent on economically justifiable work.

6.4.1 Cost Estimate

The estimated *direct costs* to build an HPRT at the VMT are calculated in Table 6.3. The direct costs are the physical infrastructure and the labor necessary to install that infrastructure. *Indirect costs* are those supporting installation such as equipment rentals, project management, crew housing and transportation.

Assumptions

The following assumptions built into the estimate tabulated in Table 6.3:

1. Combined labor rate is $95 per hour.
2. "Indirects" Factor is 75% (accounts for construction management, equipment rentals, survey etc.).
3. Contingency Factor is 30% (accounts for cost overruns).
4. Engineering labor estimated at 40 hours per week (work in Anchorage).
5. Craft labor estimated at 70 hours per week (work in Valdez).
6. Existing 4/0 Medium-Voltage wiring is fit for service.
7. Induction machine operates at distribution voltage (13.8 kV); no step-up transformer is required.)
8. Equipment installed in new module. Module placed on concrete pad adjacent to north wall of East Meters. No red mud encountered.
9. Fire suppression system is not required (module walls are porous).
10. Fire and gas detection (e.g. IRs) is sufficient.

11. No lubrication oil skid is necessary (hydrodynamic bearings utilized).

12. Taxes and equipment depreciation are excluded.

13. Equipment Monitoring Package (e.g. Bently-Nevda) not required.

14. Electric Machine: 7 MW 13.8 kV Induction Generator.

15. Switchgear includes Circuit Breakers and Protective Relays.

16. DCS includes PCU, Backplane, Analog I/O, Digital I/O.

17. Process Instrumentation includes Flow, Pressure and Temperature.

18. Module cost estimated at $750 per square foot.

Table 6.3: Estimate of the Total Installed Cost for installation and commissioning of an HPRT at the VMT. Direct costs are explicitly estimated. Indirect costs are calculated as a percentage of the direct costs. Note the listed assumptions for the estimate.

Description	Material	Crew	Weeks	Manhours	Labor	Item Total
Engineering (40 hour weeks)	N/A	6	24	5,760	$547,200	$547,200
1 x Hydraulic Turbine Skid	$950,000	8	8	4,480	$425,600	$1,375,600
2x24" Motor Operated Valve	$200,000	4	2	560	$53,200	$253,200
1x24" Strainer	$50,000	4	1	280	$26,600	$76,600
24" Piping and Steel	$250,000	10	8	5,600	$532,000	$782,000
15 kV Switchgear	$400,000	3	2	420	$39,900	$439,900
DCS Node	$100,000	3	2	420	$39,900	$139,900
Process Instrumentation	$40,000	2	4	560	$53,200	$93,200
Fire & Gas Detection	$25,000	2	2	280	$26,600	$51,600
Instrument and Control Wiring and Terminations	$50,000	3	4	840	$79,800	$129,800
Medium Voltage Wiring and Terminations	$50,000	4	4	1,120	$106,400	$156,400
Low Voltage Wiring and Terminations	$10,000	4	4	1,120	$106,400	$116,400
40 Cubic Yard Concrete Foundation	$40,000	6	2	840	$79,800	$119,800
Pump Module, steel, porous-1000 SF	$750,000	8	2	1,120	$106,400	$857,530
Commissioning and Training	$10,000	4	1	140	$13,300	$23,300
Inspections and Testing	$10,000	1	4	280	$26,600	$36,600
Net Total	$2,935,000			18,060	$1,715,700	$4,651,830
Net Total (Rounded)						$4,660,000
Indirects						$3,500,000
Contingency						$1,050,000
Total						$9,210,000

Table 6.4: Estimated ten-year cash flow for installation of an HPRT. Note the listed assumptions for the cash flow.

Year	Cash Flow	Payback Ratio
0	(9,210,000)	
1	1,463,000	0.16
2	1,492,000	0.32
3	1,522,000	0.49
4	1,552,000	0.65
5	1,583,000	0.83
6	1,615,000	1.00
7	1,647,000	1.18
8	1,680,000	1.36
9	1,714,000	1.55
10	1,748,000	1.74

6.4.2 Cash Flow

The cash flow for the project is tabulated in Table 6.4. Assumptions used in calculation of the cash flow:

1. The HPRT is constructed and installed in one year.
2. Average diesel cost is $2.65 per gallon. Costs are adjusted for inflation.
3. Inflation is 2% per year.
4. Ongoing operations and maintenance costs are $50,000 per year.
5. Average pipeline flowrate is 500,000 BBL/day.
6. Flow diverted through HPRT is 400,000 BBL/day with the balance through the existing backpressure control valves.
7. Annual fuel savings are 560,000 gallons per year.

6.4.3 Internal Rate of Return and Sensitivity Analysis

The internal rates of return are calculated using Equation 6.7 for the various scenarios as follows:

Base Case

For the base scenario with the cash flow tabulated in Table 6.4 the IRR is 11%.

Base + Low Fuel Costs

Assume average diesel costs are $2.00 per gallon. The IRR for this scenario is 5%.

Base + High Fuel Costs

Assume average diesel costs are $3.50 per gallon. The IRR for this scenario is 18%.

Base + Zero Contingency

Assume the HPRT is installed with zero contingency (contingency is 0%; total installation is $8,160,000). The IRR for this scenario is 14%.

Base + Under Budget

Assume the HPRT is installed under budget (contingency is calculated as -30%; total installation is $7,110,000). The IRR for this scenario is 18%.

Base + 60% Contingency

Assume the HPRT is installed over budget (contingency is 60%; total installation is $10,260,000). The IRR for this scenario is 9%.

CHAPTER 7
CONCLUSION

The route over which the Trans-Alaska Pipeline System is built presents an opportunity for energy recovery. Today the energy expended by Pump Station 9 to push oil over Thompson Pass is lost to entropy at the Valdez Marine Terminal. Ideas to capture this energy date back half a century when the design of the pipeline and the VMT were still lines on paper in Houston. Technical, economic and legal challenges at the time prevented these ideas coming to fruition. By maintaining a tight focus on improvements to existing Power/Vapor process and maximizing use of existing infrastructure, this project has advanced the design of a hydraulic power recovery turbine.

To assure the mechanical integrity of the pipeline as it crosses Thompson Pass, the location of the slackline interface must be carefully selected. Regulation of incoming pressure at the VMT allows pipeline controllers to optimize placement of the interface. This necessitates operation of the backpressure control system at the VMT. The hydraulic theory applied in this project demonstrated the operation of this system and how it could be harnessed for energy recovery. The magnitude of this energy resource–accounting for the variable characteristics of crude oil–was calculated as approximately 3.8 megawatts at today's pipeline throughput.

As crude oil fills the storage tanks, the vapors generated must be carefully managed. The Power/Vapor facility was designed to simultaneously capture these vapors, balance tank head pressures and ensure a flammable or explosive atmosphere cannot form inside the tanks. As a byproduct of this process, electricity is generated for local use. To determine opportunities for improving the efficiency of this Power/Vapor process, it's operation was studied in detail. A thermal survey was conducted to

calculate the actual performance of the Rankine cycle. The average heat rate of the plant is approximately 15%.

To integrate power generation from an HPRT into the local power system, three major classes of electric machines were studied: DC, AC synchronous and AC induction. Of the three, the induction generator was deemed the most practical. Induction generators can tolerate variable shaft speeds although they remain dependent on parallel operation with synchronous machines to establish system frequency and voltage. Calculations of the reactive power demands of an induction generator were performed to ensure existing generation could operate together.

Utilizing an HPRT to "peak shave" the electrical load on the existing Power/Vapor synchronous generators will save diesel. Realistic efficiency factors and real operational data were used to simulate fuel savings. At an average pipeline flow rate of 550,000 BBL/day, an HPRT could generate 3.5 MW of electricity and save more than 600,000 gallons of diesel every year. At 300,000 BBL/day more than 500,000 gallons of diesel saved every year, potentially improving the economic life of TAPS.

The selected design would tie into existing crude piping at the East Meters facility, operating in parallel with the backpressure control valves. Power would be exported to the VMT grid using nearby 13.8 kV cabling. Operation of the HPRT would not place restrictions on pipeline throughput or adjust slackline pressure controls. The base case estimated installation and commissioning costs at $9.2 million with an internal rate of return of 11%.

TAPS is—and will remain—a dynamic system. Designing, operating and maintaining equipment that can accommodate variations in crude oil composition and flow rate is challenging. By capitalizing on existing infrastructure and previous engineering studies, this project has advanced the design of a practical HPRT installation at the VMT.

REFERENCES

[1] R. D. Mead, *Journeys Down the Line Building the Trans-Alaska Pipeline*. Garden City, New York: Doubleday and Company, Inc., 1978.

[2] Alyeska Pipeline Service Company, "Trans alaska pipeline system low flow overview," Alyeska Pipeline Service Company, Tech. Rep., Oct. 2017.

[3] *Trans Alaska Pipeline System The Facts*. Alyeska Pipeline Service Company, Alyeska Pipeline Service Company.

[4] C. E. Heuer, "The application of heat pipes on the trans-alaska pipeline," United States Army Corps of Engineers Cold Regions Research and Engineering Labratory, Tech. Rep., July 1979.

[5] Y. A. Cengel and M. A. Boles, *Thermodynamics An Engineering Approach*, Fifth. McGraw-Hill, 2006.

[6] "Department of environmental conservation air quality operating permit AQ0082TVP02," Alaska Department of Environmental Conservation, Tech. Rep., 2012.

[7] B. A. Hauser, *Practical Hydraulics Handbook*. 121 South Main Street, Chelsea, Michigan 48118: Lewis Publishers, 1991.

[8] M. J. Economides, A. D. Hill, C. Ehlig-Economides, and D. Zhu, *Petroleum Production Systems*, Second. Prentice Hall, 2013.

[9] H. Addison, *A Treatise on Applied Hydraulics*, Fifth. London: Chapman and Hall Limited, 1964.

[10] Alyeska Pipeline Service Company, *Summary Report Hydraulics Design for the Trans Alaska Pipeline System*. Alyeska Pipeline Service Company, Feb. 1974.

[11] E. F. Brater and H. W. King, *Handbook of Hydraulics for the Solution of Hydraulic Engineering Problems*, Sixth. McGraw-Hill Book Company, 1976.

[12] J. P. Ellenberger, *Piping and Pipeline Calculations Manual*. Elsevier, 2010.

[13] V. S. Lobanoff and R. R. Ross, *Centrifugal Pumps Design and Application*. Houston, Texas: Gulf Publishing Company, 1985.

[14] H. M. Morris and J. M. Wiggert, *Applied Hydraulics in Engineering*, Second. New York: The Ronald Press Company, 1972.

[15] "Department of environmental conservation air quality operating permit AQ0074TVP03," Alaska Department of Environmental Conservation, Tech. Rep., 2016.

[16] Office of Air Quality Planning and Standards, "Federal standards for marine tank vessel loading operations and national emission standards for hazardous air pollutants for marine tank vessel loading operations," United States Environmental Protection Agency, Technical Support Document, Jul. 1995.

[17] "May 2018 monthly energy review," U.S. Energy Information Administration, Tech. Rep., May 2018.

[18] S. J. Chapman, *Electric Machinery Fundamentals*, Fourth. 1221 Avenue of the Americas, New York, NY 10020: McGraw-Hill, 2005.

[19] P. E. Scheihing, "U.S. department of energy's motor challenge program: A national strategy for energy efficient industrial motor-driven systems," U.S. Department of Energy, Washington, DC, USA, Tech. Rep., 2012.

[20] J. E. Barkle and R. W. Ferguson, "Induction generator theory and application," *Transactions of the American Institute of Electrical Engineers. Part III: Power Apparatus and Systems*, vol. 73, no. 1, Jan. 1954.